

International
Progress Report

IPR-06-28

Äspö Hard Rock Laboratory

Cleaning and sealing of Borehole

Report of Sub-project 1 on design and modelling of the performance of borehole plugs

Roland Pusch
Geodevelopment International AB

Gunnar Ramqvist
Eltekno AB

November 2006

Svensk Kärnbränslehantering AB

Swedish Nuclear Fuel
and Waste Management Co
Box 5864
SE-102 40 Stockholm Sweden
Tel 08-459 84 00
+46 8 459 84 00
Fax 08-661 57 19
+46 8 661 57 19



**Äspö Hard Rock
Laboratory**

Report no.
IPR-06-28

Author
**Roland Pusch
Gunnar Ramqvist**

Checked by
**Christer Svemar
Jukka-Pekka Salo
Antti Öhberg**

Approved
Anders Sjöland

No.
F98K

Date
November 2006

Date
May 2007

Date
2007-06-21

Äspö Hard Rock Laboratory

Cleaning and sealing of Borehole

Report of Sub-project 1 on design and modelling of the performance of borehole plugs

Roland Pusch
Geodevelopment International AB

Gunnar Ramqvist
Eltekno AB

November 2006

Keywords: Plugging, Sealing, Bentonite, Borehole, Concrete

This report concerns a study which was conducted for SKB. The conclusions and viewpoints presented in the report are those of the author(s) and do not necessarily coincide with those of the client.

Abstract

Sub-project 1 is focused on concepts of potential use, represented by the clay plugs of "Basic", "Container", "Couronne" and "Pellet" types with focus on the design principles, maturation in rock, and manufacturing. For concrete plugs, which are proposed to be constructed where intersected fracture zones have previously been cement-stabilized, a special criterion is that the plugs must serve acceptably even if the cement component is dissolved and lost.

The experimental part led to the conclusion that two of the concepts, i.e. the "Basic" type, which makes use of jointed perforated copper tubes filled with highly compacted smectite-rich clay, and the "Container" type, implying placing of such clay in closed tubes, serve acceptably in both short and very deep holes under certain conditions respecting groundwater salinity and time of insertion. While long holes require particularly safe techniques, shorter holes may preferably be sealed by using simpler types, i.e. the "Couronne" (ring-shaped compacted clay stacked around a central copper rod) and "Pellet" concepts.

Summary

The purpose of the Borehole Plugging Project is to develop and test plugs for sealing boreholes that extend deep from the ground surface or reach out from tunnels, drifts and rooms of a repository. Both long-extending and short holes of the latter type shall be considered. The objective of the project is to indicate methods and materials of plugging that seal the holes so that they will not serve as migration paths of water carrying radionuclides that may ultimately be released from the HLW canisters. The main seals proposed by the study are clay-based plugs that prevent axial flow of water and are placed in those parts of the holes that do not intersect significantly water-bearing fracture zones, while the parts of the holes that intersect such zones do not need to be tight and can be filled with concrete. Both clay and concrete plugs must remain physically stable for at least 100 000 years [4].

Sub-project 1 describes concepts of potential use, represented by the clay plugs of "Basic", "Container", "Couronne" and "Pellet" types with focus on the design principles, maturation in rock, and manufacturing. For concrete plugs, which are proposed to be constructed where intersected fracture zones have previously been cement-stabilized, a special criterion is that the plugs must serve acceptably even if the cement component is dissolved and lost.

The experimental part of the study included testing of the maturation rate, erosion, piping and homogenization, led to the conclusion that two of the concepts, i.e. the "Basic" type, which makes use of jointed perforated copper tubes filled with highly compacted smectite-rich clay, and the "Container" type, implying placing of such clay in closed tubes, serve acceptably in both short and very deep holes under certain conditions respecting groundwater salinity and time of insertion. While long holes require particularly robust techniques, shorter holes may preferably be sealed by using simpler types, i.e. the "Couronne" (ring-shaped compacted clay stacked around a central copper rod) and "Pellet" concepts.

Sammanfattning

Syftet med Borehole Plugging Project är att utveckla och testa pluggar för tätning av djupa borrhål eller hål som når ut från tunnlar, orter och rum i ett slutförvar. Både långa och korta hål för den sistnämnda tillämpningen skall beaktas. Studiens mål är att indikera pluggkonstruktionen som förhindrar att radionuklider, som i ett mycket långt tidsperspektiv möjligen kan avges från HLW-kapslarna, kan migrera i hålen. Den viktigaste tätningsfunktionen ges av lerbaserade pluggar som hindrar strömning i axiella led och som placeras i de delar av borrhålen som inte genomskärs av vattenförande sprickzoner, medan de delar av hålen som skärs av sådana zoner inte behöver effektiv tätning och därför kan fyllas med betong. Både ler- och betongpluggarna måste vara fysiskt stabila i minst 100 000 år [4].

Sub-project 1 beskriver pluggkoncept av potentiellt användbart slag, som representeras av typerna "Basic", "Container", "Couronne" och "Pellet", med fokus på designprinciper, mognadsförlopp i berget, och tillverkning. För betongpluggar, som föreslås bli gjutna där genomskurna sprickzoner, som cementstabiliserats före pluggningen, gäller ett särskilt kriterium, nämligen att pluggarna måste fungera tillräckligt väl även om cementkomponenten löses och försvinner.

Den experimentella delen av undersökningen, som omfattade testning av mognadshastigheten, erosion, piping och homogenisering, gav slutsatsen att två av koncepten, dvs "Basic"-pluggar bestående av kopplade perforerade kopparrör fyllda med högkompakterad lera, samt "Container"-pluggar, som innebär anbringande av sådan lera innesluten i rör, fungerar tillräckligt väl i både korta och långa hål under vissa förutsättningar beträffande grundvattnets salthalt och tiden för anbringandet. Medan långa hål kräver användning av mycket säker teknik kan korta hål med fördel pluggas med enklare metoder, t ex med användande av "Couronne"- (ringar av kompakterad lera placerade runt en central kopparstång) och "Pellet"- koncepten.

Contents

1	Introduction	11
2	The four clay plug concepts	13
3	The "Basic" concept	15
3.1	Design	15
3.1.1	Materials and dimensions	15
3.2	Maturation - processes and predictions	16
3.2.1	Conditions	16
3.2.2	Idealized rock - unlimited access to water	16
3.2.3	Homogenization of saturated clay	18
3.2.4	Real rock - possible limited access to water	19
3.3	Performance in situ	29
3.3.1	Practical design issues	29
3.3.2	Erodability	30
3.3.3	Manufacturing	33
3.3.4	Equipment for placement	33
4	The "Container" concept	35
4.1	Design	35
4.1.1	Materials and dimensions	35
4.2	Maturation - processes and predictions	36
4.2.1	Unlimited access to water in fractured rock	36
4.2.2	Limited access to water in rock with few fractures	36
4.3	Performance in situ	38
4.3.1	Practical design issues	38
4.3.2	Erodability	38
4.3.3	Manufacturing	38
4.3.4	Equipment for placement	38
5	The "Couronne" concept	39
5.1	Design	39
5.1.1	Materials and dimensions	39
5.2	Maturation - processes and predictions	40
5.2.1	General	40
5.2.2	Limited access to water in rock with few fractures	40
5.3	Performance in situ	41
5.3.1	Practical design issues	41
5.4	Erodability	42
5.5	Manufacturing	42
5.6	Equipment for placement	42

6	The "Pellet" concept	44
6.1	Design	44
6.2	Materials and dimensions	44
6.3	Maturation - processes and predictions	45
6.3.1	Microstructural evolution	45
6.3.2	Unlimited access to water in fractured rock	46
6.3.3	Limited access to water in rock with few fractures	46
6.3.4	Piping resistance	46
6.4	Performance in situ	49
6.4.1	Practical design issues	49
6.4.2	Erodability	49
6.4.3	Manufacturing	49
6.4.4	Equipment for placement	49
7	Construction of cement-based plugs	50
7.1	Basic	50
7.2	Recipe for borehole plugs of concrete	50
8	Discussion and recommendations	52
8.1	Discussion	52
8.1.1	Performance	52
8.1.2	Possible improvements	53
8.2	Concrete plugs	53
9	References	54
	Appendices	55

1 Introduction

Sub-project 1 covers five items that are dealt with in the present document:

- Design of four clay plug versions
- Maturation of clay plugs, processes and prediction
- Performance in situ of clay plugs
- Manufacturing of clay plugs
- Construction of cement-based plugs

The reason why several clay plug types are investigated is because the different conditions that are met with in practice calls for plugs with different properties and placeability. Thus, while very deep holes require a particularly robust technique that is presently represented by plugs of "Basic" case" but with a simpler version, "Container" case", as competitor, shorter holes may preferably be sealed by using even simpler types: "Couronne" case" and "Pellet" case. A further reason is that the rate of maturation of the clay may be a problem if it matures too quickly since it can then make it difficult to insert plugs of "Basic type" in very deep holes and to retrieve them if necessary. "Container" plugs would be ideal from this point of view. Plugging of short holes should not require these two rather sophisticated design principles and simpler types represented by the "Couronne" and "Pellet" concepts may be more suitable.

Construction of cement-based plugs is different from the other plugging techniques in the sense that it is made down-the-hole in rock that has been stabilized by grouting and reborings. Such plugs do not need to be tighter than the surrounding, fractured rock but must remain physically stable for the same period of time that is required for the clay plugs.

The Borehole Plugging Project has developed according to the plans described in [1].

2 The four clay plug concepts

The four clay plugs are illustrated in Figure 2-1. They are primarily intended to be used in boreholes with diameters ranging from 56 to 100 mm but at least the "Basic" and "Pellet" plugs can be used in much wider holes. This latter type and the "Couronne" plug can hardly be used in very deep holes while the other two may be used in kilometer-deep holes. The density of the matured clay should be on the order of 2000 kg/m³, corresponding to a dry density of 1590 kg/m³, for fulfilling the criterion that the hydraulic conductivity must be lower than that of the surrounding rock irrespectively of whether the groundwater is fresh or salt. For uniform maturation the boreholes to be plugged should be filled with tap water when plugging starts.

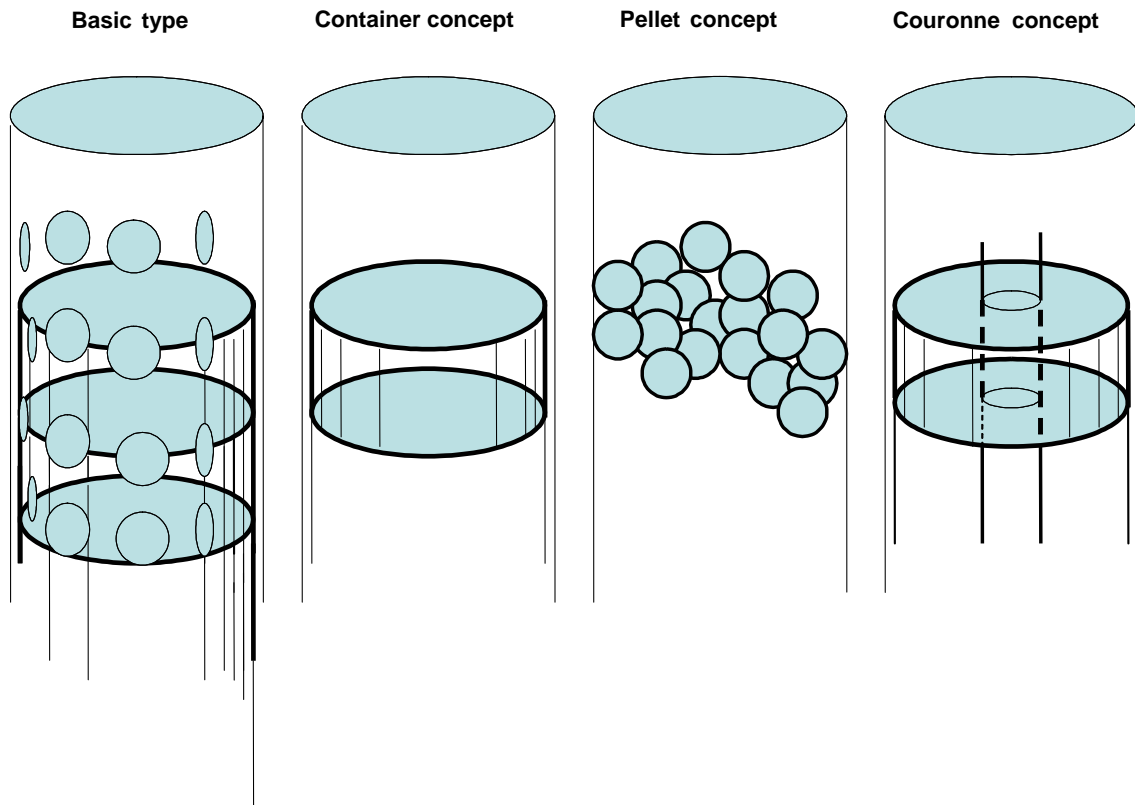


Figure 2-1. The four alternative clay plug concepts. Left: The "Basic" plug with highly compacted MX-80 clay columns confined in perforated copper tubes. Second left: The "Container" plug with highly compacted MX-80 clay blocks contained in a cylinder attached to drilling rods and released when the tip of the cylinder is in the desired position. Third left: MX-80 pellets poured into the hole without compaction. Right: The "Couronne" plug with annuli of highly compacted MX-80 clay stacked around jointed copper rods that are pushed into the hole.

3 The "Basic" concept

3.1 Design

The "Basic" plug has been used successfully for plugging short and long holes as demonstrated by the OL-KR24 project (Sub-project 3). The method is very robust since there is complete control of the position of each individual segment and good opportunities to pull up those that may not be placeable because of roughness of the borehole walls or too small radius of curvature of the hole.

3.1.1 Materials and dimensions

The perforated tubes with the dense clay blocks placed in them must have sufficient strength to be handled in the placement phase without being deformed or break. This puts a limit to the degree of perforation and to the thickness of the tube walls and a comprehensive study was made in the early phase of the project for finding an optimum geometry. The variables are:

- metal type for minimizing corrosion and impact on the clay
- perforation ratio (size of open surface area and total tube wall area)
- strength as function of the perforation ratio and tube wall thickness
- safety in placement and retrieval

Metal type

Four metals were considered: copper, navy bronze, titanium, and steel [2]. Copper is naturally a possible candidate material referring to the KBS3 concept. Navy Bronze is an alloy with 90-95 % Cu and 5-10 % Zn and a chemical stability that is assumed to be similar to that of copper. It has a tensile strength that is close to that of steel. Titanium, which is significantly lighter than copper (8930 kg/m^3 and 4500 kg/m^3 , respectively), is assumed to be as chemically stable as copper and has a tensile strength that significantly exceeds that of copper. Steel can be only slightly less chemically stable than the other candidates depending on pH, salt and oxygen in the groundwater.

Assessment of the four metal types led to selection of copper for three reasons: 1) the chemical stability and impact on the clay are judged to be superior, 2) the relatively low strength makes results from field experiments conservative if stronger metals will be ultimately selected, and 3) the more deformable copper tubes can better adaptate to the curvature of the holes in the placement phase. Copper was therefore taken as metal for manufacturing the tubes.

Perforation ratio

The degree of perforation is a determinant of the rate of maturation of the clay component and of the compressive and tensile strength of the tubes. For plugs in deep holes the high water pressure implies that access to water for maturation of the clay is not a limiting factor while geometrical constraints in the form of the size and spacing of the perforation holes control the rate of migration of clay to form a clay gel in the gap between tube and rock. For plugs close to the ground surface or located in those parts of a repository where the water pressure is low in the construction and waste placement phases the ability of the rock to give off water to the clay determines the maturation rate.

Earlier field experiments with 50 % perforation ratio and 10 mm hole diameter and 2 mm tube wall thickness gave acceptable performance with respect to the maturation rate of the clay and to the mechanical performance of the tubes and these measures were found to be at optimum in the study performed by Clay Technology AB in the present project. Thus a FEM-based model developed for determining the optimum diameter of the perforation hole diameter for reaching a high degree of homogeneity and highest density of the clay. It was found to be 10 mm for 50 % perforation ratio provided that all holes are equal and that the spatial distribution is symmetric with a half hole shift [Appendix I].

3.2 Maturation - processes and predictions

3.2.1 Conditions

The potential of the surrounding rock to provide the clay plug with water determines the maturation rate as demonstrated by pilot field tests at Stripa, reported in the report "Borehole Plugging Project", December 2004 [1]. Thus, where clay plugs were placed in shallow rock with low water pressure and hydraulic conductivity, they did not become fully water saturated even in several months, while where the water pressure was high and the frequency of water-bearing fractures was high, the plugs reached complete water saturation in due time. In this report we will distinguish between two conditions: 1) water is available without limitation at the plug/rock contact, and 2) water is available from discrete fractures that may imply limitation of the access to water. Both will be considered here.

3.2.2 Idealized rock - unlimited access to water

Equilibrium equations were formulated by Clay Technology AB [Appendix II] for forces in the clay in axial and radial directions, the forces representing swelling pressures in the system with internal friction as counteracting factor. Isotropic and anisotropic swelling conditions were assumed and different friction angles (8 to 22.4 degrees) were considered. The influence of the friction angle was found to be significant, which makes the selection of a representative value important.

Stepwise calculation had to be made because of the impact of the swelling pressure on the friction angle. The iterative procedure involved assumption of an initially low swelling pressure representing early penetration of a clay gel through the perforation.

The gel consolidates by being compressed by the successively expanded clay inside the perforated tube, yielding a higher density and therefore a higher friction angle. Using these new values the swelling pressure was calculated yielding a new density and friction angle data etc. Equilibrium was finally obtained giving the swelling pressure and corresponding density. Mean pressures were predicted for fresh water and found to be in good agreement with recordings while those representing saline water deviated substantially from the recorded pressures. The most important practically important results from the theoretical modelling and supporting laboratory tests were:

- The minimum theoretical swelling pressure against the rock was 1.96 MPa for fresh water and 0.95 MPa for saline water.
- Long term laboratory tests showed that complete swelling and homogenisation is obtained after 10-20 days. The measured mean swelling pressure against the rock was 2.8 MPa for fresh water and 0.6 MPa for saline water. This is in good agreement with the predicted mean pressure for fresh water but not for saline water.
- Measurement of the hydraulic conductivity of the clay paste formed between tube and confining tube, representing rock (Figure 3-1), after 20 days of maturation gave $5E-13$ to $9E-13$ m/s for fresh water and $2E-12$ m/s for saline water. Both are below typical conductivity values for the surrounding rock, i.e. $E-11$ to $E-8$ m/s.

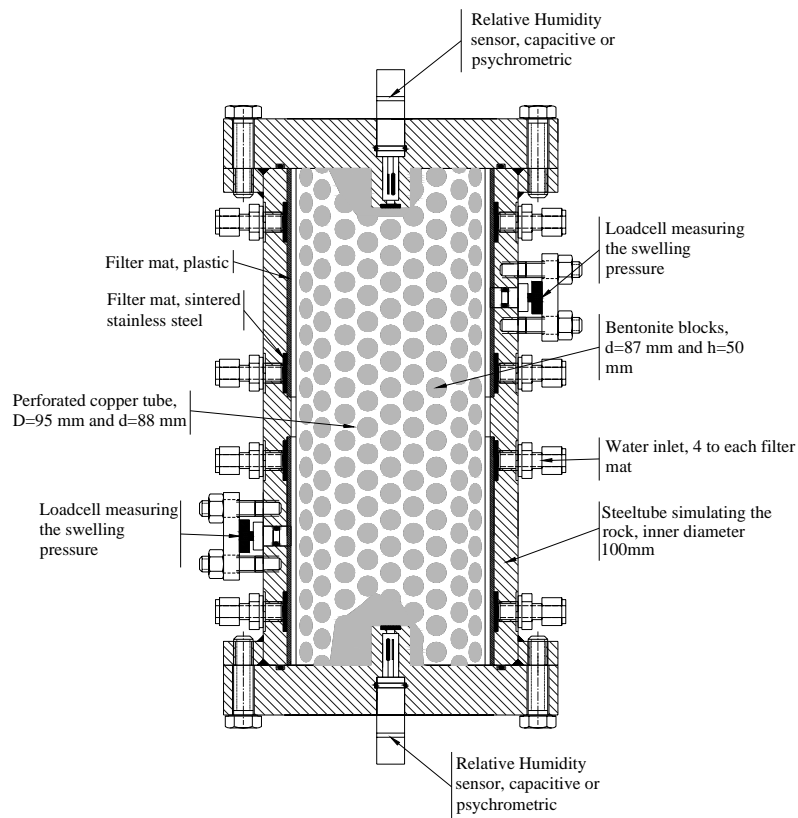


Figure 3-1. Section of test set-up for wetting and simultaneous recording of the evolution of the swelling pressure (load cells) and wetting ("RH" sensors) of "Basic" type [2].

3.2.3 Homogenization of saturated clay

For unlimited access to water it is concluded that complete water saturation is reached within less than a month for plugs in holes with up to 80 mm diameter. This does not imply that complete homogenization is reached in this time and a practical issue is whether the clay, which has somewhat different density in the centre and in the gap between tube and rock after reaching complete water saturation, will ultimately become totally homogeneous or have permanent differences in density. This was investigated in experiments with duration of one month and 1 year, respectively, using the equipment in Figure 3-1. The 1 month experiment was made by using clay blocks that had been "eroded" by flushing water along the plug units or by scraping off clay, both implying a loss of solid clay by 7.5%. One can draw two major conclusions from the experiments: 1) After 1 month the differences in density and water content of the shallow "skin" and central part of the dense core was very obvious, and 2) The "skin" and the central dense core were nearly water saturated (Figure 3-2). The latter finding means that there is no driving force for evening out the differences in density, suggesting that they will be permanent.

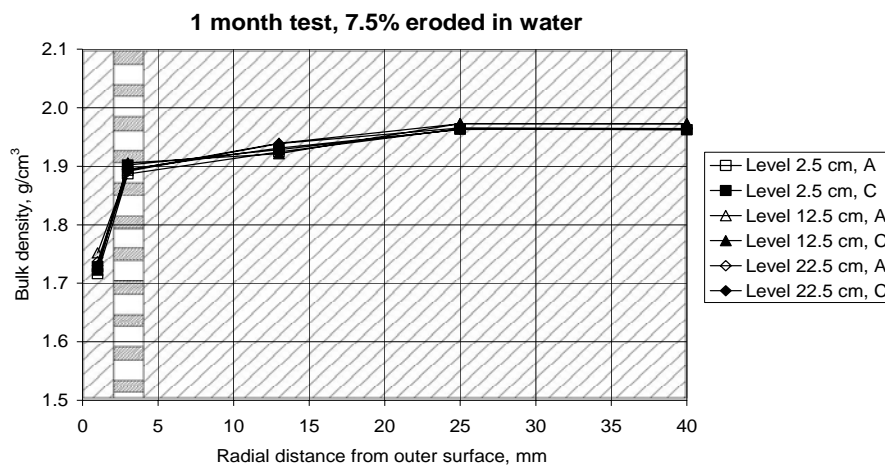


Figure 3-2a. Radial bulk density on three levels and in two directions after 1 month (Clay technology AB)

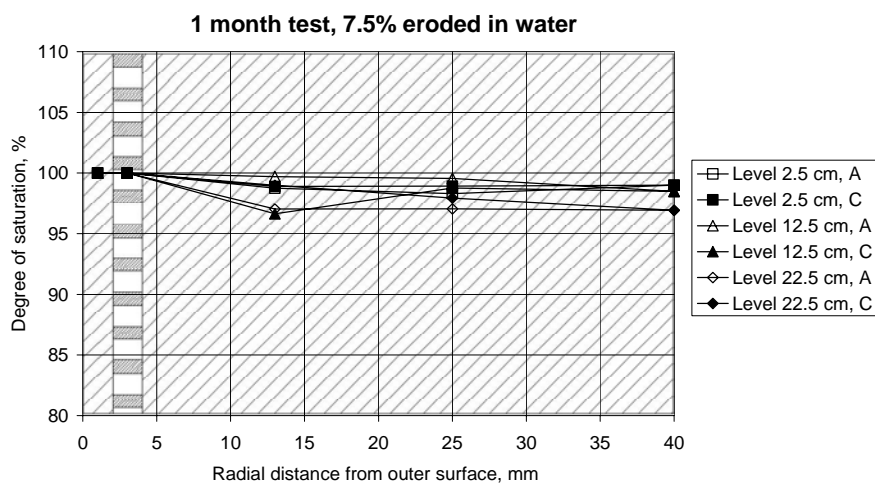


Figure 3-2b. Radial degree of saturation on three levels and in two directions after 1 month (Clay Technology AB).

The tests are fully reported in Appendix II.

3.2.4 Real rock - possible limited access to water

Controlling conditions

The factors affecting the rate of water saturation are:

- the hydraulic conductivity of the rock.
- the location of water-supplying fractures.
- the water pressure.
- the type, density and initial degree of water saturation of the clay plug.
- the geometrical conditions with respect to the perforation of the central tube, gap between tube and rock and between tube and clay.

The matter has been dealt with by using FEM and for predicting the water saturation process of the clay plug with the geometrical configuration in Figure 3-3, (cf. Appendix I). The diameter of the hole and plug were assumed to be 80 and 76 mm, respectively.

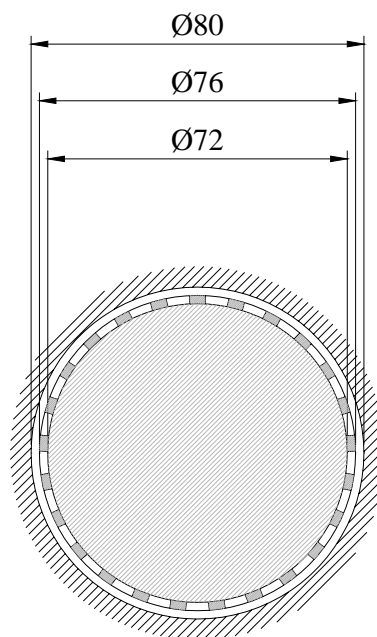


Figure 3-3. Assumed geometry of the plugged borehole. Borehole diameter 80 mm, perforated copper tube diameter 76/72 mm.

The calculations of the wetting and saturation of MX-80 clay confined in a borehole were made on the assumption that water for saturation is supplied by a single fracture in which a constant water pressure prevails (Figure 3-4). Considering the structural conditions in the rock as described above, this assumption implies that the availability of water for saturation of the clay is strongly underrated. The calculations did not include the displacement of solid clay material that is known to take place and no definite conclusions concerning the rate of homogenization can hence be drawn from them.

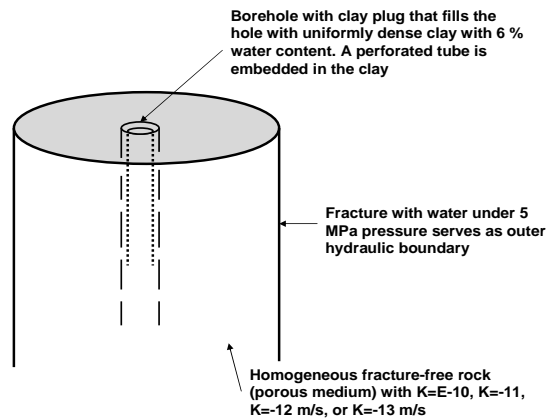


Figure 3-4. Geometry of ABAQUS model (Clay Technology AB).

The calculations gave the relation between the wetting time and hydraulic conductivity of the rock for two specific distances between the hole and the fracture: 2.5 and 25 m. The fracture was assumed to be currently saturated with water with a pressure of 5 MPa, corresponding to the conditions at 500 m depth.

The clay was assumed to be the often used Wyoming bentonite MX-80. Its initial dry density was defined with respect to an assumed loss of 5 % of the solid clay mass by erosion in the emplacement phase, i.e. 1590 kg/m³ (2000 kg/m³ after water saturation).

The following initial conditions of the clay were assumed:

- void ratio $e=0.78$ (porosity 56%)
- initial degree of saturation $S_r=21\%$
- initial pore water pressure $u=-150$ MPa (derived from the retention curve)

The following initial conditions of the rock were assumed:

- void ratio $e=0.00311$ (porosity 99.69%)
- initial degree of saturation $S_r=100\%$

The FEM calculations were made by using the code ABAQUS and an axial-symmetric element mesh. Only radial hydraulic and mechanical processes were considered, i.e. water uptake in the clay from the surrounding rock and associated swelling and changes in density of the clay. It was assumed that the clay fills up the hole from start with uniform density and that the only function of the perforated tube is to serve as a filter with a hydraulic conductivity equal to 50 % of that of the clay. The starting conditions were that the initial pore water pressure was $u=0$ kPa in the borehole and $u=5$ MPa water pressure at the rock boundary. In a corresponding field experiment that was part of Sub-project 2, the hole was filled with water from start.

Figure 3-5 shows the time to reach saturation as a function of the hydraulic conductivity of the rock for the two different boundary conditions. According to the model, the influence of the hydraulic conductivity of the rock and of the distance to the concentric water-bearing fracture on the time for saturation is not very important. Thus, for hydraulic conductivities higher than E-12 m/s the clay plug will be water saturated in less than a month. For rock with a conductivity equal to E-13 m/s it will take about 3 months, while for the common conductivity E-10 m/s it will take about 2 weeks.

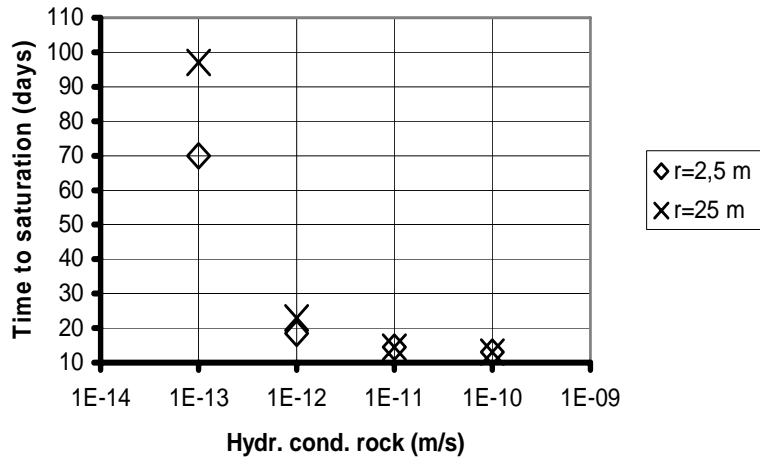


Figure 3-5. Time to full saturation of the clay-plugged borehole as a function of the hydraulic conductivity of the rock at two different boundary distances.

Numerous experiments [2] have shown that the rate of water saturation of a rigidly confined block of smectite clay can be described as a diffusive process with a diffusion coefficient of E-10 to E-9 m²/s. Using the figure 3E-10 m²/s for the coefficient and making the same simplification as in the ABAQUS modelling, i.e. that the clay fills up the hole from start and initially has a uniform density, one finds that complete water saturation of the clay plug will be reached in about the same time as obtained in the ABAQUS calculations for the case of unlimited access to water for hydration of the clay, i.e. the case with a rock conductivity of at least E-12 m/s. Thus, the upper curve in Figure 3-6, representing the conditions after 120 days, shows that the degree of saturation is in the interval 87-100 % for 1D conditions. For the actual axisymmetric case this would correspond to practically complete saturation.

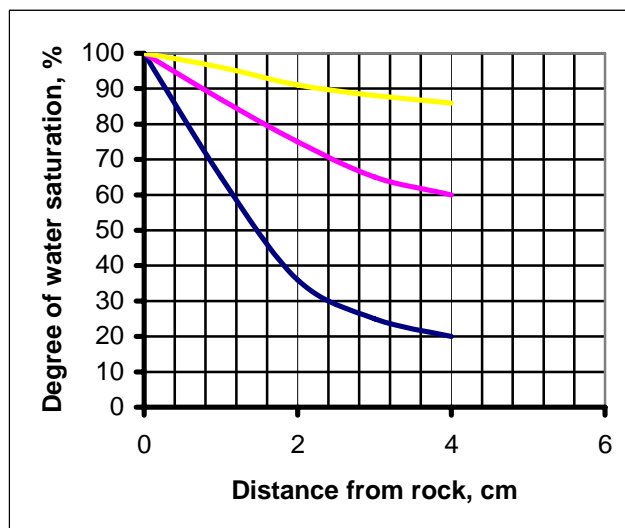


Figure 3-6. Evolution of the degree of saturation of the clay plug assuming electrolyte-poor water and assuming the process to take place by diffusion in 1D for $D=3E-10$ m²/s. Lower curve: 12 days, Central curve: 72 days, Upper curve: 120 days.

As for the ABAQUS study the actual water saturation rate of the clay plug is expected to deviate from the theoretical prediction because of the retarding influence on water migration of the perforated tube and by the transient migration of clay from the dense core through the perforation towards the rock. The internal friction will retard homogenization of the clay and lead to permanent differences in density in outer and central parts of the clay core according to the model, which is being investigated as described later in this chapter.

For the alternative plug types shown in Figure 2-1 the same maturation process applies but the water saturation and homogenization are expected to be faster in the absence of the perforated tube, which retards water migration into the central plug core and migration of clay from the core and outwards.

Water uptake and saturation

For the "Basic" concept a proposed simplified maturation process is shown in Figure 3-7. It implies that water does not primarily enter the hole in the form of uniform radial flow through the rock but through fractures intersecting the hole from which it migrates to and through the clay. The condition for this type of wetting is that a sufficiently high water pressure prevails in the fractures to make them control the hydration of the clay plug, i.e. that water flow through the rock crystal matrix is negligible. This model fits typical clay plug tests performed at Stripa [1].

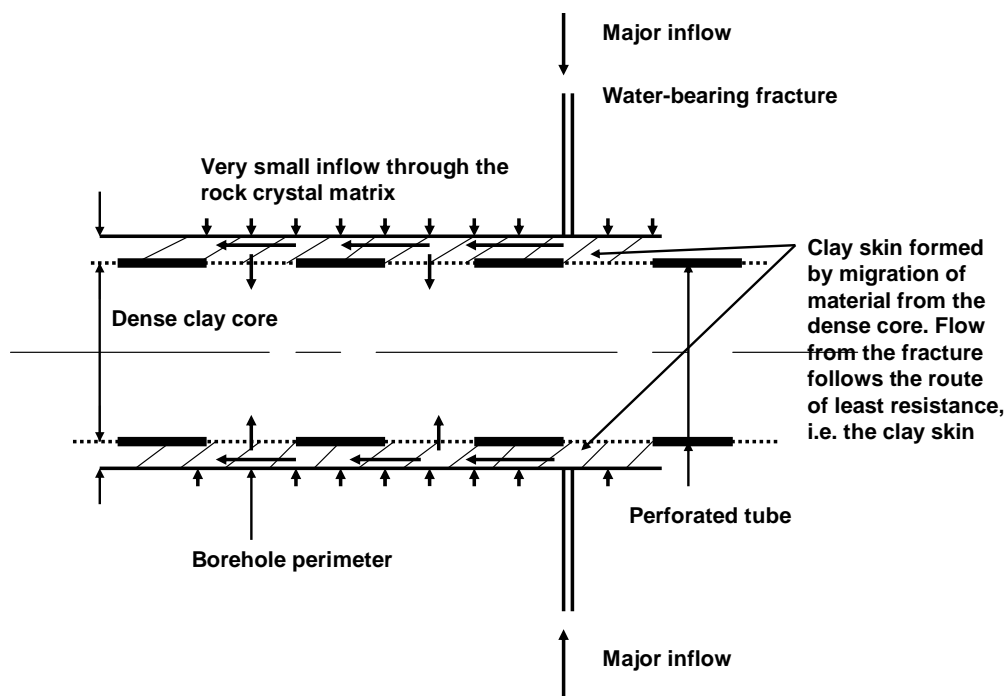


Figure 3-7. Conceptual model of the inflow path of water from water-bearing fracture. Least resistance to the flow is through the clay "skin" around the perforated tube since it is more permeable than the dense clay core for several weeks.

According to the model the supply of water for saturation and maturation of the clay "core" of the basic concept takes place in the initially soft but successively denser clay "skin" that is formed by material moving out through the perforation of the tube.

Figure 3-8 illustrates the first phase of maturation of a plug of "Basic Type". It is characterized by formation of clay columns ("plugs") growing from the dense clay core through the perforation of the tube and forming, in the first phase, an embedment of the tube of different densities. After about 24 hours the clay components in the space between the tube and the rock wall have become relatively homogeneous but it takes weeks and months for them to reach a high degree of homogeneity and a density that approaches that of the successively softening central clay core. From the point of maturation and performance they initially make up a very heterogeneous, soft and permeable "clay skin" that successively becomes denser.

The rate of growth of the clay columns has been investigated in laboratory tests, which have given values of the density of the clay skin in the maturation process.

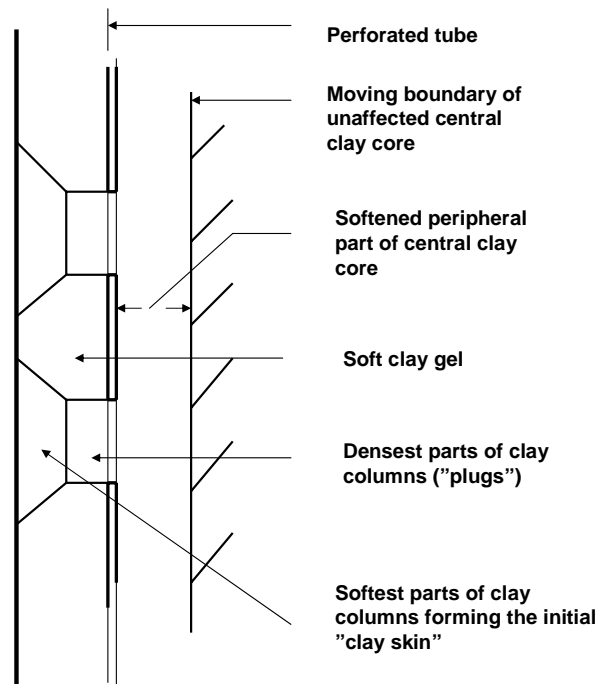


Figure 3-8. Schematic picture of the earliest stage in the maturation of a "Basic" plug.

One can estimate what the hydraulic conditions, particularly the magnitude of the pressure in a fracture intersecting a plugged holes, must be to provide sufficient access to water in the skin zone for not limiting the maturation rate. This can be made by using experimental laboratory data and a simple theoretical model by which one can calculate the suction of water transported from the skin zone into core and comparing it with the rate of axial inflow into the zone from an intersected fracture. The results are compiled in Table 3-1.

Table 3-1. Estimated amount of tap water for unlimited hydration of a freely expanding 2.5 m long clay core as a function of time. Initial dry density 1700 kg/m³. Strength data included. For clay plugs confined by a perforated tube the rate of maturation is at least 50 % lower.

Time, hours	Density of saturated, expanded part, kg/m ³	Amount of sorbed water, litres	Hydraulic conductivity of "skin zone", m/s	Shear strength of "skin zone", m/s
6	1100	10	E-9	50
12	1150	15	5E-10	200
24	1325	33	5E-11	400
48	1400	40	2E-11	550
96	1700	70	E-12	700

For all the plug types the expansion is limited because of the confinement provided by the small-diameter boreholes, meaning that the "clay skin" starts to consolidate rather early under the compressive force exerted by the dense clay columns that move out from the dense core. This means that, in practice, only the amounts of water required for maturation in the first 12 hours are relevant since consolidation will then be the dominant process. One can estimate that about 10 litres need to enter the holes in the first 6 hours and another 5 litres in the subsequent 6 hours for avoiding retardation of the maturation of the clay plugs. For the "Basic" plug even less water is required, i.e. roughly 50 %, in the earliest stage since the formation of a "clay skin" is delayed by the perforation. For a 2.5 m long "Basic" plug, only about 3 litres would hence be needed for formation of the "skin" in the first 6 hours and somewhat more than 2 litres in the subsequent 6 hours.

One can check whether these amounts of water can enter the hole and be adsorbed by the dense clay core for forming the "skin" by using the model in Figure 3-9. It is basically the same that was used for predicting the maturation of the deep hole OL-KR24 (Sub-project 3). In contrast to the simple free expansion case described above, the present model takes geometrical and flow restraints into consideration.

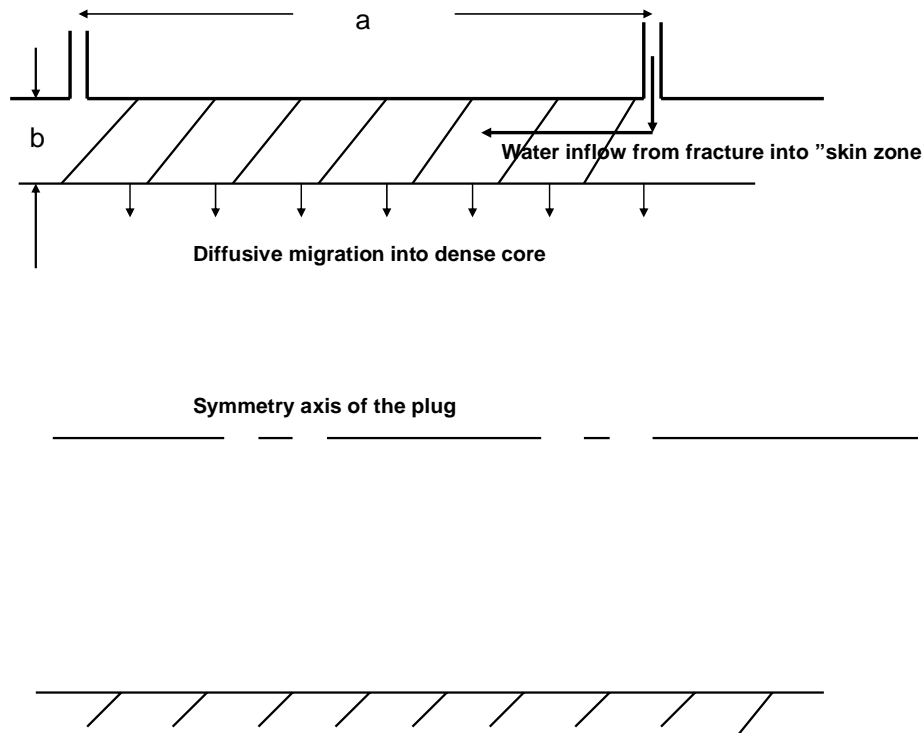


Figure 3-9. Conditions for saturation of the clay core by sorbing water from the skin zone that is supplied with water from intersecting fractures.

The rate of migration of water into the core is assumed to take place by diffusion from the interface of skin and core and can be estimated by use of the ANADIFF code (Figure 3-6). For 12 hours it is estimated that complete hydration of the dense core has taken place to 0.3 cm radial distance from the wet boundary, hence requiring about 5 litres of water for a 2.5 m long clay core. For checking if the plug has access to this amount of water over its entire periphery the issue is to find out whether such inflow can take place and maintain complete water saturation of the gap between rock and perforated tube under prevailing conditions.

Assuming a fracture spacing $a=1$ m, and considering the 0.5 m long element consisting of clay "skin and core" in Figure 3-8, it is realized that water from the fracture needs to be driven into and through the successively formed clay skin by flow, which requires that the hydraulic gradient operating over the 0.5 m length and the average conductivity of the clay skin are sufficiently high to bring water all the way to the mid distance between the two neighbouring fractures. For fulfilling the condition that the flow must be sufficient to feed the dense clay core also at the opposite end of the 0.5 m long element, the flux must hence be about 1/12 litre per hour, i.e. 0.2 litres for the 2.5 m long plug. The cross section area of the "clay skin" is on the order of 10 cm^2 , meaning that the minimum flow rate must be at least 0.6 m per day. Assuming zero water pressure at the inner end of the element and only the fracture pressure as driving force¹, this would, for a pressure of 500 kPa (50 m water head), require a hydraulic

¹ In fact the incompletely saturated core generates a suction of hundreds to thousands of kPa that contributes to the hydraulic gradient, meaning that the estimated minimum conductivity is very conservative.

conductivity K of the skin of $K > 3E-10$ m/s, which is lower than that of MX-80 with a density of about 1100 kg/m^3 , at percolation with low-electrolyte water. For brackish water of Äspö type it would be much more than required. Taking instead the distance of the neighbouring fractures to be 10 m, the minimum conductivity of the skin to serve as required would be roughly $3E-9$ m/s, which would imply insufficient supply of water the clay core at mid distance. One hence finds that the rock structure is of major importance for the maturation rate of the plugs.

Quicker densification of the skin, larger fracture spacing, or lower fracture pressure would delay maturation of the core and make it heterogeneous since only the part of the skin close to the fracture would consequently be fully mature in the early stages. Such delay is exemplified by the field experiments at Stripa [1] in which short holes extending from a drift were equipped with clay plugs of "Basic" type 1.

Piping resistance

If there are differences in water pressure along a plugged borehole, which will be the case in holes extending from tunnels or shafts where the water pressure will be low until the repository is backfilled, the plugs will be exposed to a pressure gradient that can cause piping before the clay has matured sufficiently. Tests were made in the laboratory of Clay Technology AB for investigating the sensitivity to such degradation by using the equipment shown in Figure 3-10. The tests were performed as follows:

- The tube representing a borehole was filled with tap water and the plug inserted.
- A water pressure of 500 kPa was applied for supplying the plug with water in the maturation process. This pressure was on the same order as at the test site at Äspö where plugs of the same type were tested with respect to the adhesion to the borehole walls (Sub-project 2).
- After rest for maturation under a uniform water pressure of 500 kPa, a step-wise increased water pressure was applied at one end of the plug-confining tube while the opposite end was pressure-free and connected to a pipe for measuring water flow through the plug. The pressure was increased until through-flow was initiated. When permeation took place the pressure was immediately reduced to zero after which both ends of the tube were pressurized to 500 kPa for continued maturation of the clay. The critical pressure represents the piping resistance.
- After further rest, a pressure gradient was again established for determining if self-healing can repair structural defects generated by piping. Repeated pressurizing after periods of rest was expected to show the influence of time on the critical pressure for piping.
- When the piping resistance was finally sufficient to resist the maximum water pressure that could be applied with the available GDS equipment [2], which was used for controlling the pressure and for measuring the flow, the plug was extruded by use of a hydraulic jack with 60 MPa capacity. This gave the adhesive strength of the plug, i.e. the shear strength of the clay/steel contact that could then be compared to that determined in the field experiment (Sub-project 2).
- The extruded plug was dismantled and samples taken for determining the density and water content of the clay in three evenly distributed sections.

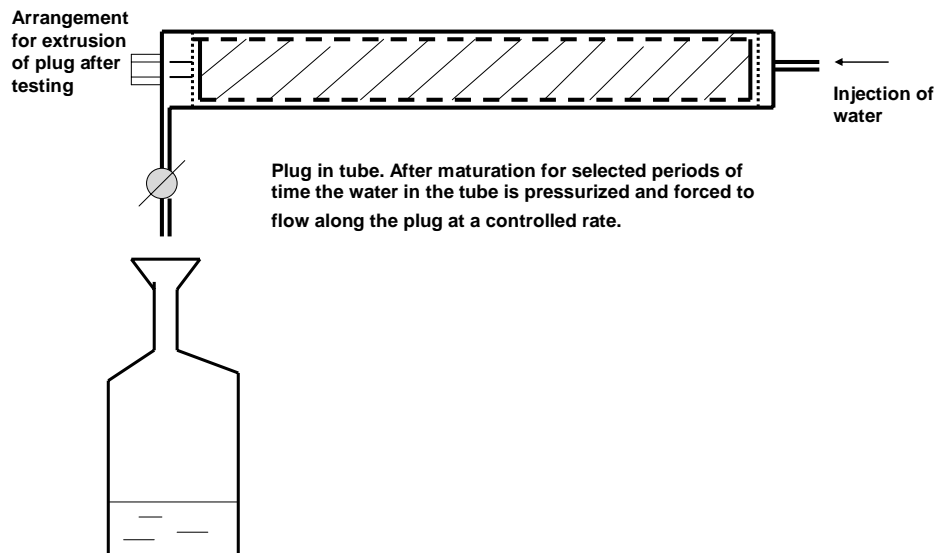


Figure 3-10. Laboratory equipment for determining the critical pressure for generating piping (Livinstone). The plug is placed in the tube, which is filled with water that is successively pressurized at one end for determining the critical pressure for "piping".

The outcome of the tests can be summarized as follows [Appendix III]:

- After 8 hours of maturation under 500 kPa uniform water pressure the critical pressure for piping was 700 kPa.
- After another 11.5 hours under 500 kPa uniform water pressure the critical pressure for piping was 900 kPa.
- After another 22 hours under 500 kPa uniform water pressure, the critical pressure for piping was 1700 kPa.
- Immediately after the last piping test extrusion of the plug was started. The plug began to be displaced but could not be extruded at the maximum capacity of the hydraulic jack, 7 tons, possibly because of deformation and locking of the perforated tube in the confining bigger tube. It is estimated that the adhesion strength was 80 to 100 kPa. Considering the fact that the test arrangement represented 5 m distance between neighbouring fractures and hence a considerable delay in maturation, the deviation from what the model predicts (550 kPa for an unshielded 2.5 m long plug, or approximately 275 kPa for a "Basic" plug) is explained (cf. Table 3-1).
- The extruded plug had a homogeneous appearance except for some small, local heterogeneities (Figure 3-11).
- Samples of the clay located outside the perforated tube had a density and water content of 105 % at 0.5 m distance from the pressurized end, 94 % at 1.25 m distance and 93 % at 2 m distance from this end. The clay core inside the tube had a density that was unchanged from the initial state.

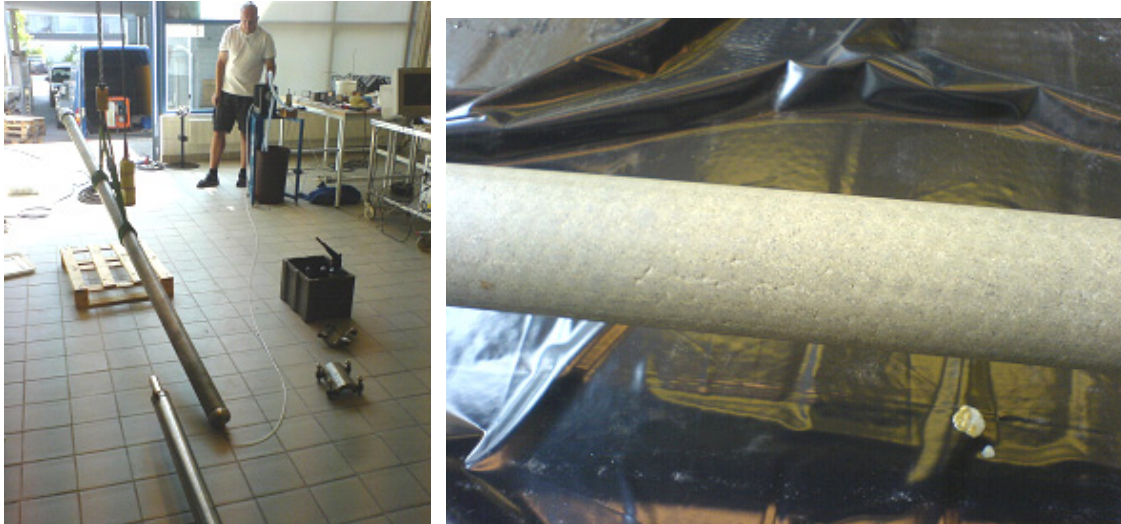


Figure 3-11. Left: The steel tube with the plug being exposed to a water pressure at the lower end. Right: Appearance of "Basic" plug extruded after 3 weeks of maturation under 500 kPa uniform water pressure.

Practical function of the clay plug of "Basic" type

The following major conclusions from the various test series were drawn:

- After 4 hours in low-electrolyte water, clay from plugs of MX-80 penetrates the perforation but will not form a homogeneous paste around the tube (Figure 3-12), while after 8 hours such a paste is formed.
- The clay paste formed around the perforated tube will cause resistance to insertion of clay plugs in boreholes, which must therefore be made within a limited period of time. In saline water the clay plug must be placed within one hour, while in electrolyte-poor water the corresponding time is 5-10 hours.
- For avoiding very rapid expansion and erosion of the clay gel formed early in the space between tube and rock the water in the borehole must be poor in electrolytes. In practice, this means that the natural water should be replaced by tap water.
- After a few weeks the clay between the tube and the rock becomes dense and after several months the entire clay mass tends to become homogeneous and sufficiently dense for providing the required tightness. Complete homogeneity may require years or decades and it may in fact never be reached.
- The long term tests show that nearly complete swelling and homogenisation are obtained after 10-20 days. The measured mean swelling pressure against the rock for the initial dry density 1905 kg/m^3 of the clay plug core was 2800 kPa using fresh water and 600 kPa for saline water. Measurement of the hydraulic conductivity of the clay paste between tube and rock showed that it was lower than $9\text{E-}13 \text{ m/s}$ for fresh water and $2\text{E-}12 \text{ m/s}$ for saline water.
- Only clays with Na as major adsorbed cation should be used since Ca-saturated expansive clays behave like clay in salt water.
- For very strongly compacted MX-80 powder (compressed under more than 250 MPa) the clay is expected to migrate slower through perforation than ordinarily compacted clay.



Figure 3-12. Growth of soft clay through the perforation of a copper tube confining a dense MX-80 clay core in an 80 mm diameter oedometer. Appearance at removal of the lid 8 hours after start. The larger part of the core is still unaffected by water.

3.3 Performance in situ

3.3.1 Practical design issues

Plugs of "Basic" type are suitably made by coupling 2-5 m long units to 10-25 m long segments using drilling rigs that have enough lifting capacity to hoist and lower them. Their maximum length with clay contained in the tubes is determined by the tensile strength of the metal tubes applying a safety factor of 3, which suggests that a practical length of coupled plug segments is about 25 m. Shorter lengths are required if the curvature of the borehole leads to contact between the ends of the plug segments and the borehole walls. For plugging the borehole OL-KR24 the units consisted of 4 units forming a 10 m long segment (Sub-project 3).

The following major conclusions are drawn from the various investigations:

- The tensile strength of the perforated tubes determines the maximum length of the plug segments.
- Copper, Navy Bronze, steel, and titanium have been considered and deemed possible as tube metal.
- A practical solution for use of copper tubes implies 24 m long segments consisting of jointed 3 m long parts. The tensile strength is sufficient, assuming 4-fold safety and that safe attachment to the drill string can be achieved. The thickness of the tube wall will be 2-3 mm and the outer diameter about 6 mm smaller than the diameter of the hole.
- Each 24 m segment is lowered into the desired position, i.e. in the space between two stabilized fracture zones, and left there. Several segments will be placed in series without coupling them together. Their weight guarantees that they will rest on the underlying ones without moving in the axial direction.
- Before a clay plug segment is emplaced a previously cast quartz/cement plug must have hardened sufficiently to be able to carry it. With a suitable concrete recipe this shall be possible in one day.

3.3.2 Erodability

Tests simulating the impact of water flowing along clay plugs in the installation of a clay plug have been made by Clay Technology AB using the equipment in Figure 3-13. In tests with clay components having a water content of 6 % and a density of 2050 kg/m³, water was flushed along the plug with a rate of 0.92 l/min for about one hour, corresponding to insertion of a plug down to 500 m depth. The effect of the erosion was evaluated by measuring the clay content in the percolate and by determining the dry density of the clay contained in the tube at the end of the experiment. The results showed that 6 to 9 % of the solid clay had been eroded, which would reduce the initial dry density to about 1800 kg/m³, corresponding to an average density of the fluid-saturated plug of 2130 kg/m³.

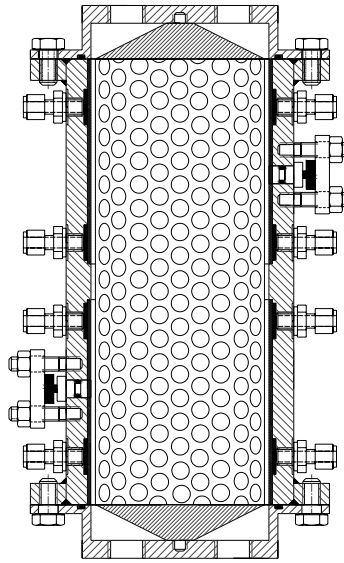


Figure 3-13. Schematic cross section of the equipment used by Clay Technology AB for the flow tests. Water was forced into the space formed by the cone at one end, flowed along the perforated tube and was discharged through the opposite end.

Although the loss of clay by erosion in the plug placement phase is moderate in boreholes with 500-1000 m depth, less erosion is asked for and various ways to achieve this were considered:

- tight fitting of the clay blocks in the perforated tubes for eliminating water flow along the inside of the tubes.
- skew drilling of the perforation holes so that water flowing along the outside of the tubes is diverted off from the tube.
- increased density of the clay blocks.

The first and third methods were used in additional series of experiments using the equipment in Figures 3-13. The high density of the blocks used in the experiments in Sub-project 1 was obtained by compacting MX-80 powder that had low water content (6 %) under a pressure of 250 MPa (Figure 3-14). A suitable grain size distribution of the clay powder was found to be 20 % 2-8 mm, 20.4 %, 1-2 mm, 42.4 % 0.1-1 mm, 17.2 % <0.1 mm.

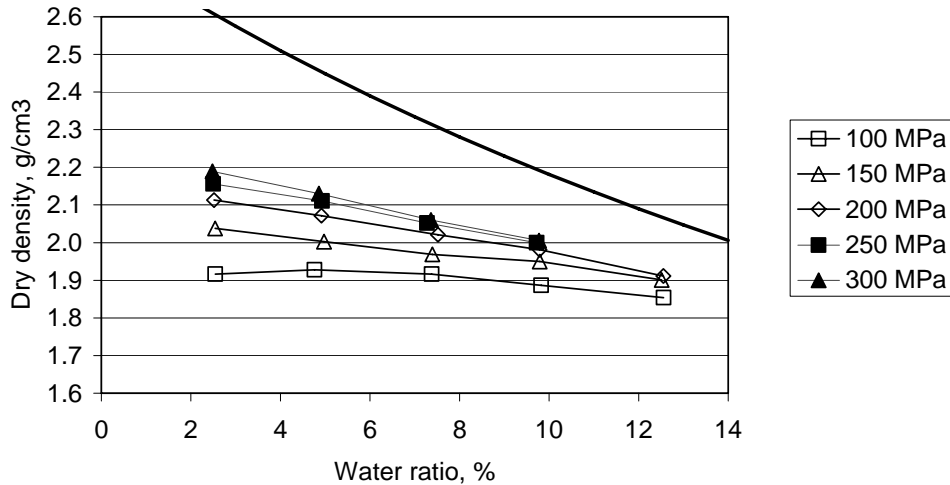


Figure 3-14. Dry densities obtained by compacting MX-80 clay powder with different water contents by using compaction pressures of 100 to 300 MPa (Clay Technology AB).

All the data from the laboratory tests, specifying the various geometries and clay properties, are compiled in Table 3-2, from which one finds that loss of solid clay material can be reduced to 4-5 % in plugging a 1000 m deep hole if the process takes less than 3 hours and the clay blocks are prepared by compacting MX-80 powder with 6 % water content under 200 MPa pressure. The experiments were performed by Clay Technology AB using the following constellations:

- Steel cells simulating the hole in the rock, inner diameter 100 mm.
- Perforated copper tube with outer diameter 95 mm and inner 88 mm. Perforation ratio 50 % with 10 mm hole diameter.
- MX-80 clay with 9.4 % water content, block pressure up to 100 MPa.
- Bentonite blocks, diameter 87 mm and height 50 mm.
- Dry density of blocks 1692 and 1905 kg/m³.

Table 3-2. Summary of test data and results from erosion experiments.

Test	Arrangement	Duration , hours	Sample length, mm	D Borehole, mm	D Tube mm	D Tube mm	Borehole depth m	Flow l/sec	Loss of clay ¹⁾	Loss of clay ²⁾
1	1 mm gap between clay and tube	1	250	100	95	88	500	0.92	8.1	5.1
2	Contact clay and tube	1	250	80	76.1	72.1	500	0.67	6.8	4.9
3	Expanden clay by 20 h exposure to water	1	250	80	76.1	72.1	500	0.67	5.7	9.4
4	Clay comp. At 200 MPa with w 6%	1	250	80	76.1	72.1	500	0.73	7.9	8.3
5	Clay comp. At 200 MPa with w 6%	1	3000	80	76.1	72.1	500	0.71	6.3	7.3
6	Clay comp. At 200 MPa with w 6%	2	3000	80	76.1	72.1	1000	0.71	15.7	15.8
7	Clay comp. At 200 MPa with w 6%	1	3000	80	76.1	72.1	500	0.70	7.6	9.2
8	Clay comp. At 200 MPa with w 6%	3	3000	80	76.1	72.1	1000	0.42	3.9	4.9
9	Clay comp. At 200 MPa with w 6%, mechanical erosion	3	3000	80	76.1	72.1	1000	0.42	10.9	10.4

1) weight loss of clay core, 2) determined by drying the suspension.

One finds that the data from sampling of the clay cores and of the percolate agree in principle and that 6-10 % of the clay is expected to be eroded when plugs of "Basic" type are moved to the bottom of 500 to 1000 m deep holes if plug rotation does not take place. If the plugs rotate, which may happen in practice, the erosion is stronger and up to 15 % may be sheared off and disintegrated at 1000 m depth.

It is concluded that quick insertion of the plugs will enhance erosion and that a suitable time interval for bringing a clay plug down to 1000 m depth is 3-8 hours. More than 8 hours is expected to initiate adhesion of the clay to the rock and cause resistance to the placement.

The lowest net density of the clay will be found at the lower end of plugs in 1000 m deep holes, i.e. 1900 kg/m³. The corresponding hydraulic conductivity and swelling pressure in saline groundwater are E-12 m/s, and 1.5 MPa, respectively. Plugs placed down to 500 m depth, corresponding to the repository level, will undergo less erosion and are estimated to have an average density of 2000 kg/m³.

3.3.3 Manufacturing

A practical and rational way of manufacturing perforated tubes with high degree of precision was developed by Livinstone AB (Figure 3-15). By this technique punching of the perforation holes could be made with great precision on a semi-industrial scale.

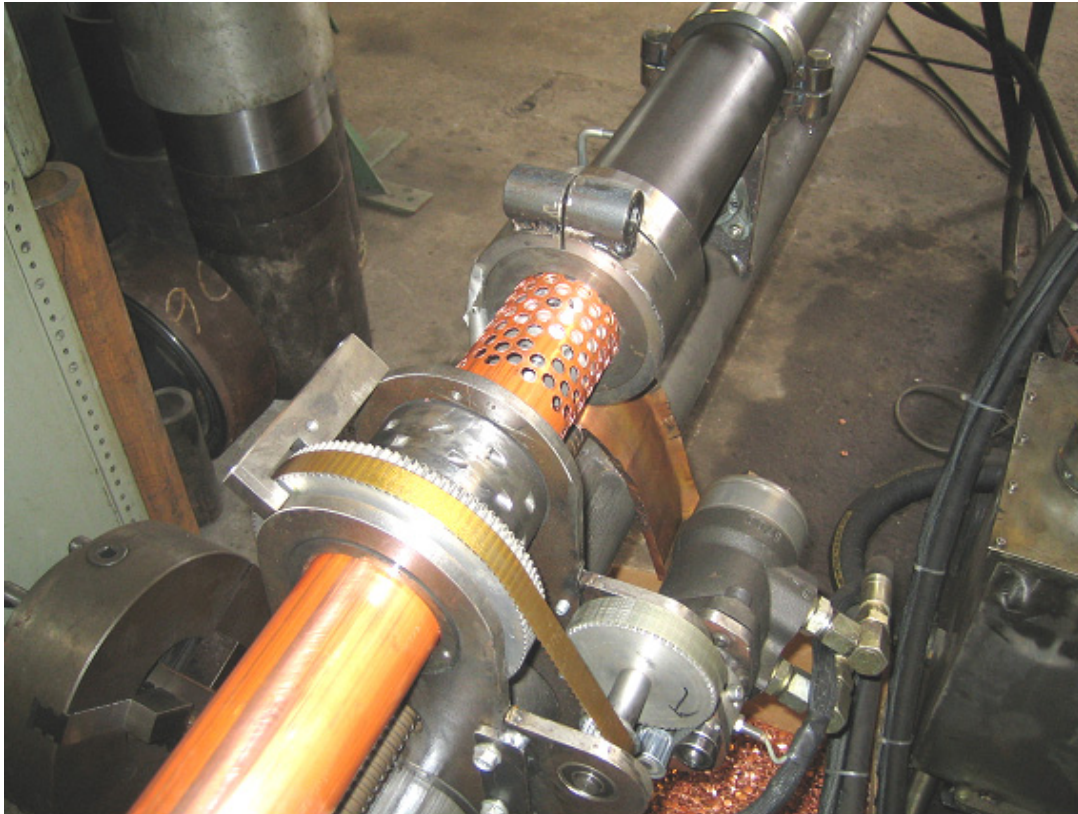


Figure 3-15. Copper tube being perforated in a lath (Liwinstone).

3.3.4 Equipment for placement

For placement of long plugs the following steps are taken:

- The plug is divided in segments with lengths that are adapted to the geometry of the holes (curvature etc)
- The plug segments are connected while being hung in a drill rig, which must provide pushing and pulling forces that can be required.

4 The "Container" concept

4.1 Design

The *Container* concept was proposed by Lars Liiv in the preparation of the borehole plugging project for eliminating the need for inserting the plug in a limited period of time. The bearing idea is to keep the plug segment confined and isolated from the water in the borehole until it reaches its predetermined position. The only difficulties that one can possibly foresee is to make the cylindrical container with highly compacted clay blocks thin enough to give the ultimately matured clay the required density, and to make strong enough. The container will be exposed to a uniform water pressure of 10 MPa in a 1 km deep hole and has to resist this pressure and be perfectly tight, which determines the thickness of the container wall. Figure 4-1 illustrates the design.

Cement/Bentonit container

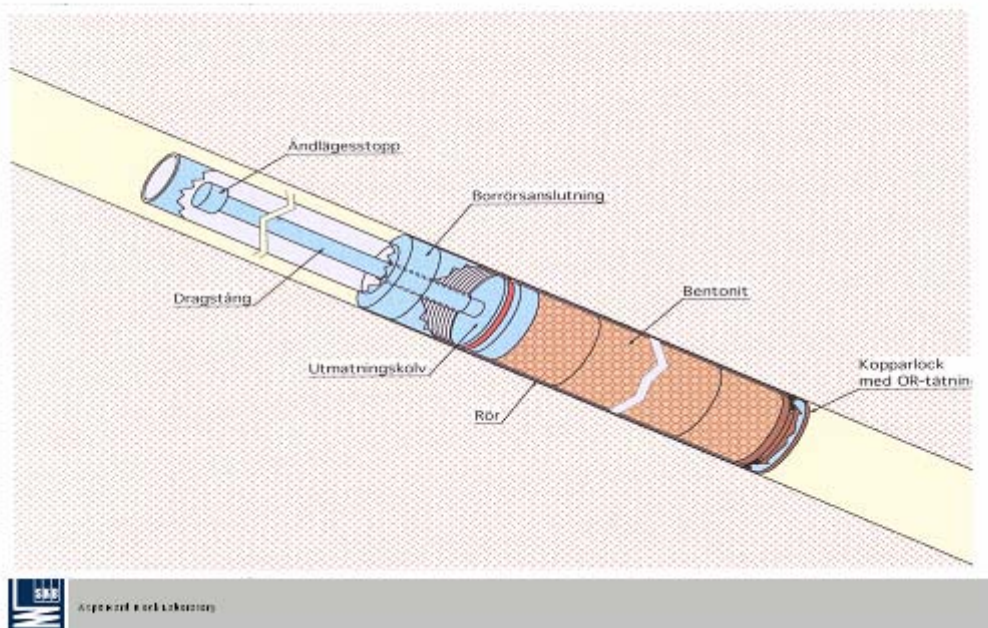


Figure 4-1. The "Container" plug.

4.1.1 Materials and dimensions

The container tube is only used in the plug installation phase and needs to remain tight and mechanically stable for which stainless steel is used. No detailed design with respect to wall thickness and other geometrical features has been made so far.

In the presently described tests the dry density of the 72 mm diameter blocks were 1700 kg/m³ yielding a net total density of 1950 kg/m³ of the ultimately matured clay in holes with 80 mm diameter. The high density was obtained by compacting MX-80 powder that had low water content (6 %) under a pressure of 250 MPa.

4.2 Maturation - processes and predictions

4.2.1 Unlimited access to water in fractured rock

Like for the "Basic" plug the potential of the surrounding rock to provide the clay plug with water determines the maturation rate and we will again consider the earlier mentioned conditions of water being available without limitation at the plug/rock contact, and of water entering from discrete fractures.

The same conditions prevail as for the "Basic" concept and the maturation rate can be estimated in the same way for both. The difference is that the maturation of the "Container plug" is considerably quicker than the plug of "Basic" type because it is exposed to water over its entire surface. Clay particle aggregates become dispersed in conjunction with extruding the clay blocks from the container and the process of gel formation and consolidation proceeds without hindrance. It is estimated that an appreciable density, at least about 1400 kg/m^3 (cf. Table 3-1), and high degree of homogeneity of the shallow part of the plug is reached in a few days. The "Container" plug can not be retrieved (in "one piece", but is easily removed by redrilling).

4.2.2 Limited access to water in rock with few fractures

The same model as for the "Basic" type can be used for predicting the maturation and performance of the clay block column extruded from the container cylinder. Thus, the initially released clay aggregates from the exposed surface of the clay blocks quickly produce a very heterogeneous, soft and permeable "clay skin" that successively becomes denser by being consolidated by the expanding dense blocks.

Applying the data in Table 3-1 and disregarding from the retarding effect of the perforation of the "Basic" plug one can estimate that 6 litres would be needed for formation of the "skin" in the first 6 hours and about 5 litres in the subsequent 6 hours. Using again the simple model in Figure 3-9 one concludes that the hydraulic conductivity of the "skin" should be roughly twice as high as the value required for the "Basic" plug, i.e. nearly $E-9 \text{ m/s}$ for 1 m distance between neighbouring water-bearing fractures that intersect the hole. This is on the same order of magnitude as the expected conductivity of the skin, implying that water will be available for undisturbed saturation of the plug.

Like for the "Basic" plug, quicker densification of the skin, larger fracture spacing, or lower fracture pressure would delay maturation of the core and make it heterogeneous since only the part of the skin close to a fracture would fully mature in the early stages.

Piping resistance

The same conditions prevail as for "Basic" plugs and the same type of laboratory experiment with a 2.5 m long "Container" plug has been performed. The following steps were taken:

- The tube with 80 mm inner diameter representing a borehole was filled with tap water and the plug inserted in it. Since the tight container was not yet available the blocks that were intended to be placed in it were assembled manually.
- A water pressure of 500 kPa was applied for supplying the plug with water in the maturation process. This pressure was on the same order as at the test site at Äspö where plugs of the same type were tested with respect to the adhesion to the borehole walls (Sub-project 2).

- After rest for maturation under a uniform water pressure of 500 kPa, a step-wise increased water pressure was applied at one end of the plug-confining tube while the opposite end was pressure-free and connected to a pipe for measuring water flow through the plug. The pressure was increased until through-flow was initiated. When this took place the pressure was immediately reduced to zero after which both ends of the tube were pressurized to 500 kPa for continued maturation of the clay. The critical pressure represents the piping resistance.
- After further rest under 500 kPa uniform pressure, a pressure gradient was again established for determining the critical pressure for piping as a function of time. Repeated pressurizing after periods of rest was expected to show the influence of self-sealing on the critical pressure for piping.
- When the piping resistance was finally sufficient to resist the maximum water pressure that could be applied with the available GDS equipment [2], by which the pressure was controlled and the flow measured, the plug was extruded by use of a hydraulic jack with 60 MPa capacity. This gave the adhesive strength of the plug, i.e. the shear strength of the clay/steel contact that could then be compared to that determined in the field experiment (Sub-project 2).

The outcome of the tests, which are fully reported in Appendix III, can be summarized as follows:

- After 6 hours of maturation under 500 kPa uniform water pressure the critical pressure for piping was 1700 kPa.
- After another 18 hours of rest under 500 kPa uniform water pressure the critical pressure for piping was 1800 kPa. Water did not penetrate the plug and the sudden inflow of pressurized water was concluded to be caused by local displacement of the softest parts of the "skin". They were successively consolidated and tightened to let no water through.
- The plug could not be extruded for the highest available force of 7 tons, meaning that the adhesion (shear) strength exceeded 115 kPa. Considering the fact that the test arrangement represented 5 m distance between neighbouring fractures and hence a considerable delay in maturation, the deviation from what the model predicts i.e. 550 kPa for a 2.5 m long plug after 2 days (cf. Table 3-1), means that the shear strength may have been far higher than 115 kPa.

Practical function of the clay plug of "Container" type

The following major conclusions from the various test series were drawn:

- The quicker maturation of the "Container" than of the "Basic" type that the model of maturation predicts is verified.
- A beneficial property of the "Container" concept is that the clay component is not exposed to water and hence not to erosion in the placement phase. After releasing it at the desired depth it is momentarily exposed to high water pressure causing dispersion and formation of an initially soft "skin" that consolidates under the pressure exerted by the expanding dense core. In contrast to the "Basic" concept there is, in principle, no need to replace the original saline water from the hole to be plugged but this is still recommended for avoiding sedimentation of the large aggregates that result from the dispersion since this would cause variations in density of the ultimately matured plug.

- After a couple of days the most shallow part of the clay plug becomes dense and able to resist piping and after several months the entire clay mass will tend to become homogeneous and sufficiently dense for providing the required tightness. Complete homogeneity may require years or decades and it may in fact never be reached.
- Only clays with Na as major adsorbed cation should be used since Ca-saturated expansive clays behave like clay in saline water.

4.3 Performance in situ

4.3.1 Practical design issues

The following practical issues need to be considered:

- The tightness of the container tube is a fundamental requirement since leakage of water into it will make the clay blocks expand and become stuck in the tube.
- Plugs of "Container" type can be made in segments that are 2-5 m long but even longer units can be prepared and placed at depths of 1000 m or more. In practice, the length is determined by the curvature of the borehole since too long plug segments may imply contact of the ends of the container tube with the borehole walls.
- For reaching a high net density of the plug the fitting between the tube and the clay blocks must be good, which means that the risk of deformation of the tube by being squeezed in the borehole or by hitting irregularities in the borehole wall must be minimized. This requires that the tube is sufficiently strong, which in turn requires a wall thickness that may significantly reduce the net density of the ultimately matured clay plug.
- Before a plug is emplaced previously cast quartz/cement plug must have hardened sufficiently much to be able to carry it. With a suitable concrete recipe this is a matter of one day.

4.3.2 Erodability

There will be no erosion of the clay.

4.3.3 Manufacturing

Manufacturing of compacted clay blocks is a standard procedure but for reaching the desired high density the need for preparing clay granulate with suitable water content that can be compressed to very dense blocks must be considered.

4.3.4 Equipment for placement

The equipment for bringing down clay blocks, i.e. the container tube and the accessories for submerging it with sufficient accuracy respecting location and interaction with the borehole walls, as well as for releasing the blocks are not commercially available. Those used in pilot tests have been developed by Lars Liiv.

5 The "Couronne" concept

5.1 Design

The "Couronne" concept was proposed a few decades ago and has been used in at least one case [1]. The bearing idea is to use a plug that consists of a central rod around which tightly fitting annular clay blocks are stacked (Figure 5-1). Submerging the plug in a water-filled hole will instantly cause dispersion as in the "Container" case and erosion will be substantial if the plug is brought down in deep holes. Delay caused by jointing plug units to form a continuous plug will cause intermittently increased dispersion and contribute to make the finally matured plug heterogeneous. One therefore may have to restrict the use of this plugging technique to holes with a depth of up to 100 m. Shorter holes, i.e. with a length of a few tens of meters can be drained so that the plug can be placed under dry conditions.

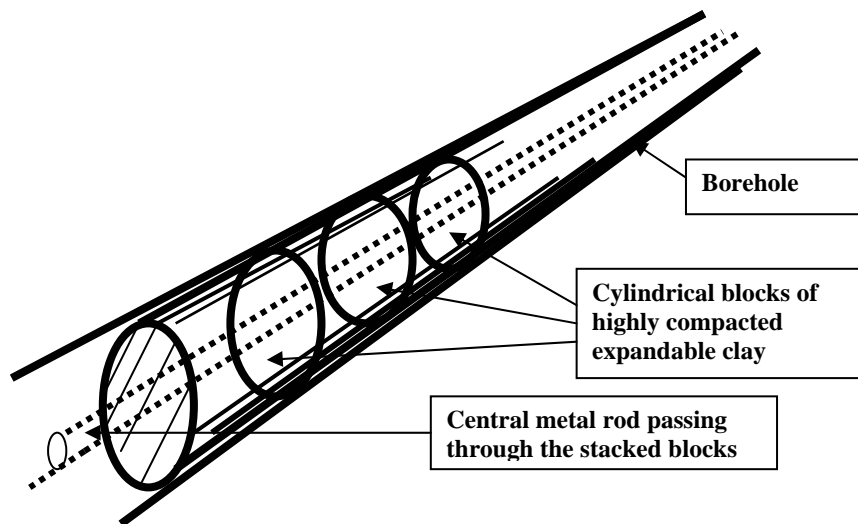


Figure 5-1. The "Couronne" plug.

5.1.1 Materials and dimensions

The central rod is left in position and hence needs to be made of a metal that is compatible with the clay, for which copper is proposed to be most suitable. No detailed design with respect to wall thickness and other geometrical features has been made so far.

In the presently described tests the dry density of the 72 mm diameter blocks was 1700 kg/m^3 yielding a net total density of 1950 kg/m^3 of the ultimately matured clay in holes with 80 mm diameter. The high density was obtained by compacting MX-80 powder that had low water content (6 %) under a pressure of 250 MPa.

5.2 Maturation - processes and predictions

5.2.1 General

Like for the other plug concepts the potential of the surrounding rock to provide the clay plug with water determines the maturation rate and we will again consider the earlier mentioned conditions of water being available without limitation at the plug/rock contact, and of water entering from discrete fractures.

The conditions for the "Couronne" plug to mature are, in principle, the same as for the "Container" plug except that, in water-filled holes, the clay starts to hydrate already in the placement phase. In holes that have been drained prior to the placement of the plug the conditions and processes after inserting the plug and filling the hole with water are exactly the same as for the "Container" plug. For the relatively short holes that can be sealed with "Couronne" plugs the difference in performance between the two conditions is not believed to be of practical importance and one can therefore estimate the maturing process to be the same as for the "Container" plug. Thus, an appreciable density, at least about 1400 kg/m³ (cf. Table 3-1) and high degree of homogeneity of the shallow part of the plug is reached in a few days. The "Couronne" plug can be retrieved only within the first few hours after emplacement.

Later stages of maturation develop as a function of the ability of the surrounding rock to give off water and we will consider the case of limited access to water as a common case for the conditions where this concept may be applied, i.e. holes extending a few tens of meters from the tunnels and shafts.

5.2.2 Limited access to water in rock with few fractures

The same model as for the "Container" type can be used for predicting the maturation and performance of the clay block column. Thus, the initially released clay aggregates from the exposed surface of the clay blocks quickly produce a very heterogeneous, soft and permeable "clay skin" that successively becomes denser by being consolidated by the expanding dense blocks. There is a difference between the two concepts, however, in that the central rod of "Couronne" plugs implies less clay and hence a lower ultimate density, which is at least partly compensated by the larger outer diameter of the clay blocks.

Disregarding from this effect one concludes that sufficient water will be available for undisturbed saturation of the plug if it is located in rock with normal structure and a groundwater pressure of at least 500 kPa.

Piping resistance

The same conditions prevail as for "Basic" and "Container" plugs and the performance is expected to be the same as for the "Container" plug. No test for determining the piping resistance was therefore made in the laboratory. However, the field experiments performed in Sub-project 2 comprised such a study and it confirmed this expectation.

Practical function of the clay plug of "Coroune" type

The following major conclusions from the various considerations were drawn:

- The "Couronne" plug should mature quicker than the "Basic" and "Container" plugs.
- Submerging the plug in a water-filled hole will instantly cause dispersion and erosion will be substantial if the plug is brought down in deep, water-filled holes. Delay caused by jointing plug units to form a continuous plug will cause intermittently increased dispersion and contribute to make the finally matured plug heterogeneous.
- This plugging technique should be confined to holes with a depth of up to 100 m. Shorter holes, i.e. with a length of a few tens of meters can be drained so that the plug can be placed under dry conditions.
- As for the "Basic" concept it is required to replace the original saline water in the hole to be plugged by tap water for minimizing sedimentation of the large aggregates that result from the dispersion since this would cause variations in density of the ultimately matured plug.
- After a couple of days the most shallow part of the clay plug becomes dense and able to resist piping and after several months the entire clay mass will tend to become homogeneous and sufficiently dense for providing the required tightness. Complete homogeneity may require years or decades and it may in fact never be reached.
- Only clays with Na as major adsorbed cation should be used since Ca-saturated expansive clays behave like clay in saline water.

5.3 Performance in situ

5.3.1 Practical design issues

The following practical issues need to be considered:

- The roughness of the borehole wall may cause abrasion of the clay block columns and heterogeneities and variations in density of the ultimately matured plug. Holes with rock fall should be stabilized and re-bored before "Couronne" plugs are emplaced. If the sealing potential of the plugs are not deemed to be high, pellets can be a suitable alternative method and if effective sealing is required the "Basic" or "Container" types are recommended.
- Plugs of "Couronne" type can be made in segments that are 2-5 m long and jointed together for creating a continuous, successively emplaced plug. The recommended length of a completed plug is estimated to be a few tens of meters.
- For reaching a high net density of the plug the fitting between the central rod and the clay blocks must be very good, and that the clearance between the borehole wall and the clay blocks must be at minimum, i.e. a couple of millimeters for very short holes and 3-4 mm for long ones.
- Before a plug is emplaced supporting quartz/cement that may have been cast in the holes must have hardened sufficiently much to stay rigid. With a suitable concrete recipe this occurs in one day.

5.4 Erodability

Emplacement of "Couronne" plugs involves strong erosion but since the length of the plugs is rather small the loss of clay will not be of practical significance.

5.5 Manufacturing

The plug components consist of a central rod, which has to have a bottom plate for the clay annuli to rest on, and the clay blocks. Manufacturing of compacted clay blocks is a standard procedure but for reaching the desired high density the need for preparing clay granulate with suitable water content that can be compressed to very dense blocks must be considered.

5.6 Equipment for placement

The equipment for bringing down the plug are a crane or hydraulic jack for placement in upward-directed holes and they are commercially available and operated by ordinary construction companies.

A small cone is required for placing the plug segments that should have suitable length. For subhorizontal holes a hydraulic jack anchored to the rock is required for pushing them in.

6 The "Pellet" concept

6.1 Design

Pellets have been used for borehole sealing in different contexts. Thus, NAGRA has conducted several experiments in downwards and upwards oriented boreholes [2] and oil companies like Texas/Chevron in the US have made experiments with rather large pellets and with mixtures of pellets of two sizes for sealing of abandoned oil and gas production holes. There does not seem to be any problems with placing them, blowing is reported to give the highest densities while dropping pellets in steeply oriented holes gives moderate and somewhat varying densities [1]. A matter of significance is whether the ultimate dry density of the pellet plug needs to be as high as specified for fulfilling the criterion that the hydraulic conductivity must be lower than that of the surrounding rock, i.e. on the order of 2000 kg/m^3 , corresponding to a dry density of 1590 kg/m^3 . None of the experiments referred to in the literature gave densities of this magnitude for which it is believed that a combination of load and vibration is required.

In practice, it seems that the pellet plugging technique is suitable for sealing holes with a length of up to about 20 m, with a further requirement that it should be used where the sealing function is not very critical, i.e. not in holes extending from deposition tunnels and definitely not in the near-field of canisters.

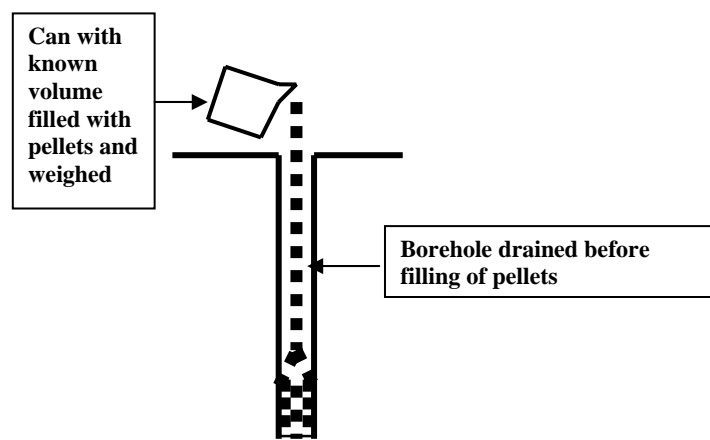


Figure 6-1. The "Pellet" concept.

6.2 Materials and dimensions

The pellets can be of tablet form or crushed blocks of highly compacted expandable clay material like MX-80. Experiments have shown that a very slightly compacted fill of pillow-shaped pellets with a large diameter of about 15 mm gets a dry density of about 1400 kg/m^3 (1900 kg/m^3 at complete water saturation with distilled water), yielding a swelling pressure of 1260 kPa, which is typical of MX-80 clay with this density. Figure 6-2 illustrates the very heterogeneous character of the fill.



Figure 6-2. Appearance of pellets filled in an oedometer with 30 mm diameter.

6.3 Maturation - processes and predictions

6.3.1 Microstructural evolution

Figure 6-3 illustrates schematically the maturation process that applies to any artificially prepared smectitic clay, showing that the grains, which contain large numbers of smectite particles, expand on hydration and release aggregates that rearrange to form soft gels that consolidate under the pressure exerted by the expanding grains. In clays with high bulk density the ultimate variation in density on the microstructural scale will not be very significant while it will be so for the rather low bulk density of a pellet fill. This means that "Pellet" plugs contain numerous continuous, rather permeable flow paths, and that they are compressible.

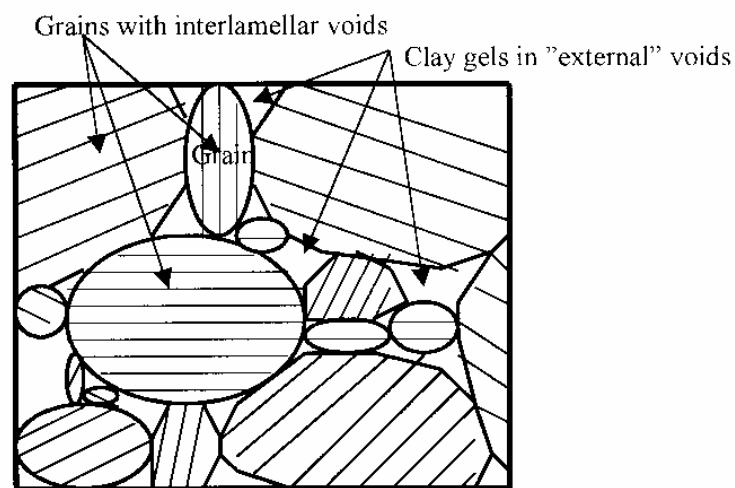


Figure 6-3. Schematic picture of the microstructural constitution. The grains are confined and take up water from the boundaries by which they expand and give off clay particles that form gels in the voids between the expanded grains.

6.3.2 Unlimited access to water in fractured rock

The very large voids in a pellet fill will be occupied by water very soon after filling the hole containing air-dry pellets with water. The main difference between the "Pellet" plug and the other plug types is that the latter become wetted from their outer boundary while the first mentioned has a high degree of water saturation in all parts from start, i.e. on the order of 70-80 %. This means that the suction, which is the main cause of saturation in the absence of high water pressure, is rather low. Another major difference between the "Pellet" plug on the one hand and the other plug types on the other, is that the "skin" formation is much less developed in the first mentioned. Both phenomena combine to cause a very slow increase in the degree of water saturation beyond the initial value even if the rock can offer significant amounts of water.

6.3.3 Limited access to water in rock with few fractures

"Pellet" plugs in rock that does not give off much water will still reach states with high degrees of water saturation rather quickly because of the aforementioned numerous continuous, permeable flow paths. In contrast to the other plug types, flow in the "skin" zone is believed to be less important than flow in the permeable paths in all the plugs. Naturally, "Pellet" plugs that are not compacted mature quicker than the other, denser plug types and that the microstructural heterogeneity makes them much more permeable.

6.3.4 Piping resistance

The "Pellet" plug would not be very vulnerable to a momentarily applied pressure gradient in the early maturation phase because water having entered into all the voids between the grains in conjunction with the placement would start to expand them and yield a significant average density very soon.

In the experiments the same conditions prevailed as for the other plugs and the same type of testing was performed of the 2.5 m long "Pellet" plug.

The procedure and observations were as follows:

- Pellets of the type shown in Figure 6-2 with 10 % water content were poured in the tube with 80 mm diameter that represented a borehole. 17 kg of pellets were filled and very slightly compacted by use of a rod. This gave the air-dry fill a density of 1150 kg/m³ corresponding to a dry density of 1035 kg/m³ and a density at complete water saturation of 1650 kg/m³.
- Tap water was pressed into the tube at low pressure after which a water pressure of 500 kPa was applied at both ends for supplying the plug with water in the maturation process. This pressure was on the same order as at the test site at Äspö where plugs of the same type were tested with respect to the adhesion to the borehole walls (Sub-project 2).
- After a short period of rest for maturation under a uniform water pressure of 500 kPa, a step-wise increased water pressure was applied at one end of the tube while the opposite end was pressure-free and connected to a pipe for measuring water flow through the plug. The pressure was increased in 50 kPa steps each lasting for 5 minutes up to 200 kPa without through-flow being initiated. The steps were then raised to 100 kPa resulting in compression and displacement of the plug but still with no permeation even at 2000 kPa pressure.

- After 24 hours of rest a pressure gradient was again established for determining the critical pressure for piping. The pressure was raised in 400 kPa steps, each lasting for 5 minutes, but no permeation occurred even at 2000 kPa. However, at 1200 kPa compression or displacement of the plug started and increased significantly at 1600 kPa pressure.
- The plug was finally extruded and examined.

The outcome of the tests, which are fully reported in Appendix III, is interpreted as follows:

- After 6 hours of rest under 500 kPa uniform water pressure the critical pressure for piping was at least 200 kPa, indicating that the plug had started to mature. For pressures exceeding about 300 kPa, corresponding to an axial force of more than 0.15 tons, the plug was compressed or displaced, implying that the "skin" had reached a shear strength of around 2 kPa if it had been mobilized over the total length of the plug. This is far less than for the "Container" plug, indicating that most of the water initially contained in the sample and taken up in the first day had been uniformly sorbed by the pellet mass without causing much consolidation of the "skin" zone. It is estimated that the uptake of water had caused expansion of the clay grains and formation of interstitial clay gels without causing much swelling pressure.
- After another 14 hours of rest under 500 kPa uniform water pressure, the critical pressure for piping was at least 800 kPa, indicating substantial microstructural homogenization. For pressures from 1200 kPa and more, corresponding to an axial force of at least 0.6 tons, the plug started to be displaced, implying that the "skin" had reached a shear strength of around 10 kPa if it had been mobilized over the total length of the plug. Also this is far less than for the "Container" plug and indicates that most of the water taken up in this period of time had been uniformly sorbed by the pellet mass still without causing much consolidation of the "skin" zone. Assuming that mobilization of the adhesion strength had only taken place over the first 0.5-1 m length, it would have been 30-60 kPa, which is on the same order of magnitude as the adhesion strength evaluated from the subsequent extrusion test.
- Extrusion of the plug after the second piping test was made by use of the hydraulic jack used for extruding plugs also in the preceding experiments. The force was found to be 3.5 tons, which gave the adhesive strength of the plug, i.e. the shear strength of the clay/steel contact, that could then be compared to that determined in the field experiment (Sub-project 2). The evaluated adhesion (shear) strength was about 60 kPa.
- The extruded plug, which appeared to be homogeneous (Figure 6-4) broke in about 0.5 m long pieces when the plug was moved out without support. The water content of differently located samples were determined and found to be as reported in Table 3-3. Since complete water saturation yields an average water content of 59 % one concludes that the plug is largely water saturated but that significant variations in density prevail.

Table 3-3. Water content and density data of the extracted "Pellet" plug. The first figure (A) represents the shallow "skin" and the other (B) the central part of the plug (A/B).

Position	Water content, %	Original density, kg/m ³	Actual density of extracted plug, kg/m ³
0.2 m from pressurized end	76/53	1035	1812/1584
1.5 m from pressurized end	66/54	1035	1718/1593
2.5 m from pressurized end	86/48	1035	1925/1532

* Constant dry density assumed



Figure 6-4. Appearance of extruded "Pellet" plug.

Practical function of clay plugs of "Pellet" type

The following major conclusions from the various test series were drawn:

- The expected quicker water saturation and homogenization of the "Pellet" plug than of the other types were verified.
- The low density of the "Pellet" plug means that its bulk hydraulic conductivity is sensitive to high salt contents, and particularly to Ca, in the groundwater. Thus, for an average bulk density of 1650 kg/m³ saturation and percolation with salt-free water the conductivity is estimated at 2E-12 m/s and around E-10 m/s for ocean water.

- The best way of placing the pellet fill is to have the borehole drained until placement is started since slight compaction can then be made. Groundwater will enter from water-bearing fractures and can produce irregular wetting of the fill, which may lead to local expansion and some variation in density along the hole.
- Only clay pellets with Na as major adsorbed cation should be used since the initially formed microstructure will be more homogeneous than if Ca-saturated clay pellets are used.

6.4 Performance in situ

6.4.1 Practical design issues

The following practical issues need to be considered:

- For reaching maximum density the pellets should be spherical and contain two sizes that are mixed. However, filling in dry holes will cause size separation and for avoiding this and for practical and cost reasons it is recommended that only one pellet size is used.
- Although one can theoretically use the "Pellet" technique in holes with a depth of a hundred meters it should be reserved for holes with a maximum depth of a few tens of meters since significant variations in density can otherwise occur and difficulties with compaction most certainly appear.
- Before a plug is emplaced previously cast quartz/cement plug must have hardened sufficiently to be able to carry it. With a suitable concrete recipe this is a matter of one day.

6.4.2 Erodability

There will be no erosion of the clay.

6.4.3 Manufacturing

Pellets are available on the market. A special type of granular smectite material that may be preferable is screened material from crushed blocks of very strongly compacted smectite clay powder with very low water content [2]. Such material matures slower than ordinary pellets but the ultimately reached density can be substantially higher.

6.4.4 Equipment for placement

The objective for bringing down the fill, i.e. a small hopper attached to a tube that reaches down in the hole for minimizing wall friction and for light compaction in the filling phase, can be of simple type. A field-adapted balance and a container with known volume shall be used for filling the hopper so that the density of the pellet mass can be continuously recorded.

7 Construction of cement-based plugs

7.1 Basic

The objective of the Borehole Plugging Project is to indicate methods and materials that make the boreholes at least as tight as the surrounding rock and to seal them so that they do not serve as conductors of radionuclide-bearing water that may ultimately emanate from the repository. Where the rock has normal structure and the average hydraulic conductivity is in the interval E-11 to E-8 m/s the hole need to be sealed by inserting plugs that are as tight as the confining rock or tighter, which requires use of clay materials. Where the holes intersect fractures zones that are permeable, plugs do not need to have a low conductivity but must be physically stable for supporting the surrounding rock and the clay plugs that rest on them or are located below them. In the construction phase they must be coherent and soon become strong enough to carry clay plugs without settling, for which cement stabilization of frictional soil has been selected. The physical stability means that chemically stable mineral grains are used for which quartz grains are suitable.

The property of quickly reaching a relatively high mechanical strength requires use of a cement binder and a suitable recipe has been worked out by CBI. For minimizing negative impact on contacting clay plugs the cement content will be very low and low-pH cement will be utilized. Likewise, the amount and type of the superplasticizer that is required for making the concrete sufficiently fluid will be at minimum. The cement is not relied on for long periods and it is assumed that it will be dissolved and lost, which requires that the physical stability of the remaining quartz fill is sufficient to provide the rock and neighbouring clay plugs with sufficient support. For this purpose the grain size distribution of the quartz grains is of Fuller-type, implying that smaller grains fill up the space between larger grains, a principle that gives a high density and prevents small particles to be moved by percolating water.

7.2 Recipe for borehole plugs of concrete

The composition of the concrete intended for use in boreholes has not yet been decided but a preliminary recipe, worked out by CBI, will be used in the boreholes plugging project. Following the principle applied in backfilling of mines, the cement content will be as low as practically possible and about 5 % was initially set for this purpose. A further requirement is that low-pH cement (pH 10 to 11) should be used, which has led to the presently suggested composition.

Table 7-1. Composition of borehole concrete (CBI).

Components	Kilograms per m ³ of concrete
White cement (Aalborg Portland)	60
Water	150
Silica Fume (Elkem)	60
Fine ground α -quartz (Sibelco)	200
Fine ground cristobalite quartz (Sibelco)	150
Superplasticizer (Glenium 51 Modern Betong)	4,38 (dry weight)
Aggregate 0-4 mm (Underås, Jehanders Grus)	1679

The concrete is self-compacting and compared to normal concrete it is fairly viscous, i.e. like syrup (viscosity 5000-10 000cp). The experiments in Olkiluoto reported in Sub-project 3, show that it is possible to construct a plug with low pH concrete in a borehole even at a fairly great depth.

The evolution of strength has been tested by CBI at 5 and 20 °C leading to the conclusion that the strength increases slowly, especially at low temperatures (cf. Table 7-2). However, the ultimate strength is higher than that of normal construction concrete that normally contains more than 300 kg of binder (cement).

Table 7-2. Strength evolution development of borehole concrete. "Cube strength".

Curing time in days	5°C Cube strenght in MPa	20°C Cube strenght in MPa
2	1.9	4.5
3	4	6.6
7	7.5	10.6
28	14	40
72	32.9	55.2
91	35.4	57.4

The concrete was also tested with respect to shrinkage. Figure 7-1 shows that, in water, the concrete can absorb water and ultimately yield some minor expansion.

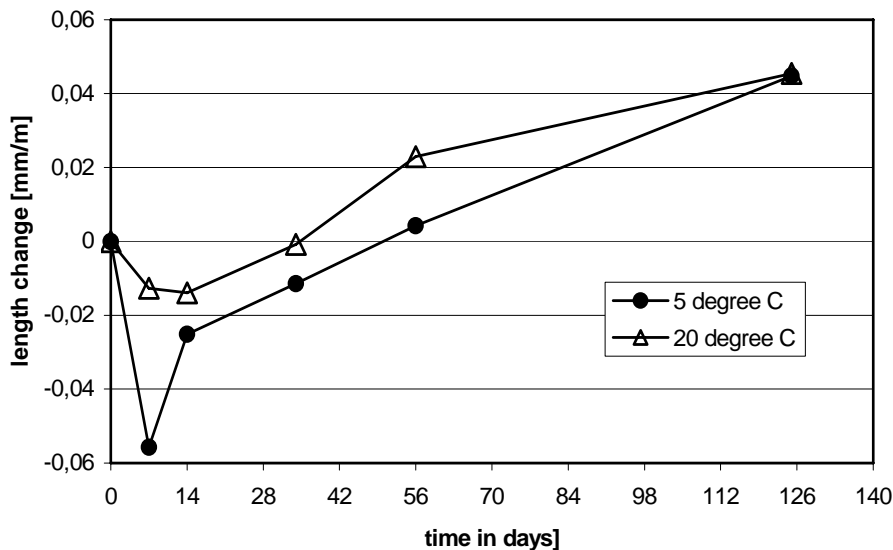


Figure 7-1. Shrinkage/swelling measurements of borehole concrete submerged in water. Measured as length changes of prism (400x100x100mm) according to CBI.

It should be noted that long-term chemical stability of the cement component is of no concern in the present context since total loss of it is assumed. This matter is therefore not considered in the project.

8 Discussion and recommendations

8.1 Discussion

This part of the Borehole Sealing Project deals with fundamental issues, primarily design of the four plug types that are considered, the ways in which the plugs mature under different rock conditions, their performance in the holes, and manufacturing issues. One of the major objectives is to design the plugs so that they become tighter than the surrounding rock, which has an average hydraulic conductivity of E-11 to E-8 m/s. This performance criterion is valid for at least 100 000 years [1].

8.1.1 Performance

"Basic" type

The major advantages of this concept are that it is robust and that plugs can be inserted, theoretically at least, to any depth and in any direction. Also, they are retrievable. Negative features are that the time for placement needs to be short enough to minimize erosion and for avoiding maturation to an extent that the placement becomes difficult. A suitable time interval for bringing a clay plug down to 1000 m depth is 3-8 hours. More than 8 hours is expected to initiate adhesion of the clay to the rock and cause resistance to the placement. An important fact is that there is sufficient experience of placement and testing of "Basic" plugs to recommend them for practical use.

Using clay of MX-80 type with 6 % water content and compression under 250 MPa the density is acceptable. Thus, the lowest net density of the clay will be found at the lower end of plugs in 1000 m deep holes, i.e. 1900 kg/m³. The corresponding hydraulic conductivity and swelling pressure in saline groundwater are E-12 m/s, and 1.5 MPa, respectively. Plugs placed at 500 m depth, corresponding to the repository level, will undergo less erosion and are estimated to have an average density of 2000 kg/m³.

"Container" type

This concept has several advantages compared to plugs of "Basic" type, primarily that the clay can be brought to the required location without exposing it to erosion. A negative feature is that placed plugs cannot be retrieved and a possible difficulty with plugs of this type is that the container tube must be perfectly tight and strong enough to resist high pressures. The thickness of the tube hence has to be large enough to provide the required strength and small enough to give the clay sufficient density. A prototype has been made but has not yet been tested in the field. The concept is very promising, i.a. because holes of any direction can be plugged, and testing on a full scale is recommended.

"Couronne" type

Plugs of this type have been installed with no difficulty. The concept is simple and practical but the problem is that erosion and abrasion of the unshielded clay may be significant, which suggests that it should not be applied for sealing boreholes longer than a few tens of meters.

The simple technique and the possibility to get a high plug density means that the technique should be applied in future R&D.

"Pellet" type

Plugs of this type have been used and tested abroad (of Pusch et al, 2003) and they can be installed with no difficulty. The concept is simple and practical but the problem is that the density of the matured plug is not very high. It is recommended that the borehole is dry before bringing in the pellets implying that the boreholes, which need to be steep and oriented downwards, cannot be very deep, i.e. only a few tens of meters. Comparison with the "Couronne" concept favours the latter.

8.1.2 Possible improvements

All the proposed plugging concepts can be improved particularly with respect to the density of the clay. Thus, it appears possible to do this by using very strongly compacted clay (>250 MPa) with a water content of a few percent [2]. This would make the matured plugs even denser and tighter. For the "Basic" and "Couronne" types slower maturation rate and hence better erosion resistance would also be expected.

A possible improvement of all these concepts, except the "Pellet" type, would be to use smectitic bore mud in the holes, firstly because this would contribute to stabilize the boreholes and to reduce erosion, as well as to contribute to the net density of the matured plugs [3].

All these suggestions should be further looked into.

8.2 Concrete plugs

The matter of further development of concrete for plugging is not discussed here since it is part of R&D performed in other contexts.

9 References

- 1. Pusch R, Ramqvist G, 2004.** Borehole sealing, preparative steps, design and function of plugs - basic concept. SKB Int. Progr. Rep. IPR-04-57.
- 2. Pusch R, Bluemling P, Johnsson L, 2003.** Performance of strongly compressed MX-80 pellets under repository-like conditions. Applied Clay Science, Vol. 23 (p. 239-244).
- 3. Pusch R, Yong R, 2006.** Microstructure of Smectite Clays and Engineering Performance. Taylor & Francis, London and New York. ISBN10:0-415-36863-4.
- 4. RD & D-Programme 2004.** Programme for research, development and demonstration of methods for the management and disposal of nuclear waste, including social science research. Swedish Nuclear Fuel and Waste Management Co. SKB TR-04-21.

Appendices

I	Design of borehole plugs of Basic Type	55
II	Homogenization of borehole plugs of Basic Type	111
III	Borehole plugging test – Piping Experiments	127
IV	Manufacturing of bentonite plugs with very high density	135
V	Silica concrete for plugging of deep bore holes	151

Appendix I

Design of borehole plugs of Basic Type

Lennart Börgesson

Torbjörn Sandén

Clay Technology AB

August 2004

Abstract

Carrying out site investigations for a future deep repository of spent nuclear fuel will involve drilling of a great number of deep boreholes for characterisation of the rock. These boreholes must be sealed, and a suggested technique is to fill them with highly compacted bentonite cylinders that are placed in perforated copper tubes to facilitate installation. After installation of the plug, the bentonite will swell through the perforation and further out between the tube and the rock. In order to obtain a good seal it is important that the bentonite has a sufficiently high density, and thus a low hydraulic conductivity and a swelling pressure which gives a good contact. The salt content of the groundwater has also an influence on the sealing function of the bentonite.

Both theoretical modelling and laboratory tests have been made to study the function of such a plug. Two different configurations have been suggested concerning the dimensions of the borehole, copper tube and bentonite block. This investigation only concerns the alternative with the larger borehole, but this alternative is probably conservative.

The following tests and analyses have been made, both with distilled water and with water with 3.5% CaCl_2 :

- Measurement of swelling rate and rate of swelling pressure build-up
- Laboratory simulations of a plugged section with swelling of bentonite through perforated copper tubes that were interrupted after one hour
- Long-term laboratory simulation of a plugged section with swelling and homogenisation of the bentonite for 78 days with a concurrent measurement of swelling pressure and wetting. Finally a thorough determination of distribution of water ratio and density were done after termination.
- Measurement of the axial hydraulic conductivity of the bentonite that has swelled out between tube and “rock” before termination of the long-term test.
- Laboratory simulation of an installation of a plug parcel in a 500 m deep borehole where 0.9 l of water per second passes the parcel during one hour
- A theoretical modelling of the swelling of bentonite through the holes of the perforated copper tube and in the slot between rock and tube. The model has since been used for prediction of long-term trials

This study has yielded the following results and conclusions:

- The swelling of bentonite is considerably faster in water with 3.5% CaCl_2 content than in distilled water. Salt water can have maximum a one-hour stop during installation while fresh water can have a 5-10 hours stop before the parcel gets stuck.
- The installation of a plug parcel at 500 m depth in fresh water results in almost a 10% loss of bentonite. The technique thus needs to be modified.
- A theoretical model of the swelling of bentonite has been made and this shows that the optimum hole diameter is 10 mm for the predicted geometry, and that the minimum swelling pressure against the rock between the holes is 1 960 kPa for fresh water and 950 kPa for salt water.
- The long term tests show that complete swelling and homogenisation is obtained after 10-20 days. The measured mean swelling pressure against the rock was 2 800 kPa for the fresh water case and 600 kPa for salt water. This mean pressure is in good agreement with the predicted mean pressure for fresh water (2 860 kPa) but not for salt water (1 950 kPa). The reason for the latter deviation might be that data for the bentonite has been obtained from tests with NaCl in the water instead of CaCl_2 . The mean void ratio between tube and rock was fairly high in both cases (1.15-1.2).
- Measurement of the hydraulic conductivity between tube and rock shows that it was $5-9 \cdot 10^{-13}$ m/s for fresh water and $2 \cdot 10^{-12}$ for salt water.

Sammanfattning

Genomförandet av platsundersökningar för ett framtida djupförvar för utbränt kärnbränsle medför att ett stort antal djupa borrhål kommer att borraras för att karakterisera berget. Dessa borrhål måste tätas och en teknik som föreslagits är att fylla hålen med högkompakterade bentonitcylindrar som placeras i perforerade kopparrör för att underlätta installationen. Efter installation av en plugg kommer bentoniten att svälla genom perforeringen och vidare ut mellan röret och berget. För att få en bra tätning är det viktigt att densiteten på bentoniten blir tillräckligt hög för att därmed få en låg hydraulisk konduktivitet och ett svälltryck som ger god kontakt. Innehållet av salt i det aktuella grundvattnet påverkar också bentonitens tätfunktion.

För att studera funktionen hos en sådan plugg har både teoretisk modellering och laboratorieförsök gjorts. Två olika konfigurationer har föreslagits vad gäller dimensioner på borrhål, kopparrör och bentonitblock. I denna undersökning har bara alternativet med större borrhål undersökts, men detta alternativ får anses som konservativt.

Följande tester och analyser har gjorts med både destillerat vatten och vatten med 3.5% CaCl_2 :

- Mätning av utsvällningshastighet och svälltrycksuppbyggnadshastighet
- Laboratoriesimulering av en pluggad sektion med utsvällning av bentonit genom perforerade kopparrör som bröts efter 1 timme
- Långtidsförsök med laboratoriesimulering av en pluggad sektion med utsvällning och homogenisering av bentoniten under 78 dygn med samtidig mätning av svälltryck och bevätning. Noggrann bestämning av fördelningen vattenkvot och densitet efter brytning.
- Mätning av axiella hydrauliska konduktiviteten av bentoniten som svällt ut mellan rör och "berg" innan långtidsförsöken bröts.
- Simulering i laboratoriet av en installation av ett pluggpaket i ett 500 m djupt borrhål med 0.9 liter sötvatten per sekund som passerar paketet under 1 timme.
- Teoretisk modellering av utsvällningen av bentonit genom hålen i det perforerade kopparröret och i spalten mellan berg och rör. Modellen har sedan använts för att prediktera långtidsförsöken

Följande resultat och slutsatser har uppnåtts av denna studie:

- Utsvällningen av bentonit är avsevärt snabbare i vatten med 3.5% CaCl₂ än i destillerat vatten. Ett stopp om maximalt 1 timme klaras i saltvatten medan 5-10 timmar klaras i sötvatten innan att paketet fastnar.
- Installation av ett pluggpaket till 500 m djup medför i sötvatten en förlust av knappt 10% av bentoniten. Tekniken måste alltså förändras.
- En teoretisk modell av bentonitutsvällningen har tagits fram och den visar att för den antagna geometrin är håldiametern 10 mm optimalt och ger ett minsta svälltryck mot berget mitt emellan hålen på 1960 kPa för sötvatten och 950 kPa för saltvatten.
- Långtidsförsöken visar att full utsvällning och homogenisering har nåtts efter 10-20 dagar. Det mätta medelsvälltrycket mot berget blev 2800 kPa för söt vattenfallet och 600 kPa för saltvatten. Detta medeltryck stämmer väl överensmed det predikerade medeltrycket för sötvatten (2860 kPa) men inte för saltvatten (1950 kPa). Orsaken till den senare avvikelsen kan vara att data för bentoniten tagits från försök med NaCl i vattnet istället för CaCl₂. Medelportalet mellan rör och berg var ganska högt i de båda fallen (1.15-1.2).
- Mätning av hydrauliska konduktiviteten mellan rör och berg visar att den blev $5-9 \cdot 10^{-13}$ m/s i sötvattenfallet och $2 \cdot 10^{-12}$ m/s i saltvattenfallet.

Contents

1	Introduction	67
2	Bore hole plugging	69
3	Theoretical modeling of the interaction between the bentonite and the perforated copper tube in a plugged borehole	71
3.1	General	71
3.2	Derived model	72
3.3	Influence of friction angle	75
3.4	Predicted swelling pressure on the rock	76
4	Laboratory tests	79
4.1	General	79
4.2	Swelling capacity	79
	4.2.1 Free swelling	79
	4.2.2 Swelling into a confined volume	82
4.3	Swelling through the perforated copper tubes	84
	4.3.1 General	84
	4.3.2 One hour pretests	87
	4.3.3 Flow test for simulating the installation of a plug parcel	87
	4.3.4 Long time tests with measurement of the wetting process and the swelling pressure	90
	4.3.5 Comparison between the measured results and the models	100
5	Summary of results and conclusions	101
	References	103

1 Introduction

The site investigation for a future deep repository for spent nuclear fuel includes drilling of deep bore holes in order to characterize the rock. These bore holes must be sealed after completed testing. One suggestion for sealing is to use highly compacted bentonite cylinders confined by a perforated copper tube in order to facilitate the installation. During wetting the bentonite will swell through the perforation and seal off the volume between tube and rock.

The study presented in this report comprises the following parts:

1. **Theoretical modeling.** Theoretical modeling of the bentonite swelling through the holes and into the slot between the copper tube and the rock surface has been done in order to study the drop in swelling pressure and density outside the copper tube. The model has also been used to optimize the geometry and size of the perforated holes.
2. **Laboratory tests for studying the swelling capacity and swelling velocity.** The time available for installation is limited by the swelling velocity since the parcels may not get stuck during installation.
3. **Simulation of the installation of a bentonite/copper parcel.** During sinking of a parcel into a 1000 m deep borehole a large amount of water flows past the bentonite. This may cause erosion and degrading of the bentonite.
4. **Long time laboratory tests for studying the swelling of bentonite through the perforated tubes and into the slot.** A part of a borehole have been simulated and the wetting and swelling processes measured.

The study is part of a project that aims at developing technique for sealing boreholes

2 Bore hole plugging

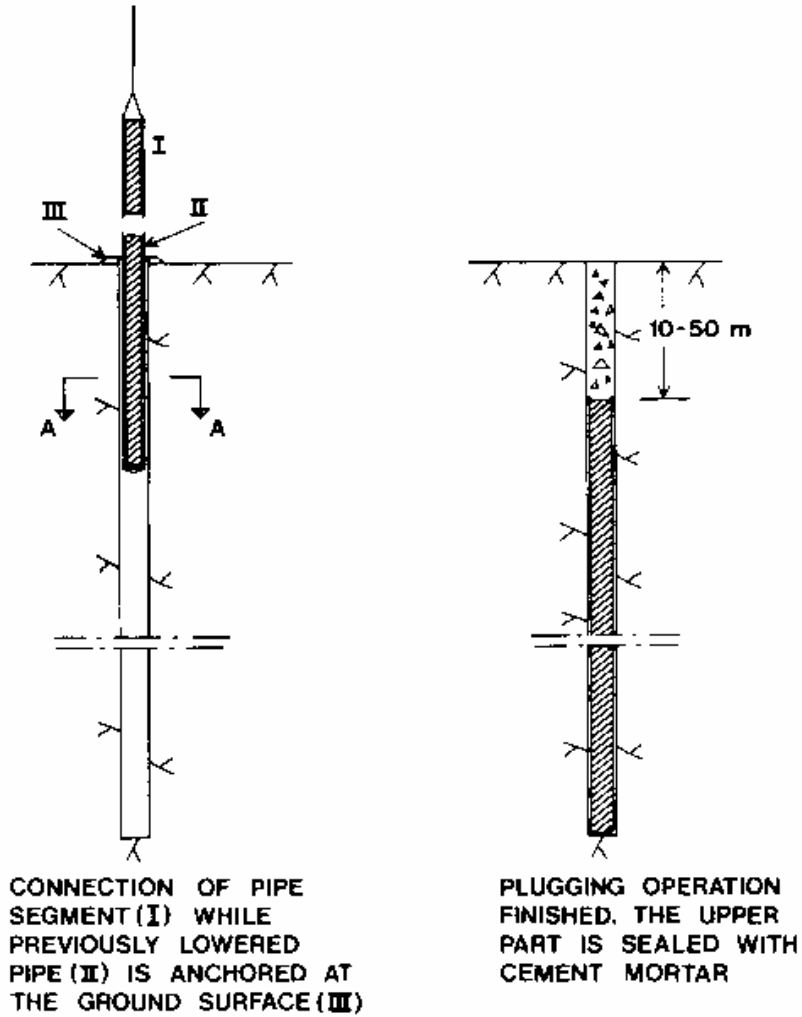
The suggestion is to plug boreholes with a combination of cement plugs and bentonite plugs. Only the bentonite plugs are considered in this study.

The proposed design of a bentonite plug is shown in Figure 2-1. Cylindrical bentonite blocks are compacted to a height of about 5 cm and placed inside a perforated copper tube. Parcels will be made in sections of 3 meters. Several parcels will be connected and lowered into the borehole.

The function of the bentonite in a plugged bore hole of many factors e.g.:

1. The final saturated average density of the bentonite.
2. The final density of the bentonite that has penetrated between the copper tube and the rock surface
3. The ion concentration in the water.
4. Problems with eroding bentonite during installation.

These factors are considered in this study.



SECTION A - A

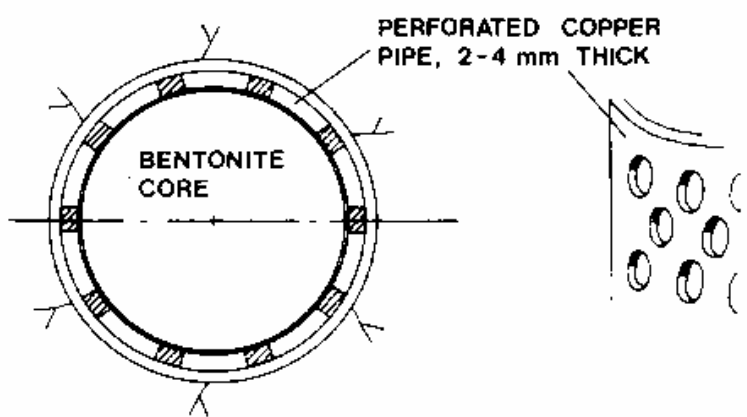


Figure 2-1. Illustration of a bentonite borehole plug /1/.

3 Theoretical modeling of the interaction between the bentonite and the perforated copper tube in a plugged borehole

3.1 General

The bentonite will swell at first radially through the holes in the perforated copper tube and then tangentially between the copper and the rock surface (see Figure 3-1). It is important that the swelling pressure from the bentonite inside the copper tube σ_0 can be transferred to the rock with a swelling pressure σ_1 and further through the gap behind the steel with a swelling pressure σ_2 , which are high enough to yield a good sealing

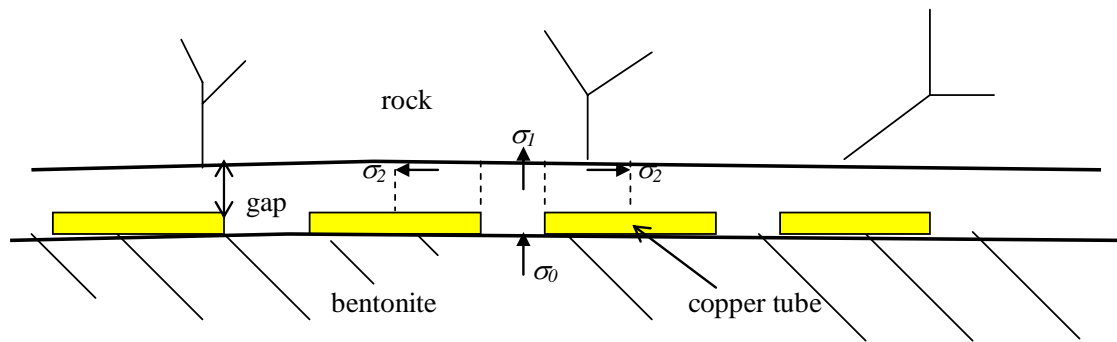


Figure 3-1. The original swelling pressure of the bentonite σ_0 is reduced to σ_1 when it swells through the holes to the rock and further to σ_2 when it swells behind the copper.

The swelling and the reduction in density and swelling pressure is a function of the geometry. In order to find the best geometry of the perforation of the steel cylinder a theoretical derivation of the swelling pressures σ_1 and σ_2 have been done. σ_1 is in these formulas assumed to be the average swelling pressure between the copper tube and the rock, i.e. the swelling pressure half way between the copper tube and the rock.

The geometry of the circular holes shown in Figure 3-2 is derived from the assumption that the “degree of perforation” (that is area holes divided to total area) is $\mu=0.5$, that all holes are equal and that the distribution is symmetric with a half hole shift.

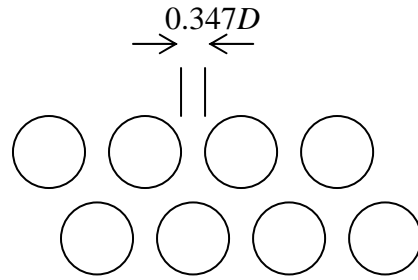


Figure 3-2. Geometry of the circular holes.

The distance between the holes is $0.347D$ ($0.694r$) while the longest distance that the buffer must swell between the holes will be $0.56r$.

3.2 Derived model

The axial swelling can be derived from an equilibrium equation of the forces in axial swelling from σ_0 to σ_1 (Equation 3-1), while the radial swelling can be derived from equilibrium of forces in radial direction from σ_1 to σ_2 (Equation 3-2). The theory behind these relations is shown in Appendix 1.

$$\sigma_1 = \sigma_0 \cdot e^{\frac{-2(d+z/2) \tan \phi}{r_1}} \quad (3-1)$$

$$\ln \sigma_2 = \ln \sigma_1 + K \ln \frac{r_2}{r_1} - \frac{r_2 - r_1}{z} \cdot 2 \tan \phi \quad (3-2)$$

where

r_1 = hole radius

r_2 = radius at σ_2

d = tube thickness

z = slot between the copper tube and the rock

$$K = \left(\frac{\nu}{1-\nu} - 1 \right)$$

ν = Poisson's ratio

ϕ = friction angle in bentonite

For the borehole plug we assume that (case 1 in Figure 4-7)

$d = 0.0035$ m

$z = 0.0025$ m

$\sigma_0 = 10\,000$ kPa

$\phi = 20^\circ$

$r_2/r_1 = 1.56$

The minimum swelling pressure σ_2 , which occurs between the holes at the radius $1.56r_1$ is plotted as a function of the hole radius in Figure 3-3. The extremes $K=0$ (isotropic swelling pressure) and $K=-1$ are assumed.

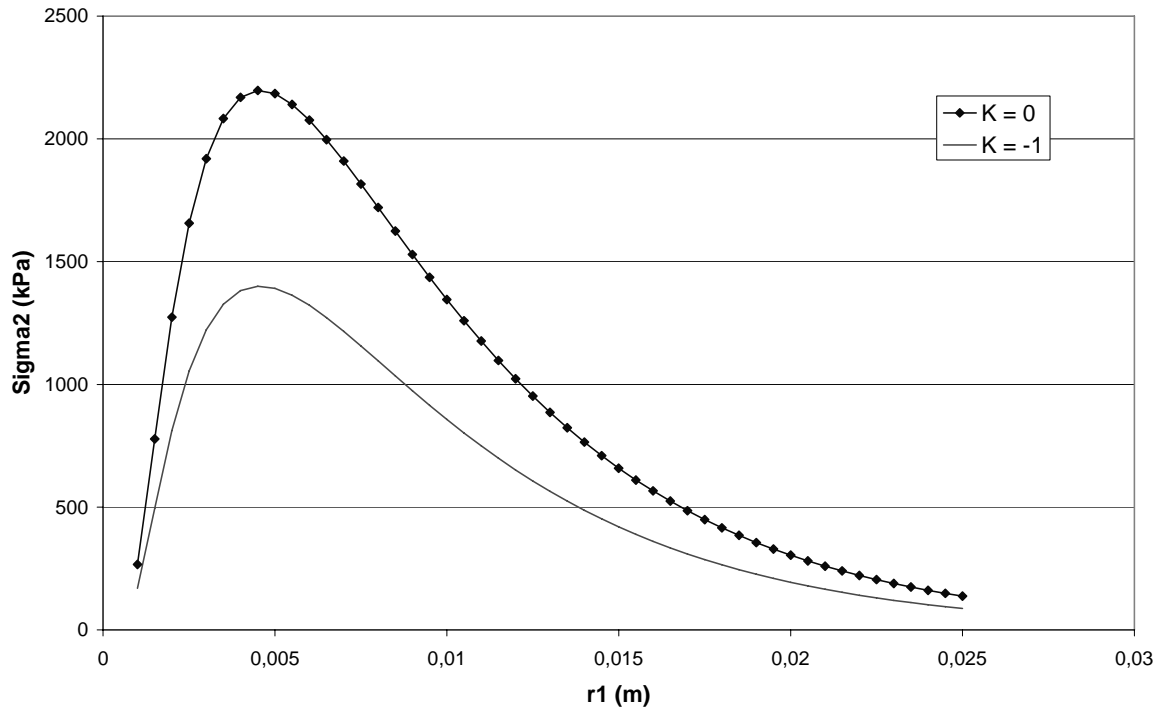


Figure 3-3. Degree of perforation $\mu=0.5$. Minimum swelling pressure as a function of the radius of the holes in the copper tube for two cases, where $K=0$ corresponds to isotropic swelling pressure. $\phi = 20^\circ$.

If the degree of perforation is changed to $\mu=0.6$ the longest distance that the buffer must swell between the holes will be $0.42r$. Thus the relation r_2/r_1 will change to

$$r_2/r_1 = 1.42,$$

which yields Figure 3-4.

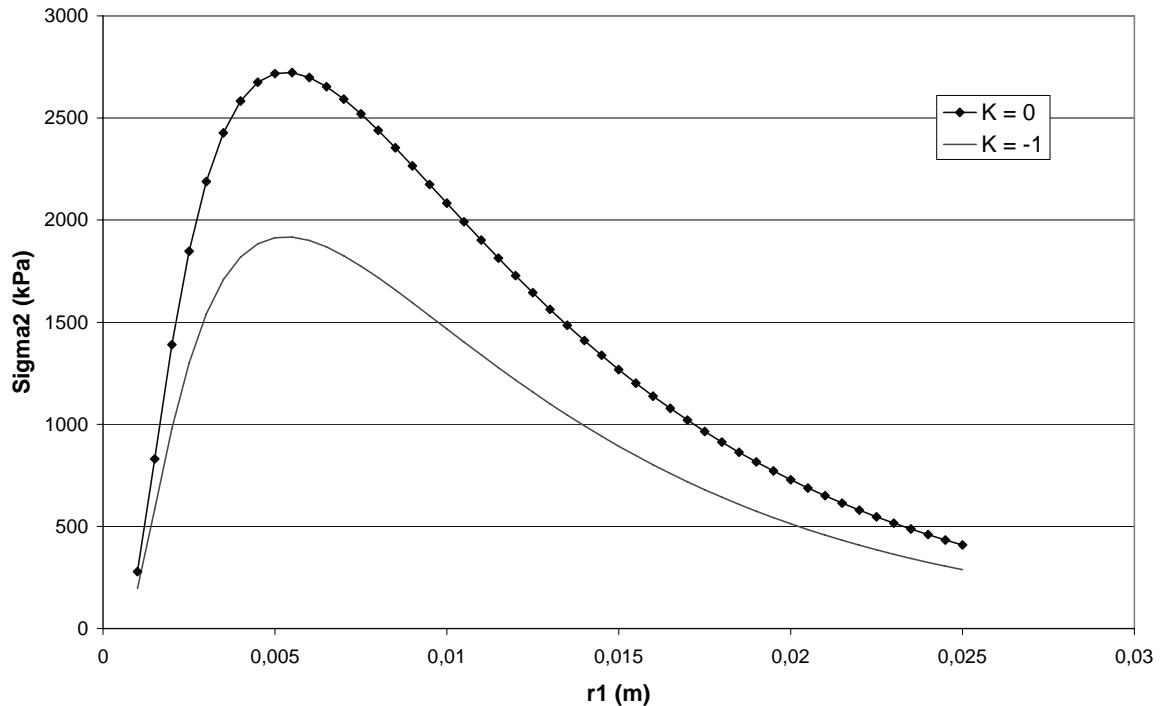


Figure 3-4. Degree of perforation $\mu=0.6$. Minimum swelling pressure as a function of the radius of the holes in the copper tube for two cases, where $K=0$ corresponds to isotropic swelling pressure. $\phi = 20^\circ$.

The calculations show that the optimum hole diameter is 1.0 cm if the degree of perforation is $\mu=0.5$ and 1.1 cm if the degree of perforation is $\mu=0.6$.

The influence of K and thus ν on the swelling pressure is a decrease in pressure of about 35% for $\nu=0$ compared to $\nu=0.5$. A value close to 0.5 is more likely since the bentonite is in a state of failure during the swelling process /2/. The results from $K=0$ (and thus $\nu=0.5$) is used in the following evaluation.

The minimum swelling pressure on the rock surface is thus (for the degree of perforation $\mu=0.5$)

$$\sigma_2=2200 \text{ kPa.}$$

The maximum swelling pressure on the rock surface is of course in the center of the holes and can be calculated with Equation 3-1, applying that the radius of the holes is 5 mm and that the total swelling distance is 6 mm ($(d+z/2)$ in Equation 3-1)

$$\sigma_2=4175 \text{ kPa.}$$

The average swelling pressure behind the copper tube will thus according to this model be about 3200 kPa if the swelling pressure inside the tube is 10 MPa and the friction angle $\phi = 20^\circ$. Another way to express it is to say that the average swelling pressure is reduced to 32% of the swelling pressure inside the tube.

3.3 Influence of friction angle

The swelling pressure shown in Figures 3-3 and 3-4 assumes that the average friction angle is 20 degrees. In reality the friction angle is dependant on both density and bentonite type. Figure 3-5 shows results from triaxial tests /2/. The deviator stress at failure is plotted as the average effective stress. The figure shows that the failure envelope is curved and that the shear strength is higher for MX-80 saturated with 3.5% NaCl than with distilled water. The data from figure 3-5 can be transformed to friction angle, which is shown in Table 3-1. However, there is no data for MX-80 saturated with 3.5% CaCl₂ so the data for 3.5% NaCl has been used instead.

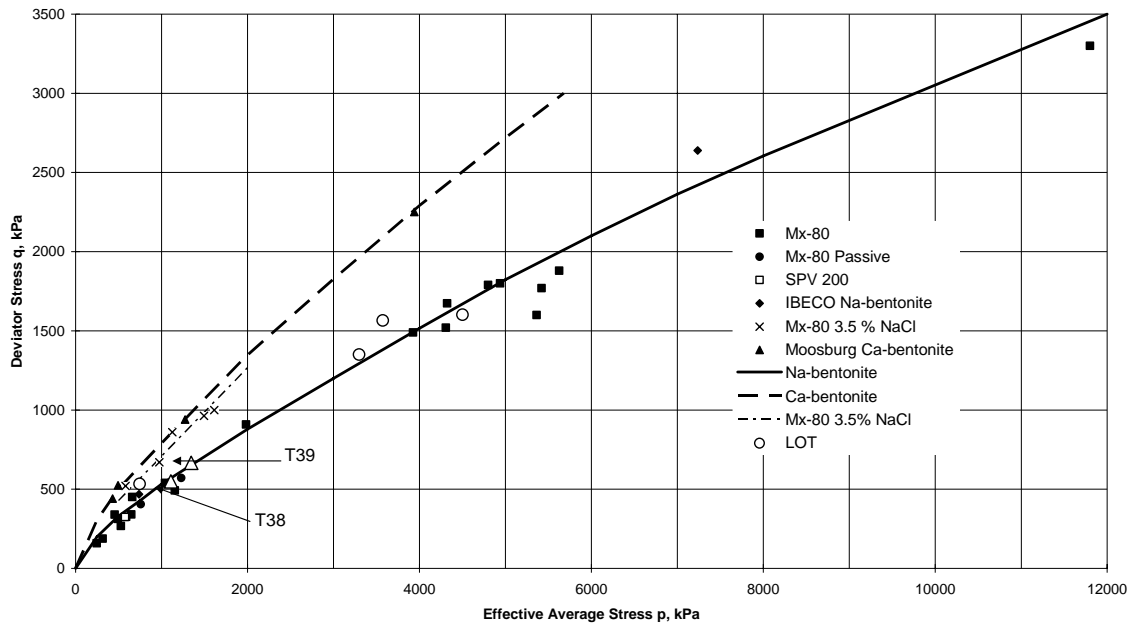


Figure 3-5. Results from triaxial tests on MX-80.

Table 3-1. Friction angle as function of effective average stress.

Average stress p (kPa)	Friction angle ϕ (degrees) Distilled water	Friction angle ϕ (degrees) NaCl water (3.5%)	Remarks
500	17.3	22.4	
1000	13.3	20.0	
2000	11.6	17.5	
5000	9.5	14.3	
10 000	8.0	-	No data for salt

The influence of the friction angle on the lowest swelling pressure behind the copper tube is shown in Figure 3-6. The influence is very strong between 10 and 20 degrees, and the influence from the swelling pressure thus high. At the average stress of about 4000 kPa the friction angle is 10 degrees and the minimum stress will be 4800 kPa instead of 2200 kPa.

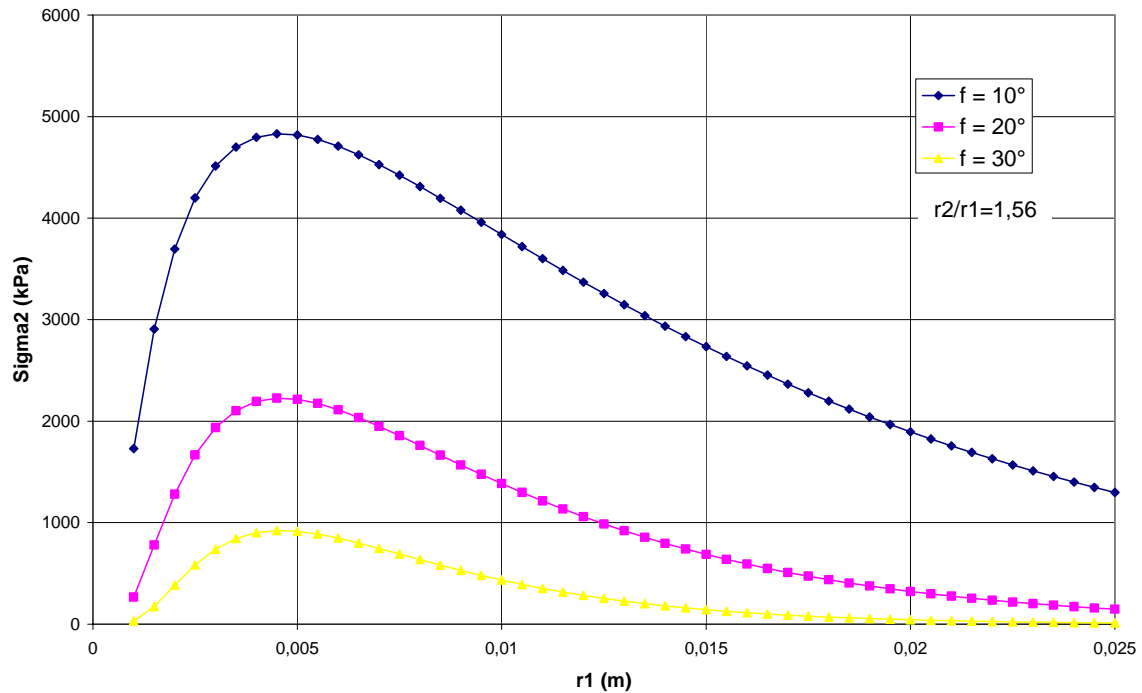


Figure 3-6. Influence of friction angle $K=0$. Degree of perforation $\mu=0.5$.

3.4 Predicted swelling pressure on the rock

With Equations 3-1 and 3-2 and the relation between swelling pressure and friction angle the expected swelling pressure on the rock surface outside the perforated copper tube can be calculated. The data for the plug is (alternative 1 in Figure 4-7)

$$d = 0.0035 \text{ m}$$

$$z = 0.0025 \text{ m}$$

$$\text{Distilled water: } \sigma_0 = 4\,500 \text{ kPa (for } e=0.82) / 2/$$

$$\text{Salty water: } \sigma_0 = 4\,000 \text{ kPa (for } e=0.82) \text{ (for 3.5\% NaCl) } / 2/$$

$$\phi = \text{according to Table 3-1}$$

$$K=0$$

$$r_2/r_1 = 1.56$$

A stepwise calculation must be done due to the dependency of the swelling pressure on the friction angle. At first we assume a low swelling pressure since we will start with a gel that penetrates the holes. The gel then consolidates from the expansion of the bentonite inside the perforated tube. With the assumed start value of the swelling pressure we can calculate the friction angle and the swelling pressure according to Equation 3-1. With this new swelling pressure we will have another friction angle and we can make a new calculation of the swelling pressure. We continue with these calculations until the swelling pressure used for the friction angle agrees with the calculated swelling pressure. This procedure yields σ_1 . The same procedure is then repeated with Equation 3-2 to yield σ_2 . Finally the average stress behind the tube is calculated according to Equation 3-3, which is based on that 50% of the swelling pressure is equal to σ_1 ($v=50\%$ perforation) and the rest is the average of σ_1 and the minimum stress σ_2 .

$$\sigma_a = v \sigma_1 + (\sigma_1 + \sigma_2) \cdot (1-v) \quad (3-3)$$

The stepwise calculation for the plug with distilled water is shown in Table 3-2.

Table 3-2. Stepwise calculation of σ_1 and σ_2 for distilled water.

Assumed σ_1 (kPa)	Corresponding friction angle ϕ (°)	σ_1 according to Equation 3-1 (kPa)
500	17.3	2500
2500	11.0	3100
3100	10.8	3140 (OK)
Assumed σ_2 (kPa)	Corresponding friction angle ϕ (°)	σ_2 according to Equation 3-2 (kPa)
500	17.3	1570
1570	12.5	1910
1910	11.8	1960 (OK)

Equation 3-3 then yields the average swelling pressure σ_a .

$$\sigma_1 = 2840 \text{ kPa}$$

Corresponding stepwise calculation for the plug with salty water is shown in Table 3-3.

Table 3-3. Stepwise calculation of σ_1 and σ_2 for salty water.

Assumed σ_1 (kPa)	Corresponding friction angle ϕ (°)	σ_1 according to Equation 3-1 (kPa)
500	22.4	1830
1830	18.0	2160
2160	17.3	2210 (OK)
Assumed σ_2 (kPa)	Corresponding friction angle ϕ (°)	σ_2 according to Equation 3-2 (kPa)
500	22.4	880
880	21.0	930
930	20.7	950 (OK)

Equation 3-3 then yields the average swelling pressure σ_a .

$$\sigma_1 = 1890 \text{ kPa}$$

However, this figure is uncertain because there is no data for 3.5% CaCl.

4 Laboratory tests

4.1 General

The following laboratory tests have been performed:

- 1 Measurement of swelling capacity in special oedometers. Two types of tests have been made: Tests of free swelling and swelling into a confined volume. The influence of salt in the groundwater has been considered.
- 2 Swelling through perforated tubes. The equipment has been designed to simulate a short part of a borehole. In these tests, bentonite has swelled out through perforated copper tubes and into the slot between copper tube and rock. The following different tests have been performed in this equipment:
 - 2.1 Two short pre-tests, one with distilled water and one with 3.5% CaCl_2 , where the experiments have been interrupted after 1 hour.
 - 2.2 A flow test that simulates the installation of a bentonite/copper parcel, where water has been flushed (0.92 l/min) through the slot for about one hour.
 - 2.3 Two long term tests with measurement of swelling pressure and the wetting process. One test was done with distilled water and then other one with 3.5% CaCl_2 .

4.2 Swelling capacity

4.2.1 Free swelling

Preparation

Two tests have been made, one with distilled water and one with 3.5% CaCl_2 . The bentonite was compacted directly in steel rings with 100 MPa, which yields a bulk density of about 2.08 g/cm^3 . The final height of the samples was aimed to be 20 mm before test start. A light plastic filter was placed on the top of the bentonite samples together with a small PVC cylinder (see Figure 4-1). The samples had free access to water on the top surface during the whole test. A displacement sensor was positioned against the PVC cylinder and the swelling of the bentonite was continuously registered.

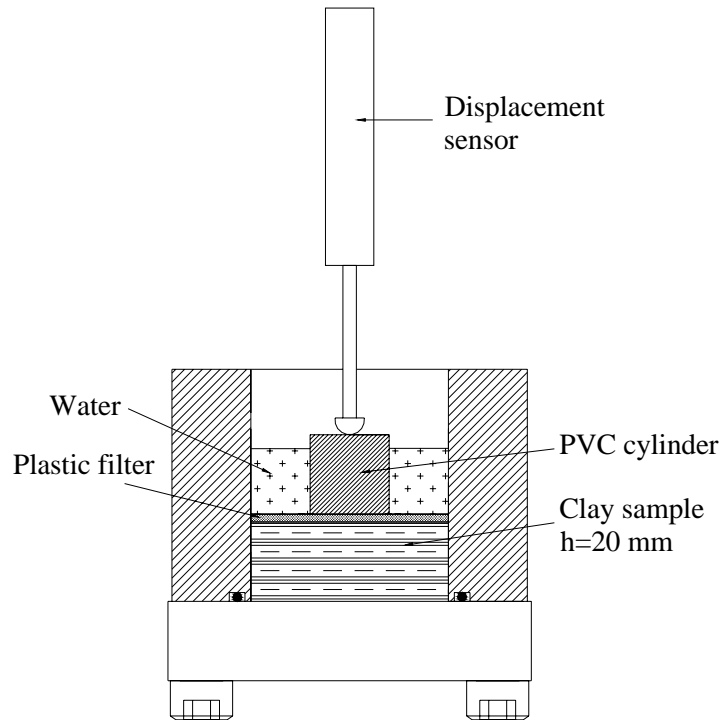


Figure 4-1 Schematic view showing the equipment used in the free swelling tests. The bentonite samples were compacted in the test cylinder with 100 MPa. The sample has free access to water from the plastic filter during the entire test period.

Results

The results are shown in Figures 4-2 and 4-3. The tests were left for 11 days and then interrupted and measured. Figure 4-2 shows the swelling as a function of time in logarithmic scale. The difference between distilled and salt water is strong. The sample supplied with salt water swells about 10 times faster, but the total swelling seems to end after a day and about 125% swelling, while the sample supplied with distilled water still swells after 11 days and 190% swelling.

Figure 4-3 shows the swelling during the first hours. After 1 hour the sample in distilled water has only swelled about 1.4 mm while the sample in salt water has swelled 8 mm. These results show thus that if the installation is stopped for an hour it is not likely that the parcel will get stuck in tap water but most likely in sea water.

Table 4-1 shows the measured water ratio distribution after completed tests. The very strong water ratio difference in the sample in distilled water shows that equilibrium is far from reached.

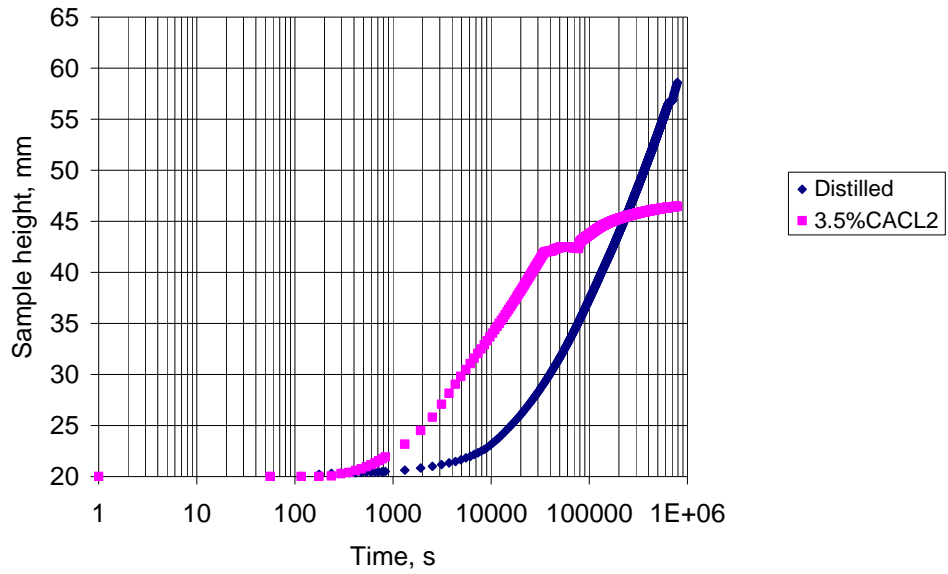


Figure 4-2. Diagram showing sample height as a function of time.

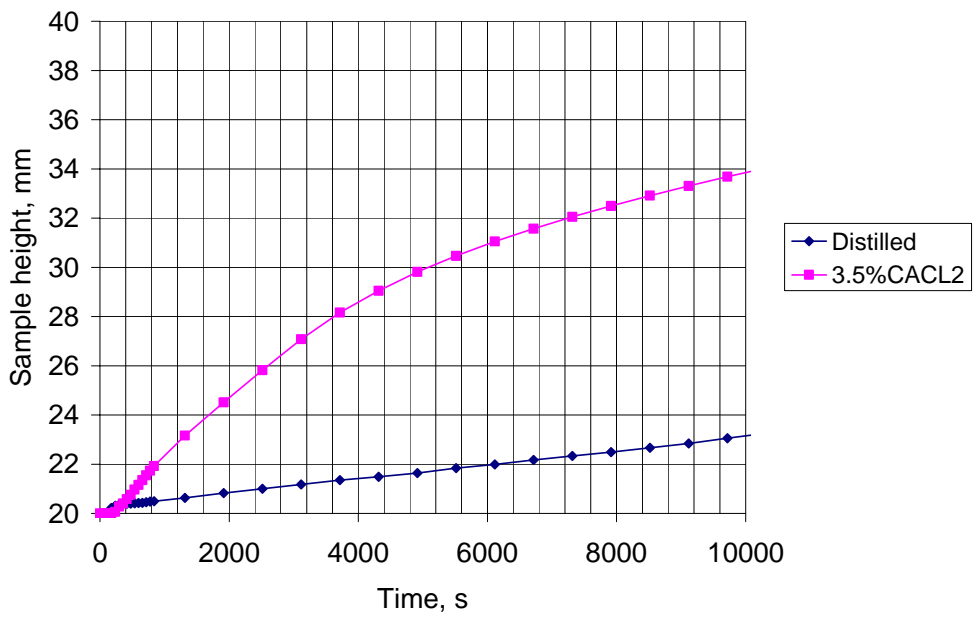


Figure 4-3 The same diagram as Figure 4-2, but showing more in detail the first hours.

Table 4-1. Measured water ratio of the two samples after interruption. Each sample was divided into 5 slices. The slices are counted from the top.

Sample	w %
Distilled-1	478.8
Distilled-2	322.4
Distilled-3	180.6
Distilled-4	73.4
Distilled-5	35.3
3.5% CaCl ₂ -1	87.5
3.5% CaCl ₂ -2	82.6
3.5% CaCl ₂ -3	76.8
3.5% CaCl ₂ -4	67.7
3.5% CaCl ₂ -5	62.4

4.2.2 Swelling into a confined volume

Preparation

Two tests have been performed, one with distilled water and one with 3.5% CaCl₂. The bentonite was compacted directly in the steel ring with 100 MPa, which yields a bulk density of about 2.08 g/cm³. The final height of the samples was aimed at being 30 mm before test start. On each sample a piston (light weight pistons made of PVC) was placed on the top. The piston was locked in order to give a slot between the bentonite surface and the piston of 6.5 mm (Figure 4-4). The samples had free access to water on the top surface during the whole test. A load cell was placed on top of the piston and the swelling pressure continuously recorded. The tests were left to run for about fourteen days.

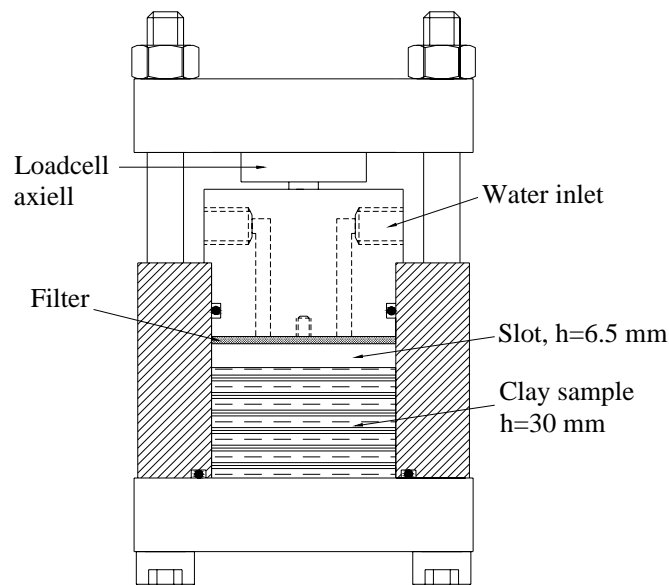


Figure 4-4. Schematic view showing the equipment used in the confined volume tests. The bentonite samples were compacted in the test cylinder with 100 MPa. The samples have free access to water during the entire test period.

Results

The results are shown in Figures 4-5 and 4-6. The tests were left for 14 days and then interrupted and measured. Figure 4-5 shows the swelling pressure as a function of time in logarithmic scale. The difference between distilled and salt water is strong in the beginning but levels out at the end.

Figure 4-6 shows the swelling pressure during the first ten hours. The sample supplied with distilled water reaches 25 kPa swelling pressure after 6 hours while the sample supplied with salt water reaches only needs 1 hour. These results confirm the conclusions from the first tests that if the installation is stopped for an hour it is not likely that the parcel will get stuck in tap water but most likely in sea water.

Table 4-2 shows the measured water ratio distribution after completed tests.

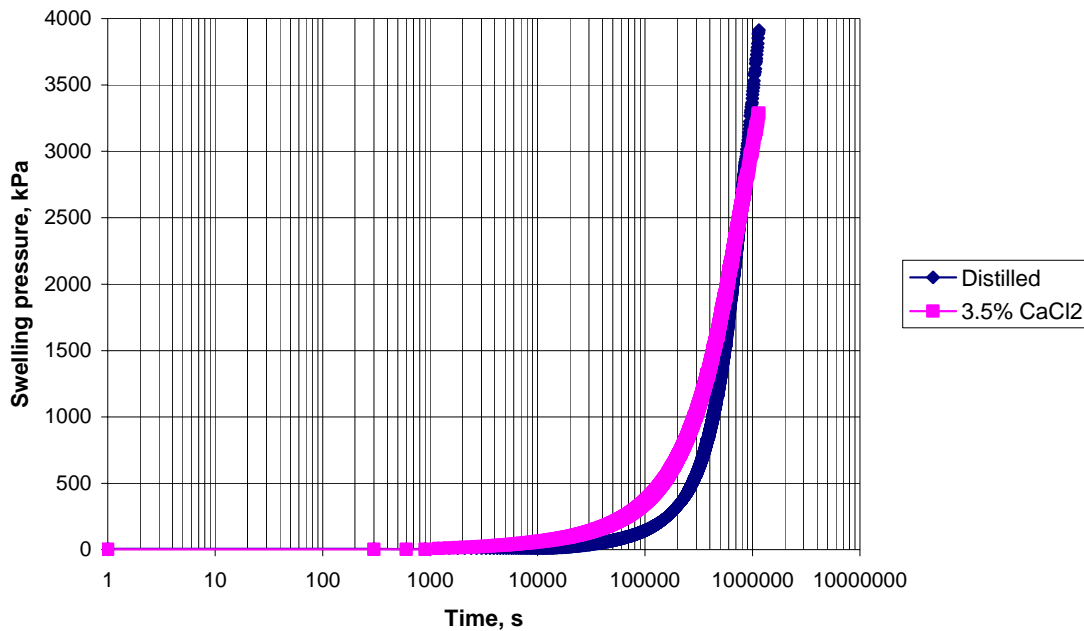


Figure 4-5. Diagram showing the swelling pressure as a function of time.

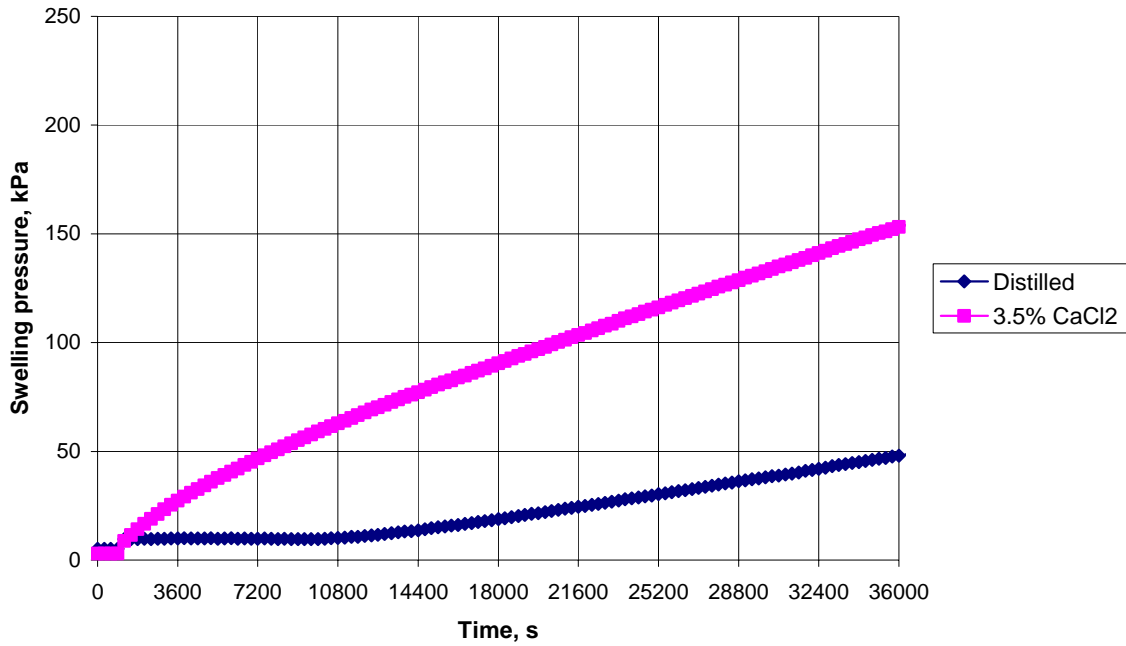


Figure 4-6 The same relation as in Figure 4-5, but showing more in detail the first ten hours.

Table 4-2. Measured water ratio of the two samples after interruption. Each sample was divided into 5 slices. The slices are counted from the top.

Sample	w %
Distilled-1	33.7
Distilled-2	27.0
Distilled-3	23.8
Distilled-4	22.5
Distilled-5	21.7
3.5% CaCl2-1	33.1
3.5% CaCl2-2	26.5
3.5% CaCl2-3	23.7
3.5% CaCl2-4	22.5
3.5% CaCl2-5	22.0

4.3 Swelling through the perforated copper tubes

4.3.1 General

Two alternative configurations regarding the dimensions of the bore hole, the copper tube and the bentonite cylinders have been considered. These alternatives are shown in Figure 4-7. Alternative 1 implies widening of the holes to 100 mm, 2.5 mm slot between the rock and the copper tube and 0.5 mm slot between the tube and the bentonite cylinders. Alternative 2 implies direct plugging of the holes and a very tight design with only 1 mm slot between the copper tube and the rock and no slot at all between the bentonite cylinders and the tube. All tests in this report refer to alternative 1.

Alt.1 Bentonite properties		Alt.2 Bentonite properties	
Start values		Start values	
Bulk density, kg/m ³	2085	Bulk density, kg/m ³	2085
Dry density, kg/m ³	1905	Dry density, kg/m ³	1905
Degree of sat. %	57.2	Degree of sat. %	57.2
Void ratio	0.459	Void ratio	0.459
Saturated values		Saturated values	
Saturated density, kg/m ³	1983	Saturated density, kg/m ³	2086
Dry density, kg/m ³	1533	Dry density, kg/m ³	1692
Void ratio	0.820	Void ratio	0.649

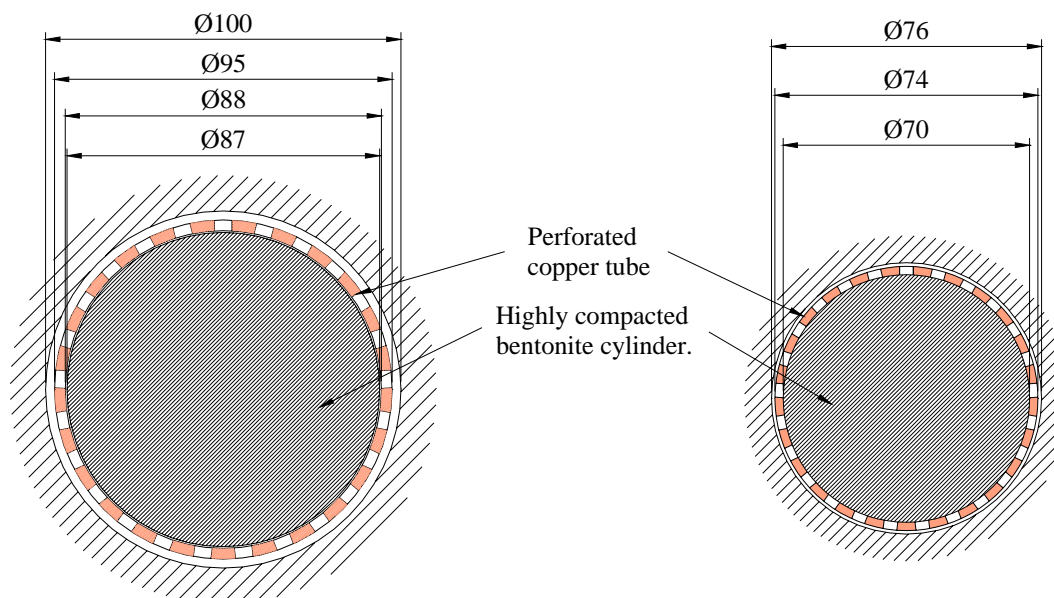


Figure 4-7. Picture showing the dimensions of the two alternatives. The table above shows the initial properties of the bentonite during installation (start values) and the average properties after water saturation and swelling through the holes (saturated values).

Two identical sets of test equipment have been manufactured in order to simulate a short part of a borehole. The test equipment is shown in Figure 4-8. It contains of a test cylinder made of stainless steel simulating the rock confinement, a perforated copper tube and pre compacted bentonite cylinders. The radial swelling pressure is measured in two positions at the periphery and the relative humidity in two positions in the centre of the hole. Water is supplied in the periphery by plastic filter mats. There is a small section in the center of the periphery where no filter is installed with the purpose to measure water flow between the filters and thus study the sealing capacity of the plug.

The bentonite used in these tests is Mx-80. The cylinders have been compacted to the axial pressure 100 MPa. The height is about 50 mm and the diameter 86.6 mm. The bulk density is 2.08 g/cm^3 and the water ratio 9.4%.

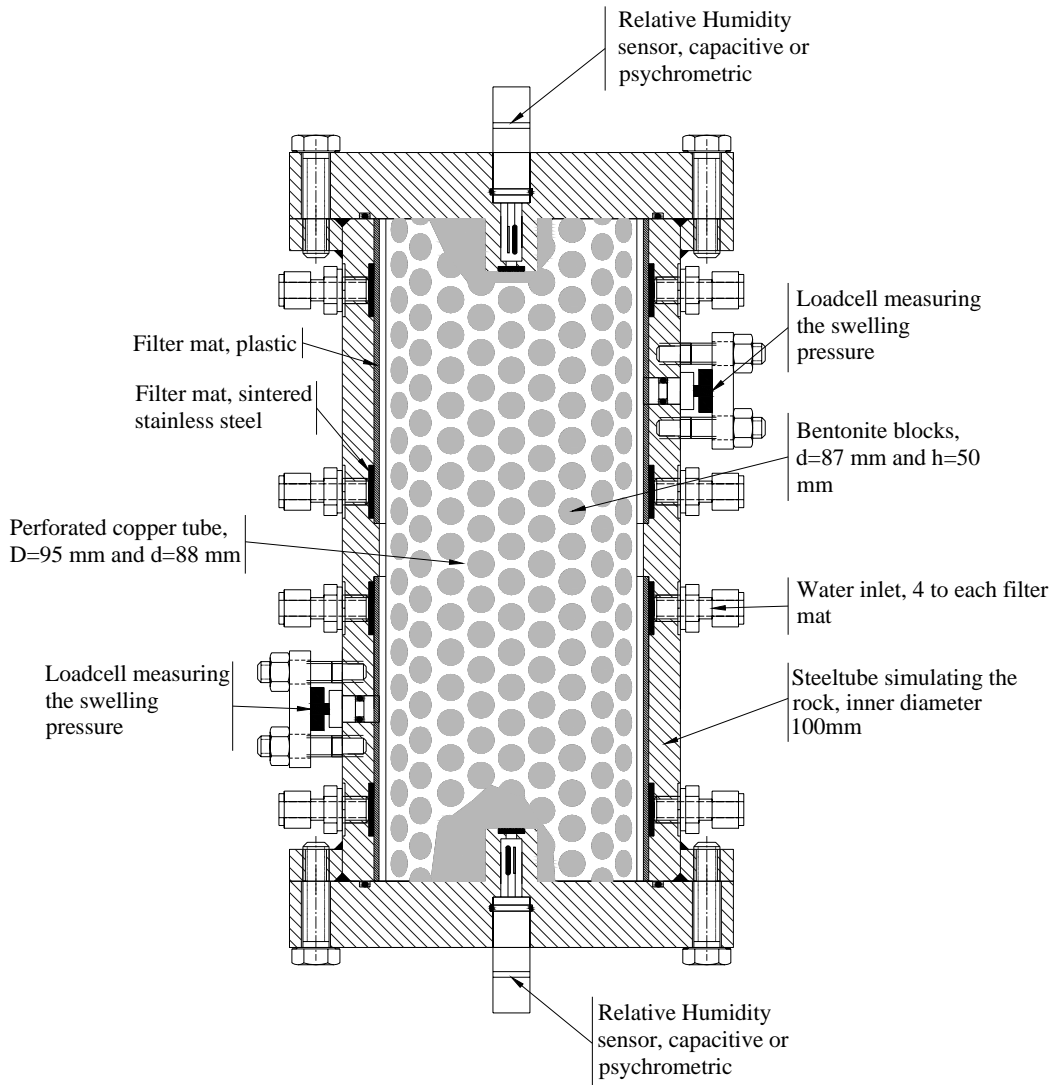


Figure 4-8. Schematic view showing the equipment used in these tests. The samples have had free access to water during the test period.

Three types of tests have been performed in this equipment:

- 1 Short one hour pretests for checking the swelling behavior
- 2 Flow tests for simulating the installation of a plug parcel
- 3 Longtime tests for studying the wetting, swelling and homogenization of the bentonite..

4.3.2 One hour pretests

Two pretests have been performed, one with distilled water and one with 3.5% CaCl_2 added to the water. After preparation of the tests, water was filled into the slot from the bottom for de-airing purpose. The samples had access to water during the 1 hour test period, but the water was not pressurized.

No radial swelling pressure was recorded for any of the test samples. Both samples were easy to extrude and dismantle. The clay in the sample exposed to the salty water had swelled and filled most of the slot, but it was still very easy to take out the copper tube with the clay from the sample holder. Figure 4-9 shows the tubes after extrusion.



Figure 4-9. Pictures taken after interruption of the 1 hour tests. The left picture shows the sample which has been surrounded by distilled water and the right shows the sample which has been surrounded by 3.5% CaCl_2 water. The water ratio of the clay outside the copper was for this sample about 118%.

The results confirm the findings from the swelling tests that one hour is not critical if the hole is filled with salt-free water and that the swelling bentonite in the hole with salt water will reach the rock wall. However, the perforation seems to delay the swelling somewhat, which explains why the sample in salt water was not stuck.

4.3.3 Flow test for simulating the installation of a plug parcel

A flow test simulating the installation of a plug parcel in a full scale water filled borehole has been performed. Lowering a perforated tube with compacted clay into a borehole with a depth of 500 meters implies that about 3.9 cubic meters of water (2.3 cubic meters with the alternative dimensions) have to pass the outer periphery. In order to simulate this event, the confining steel cylinder was equipped with special lids, as shown in Figure 4-10. During 1 hour water from three taps was flushed past the sample. The amount of water was registered and was found to be 3306 liters or 0.92 liters per second.

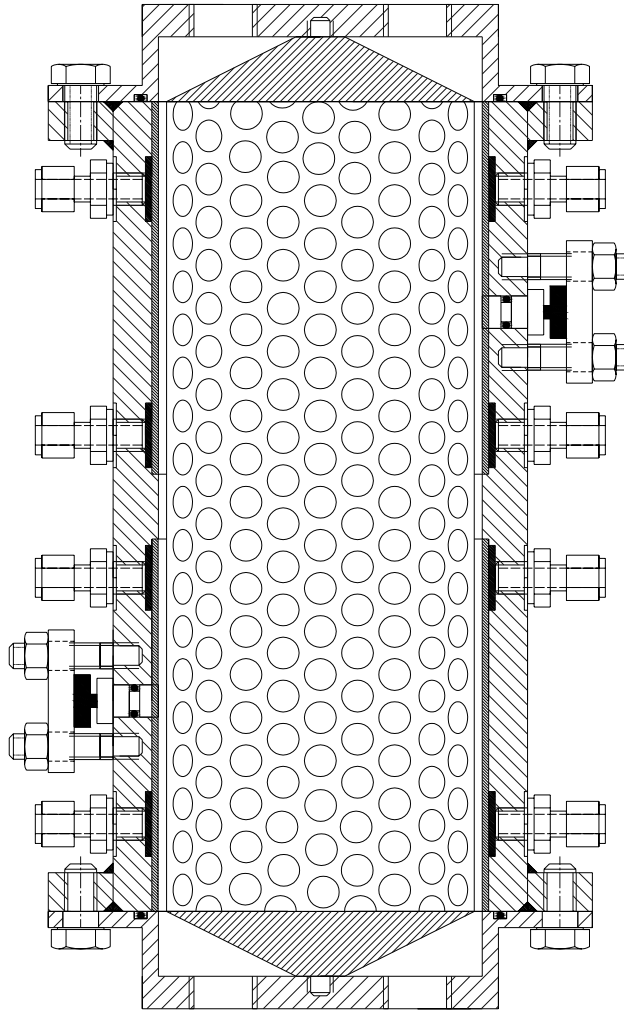


Figure 4-10. Schematic view showing the equipment used in the flow tests. The steel cylinder was equipped with special lids and conical end parts, where the water was let in and forced to pass in the slot between copper tube and rock.

Figure 4-11 shows the test arrangement during testing and directly after interruption. Figure 4-12 shows the perforated tube with the bentonite cylinders after removal from the enclosing. The influence of the flushing water with erosion of bentonite is visible in these pictures, but the amount of bentonite lost is not evident.

The amount of eroded and lost bentonite could be estimated with two techniques, namely by measurement of the dry weight of the bentonite rings before and after the test and by measurement of the bentonite concentration in the out-flowing water.



Figure 4-11. The left picture shows the arrangement of the test. The right picture shows the top of the sample directly after interruption of the test.

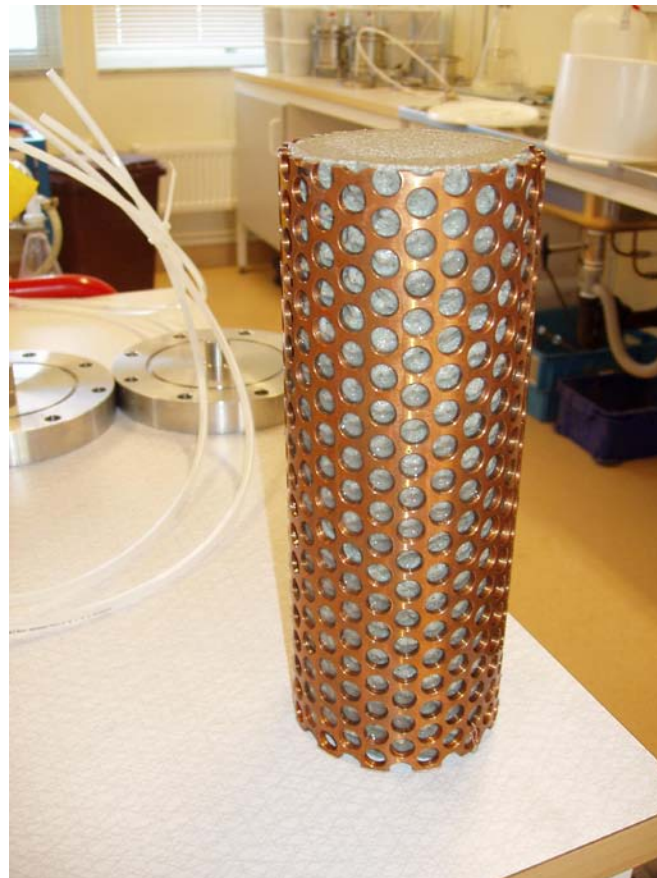


Figure 4-12. Picture showing the copper tube and the installed bentonite immediately after interruption of the test.

Installed amount of dry mass of bentonite in the sample holder was 2785 g. The loss of solid mass during the test was determined by drying and weighing of the remaining bentonite, which yielded a loss of 225 g i.e. 8.1 %.

Samples of the out-flowing water were taken during the test at different times. Each sample was about 1 liter. The water was dried and the amount of solid mass of each sample determined. The result is shown in Table 4-3. A calculation of lost mass gives an amount of about 142 g during 1 hour or 5.1%. This is 83 g less than the weighed mass in the sample holder, but the method is very uncertain since only 5 out of 3306 liters were sampled.

Table 4-3. Measured dry weight of bentonite in the 5 1 litre samples taken during the test

Time after start (min)	Solid mass in water (g)
5	0.019
10	0.029
15	0.021
30	0.041
60	0.054

The loss of bentonite is thus very high (5-8%), which shows that this is a real problem that has to be solved. The loss will of course be higher in 1000 m holes and probably also higher if the water in the hole is salty.

4.3.4 Long time tests with measurement of the wetting process and the swelling pressure

Test start

Two identical tests were performed with the equipment described in Figure 4-8. The only difference between the tests was the water used to saturate the samples, which in one test contained no salt and in the other test contained 3.5 % CaCl₂. After preparation of the tests, water was filled into the slot from the bottom for de-airing purpose. The samples had access to water from the filters during the whole test. The water pressure was raised to 4 MPa in two steps. Figure 4-13 shows a picture of the test arrangement.

Measurement of swelling pressure and the wetting process

The radial swelling pressure was measured in the periphery outside the perforated tube in two points as shown in Figure 4-8. The pressure was measured by use of a small piston with the diameter $d=10$ mm in contact with a load cell. In order to detect if there is a difference in swelling pressure just opposite to a hole in the perforated copper tube and in the between the holes, the two pistons were placed according to this.

Relative humidity (RH) was measured in two points in the centre of the samples as shown in Figure 4-8. A capacitive sensor was placed in the top and a psychrometer in the bottom. The reason for using two different devices is that although the measuring range for the capacitive sensors is 0-100% the accuracy between 90 and 100% is not good (+/- 2%). The measuring range for the psychrometers is only 95-100% but the accuracy in that limited range is very high.

The tests were left for almost 80 days for wetting and homogenization. The measured results are shown in Figures 4-14 and 4-15. The time until equilibrium in swelling pressure and RH are about 20 days for both tests but the total pressure differs significantly. At equilibrium the swelling pressure defined as the measured total pressure minus the water pressure was

$\sigma_s = 2800$ kPa for the sample with distilled water and

$\sigma_s = 600$ kPa for the sample with salt water.

The results also show that the difference between the swelling pressure measured at the holes and between the holes was insignificant for the salt water test and about 300 kPa for the distilled water test

The measured RH is very logic in the distilled water test with an increase in RH with time until 100% after 20 days for both transducers. The increase in RH in the salt water test is a little faster but ends in a different RH for the two transducers. The psychrometer ends at RH=99.5% while the Vaisala transducer ends at RH=94%. The expected value is 98.5% since that is the tabulated value for 3.5% CaCl₂. The reason for the difference is not clear.



Figure 4-13. Picture of the test equipment for the long time tests.

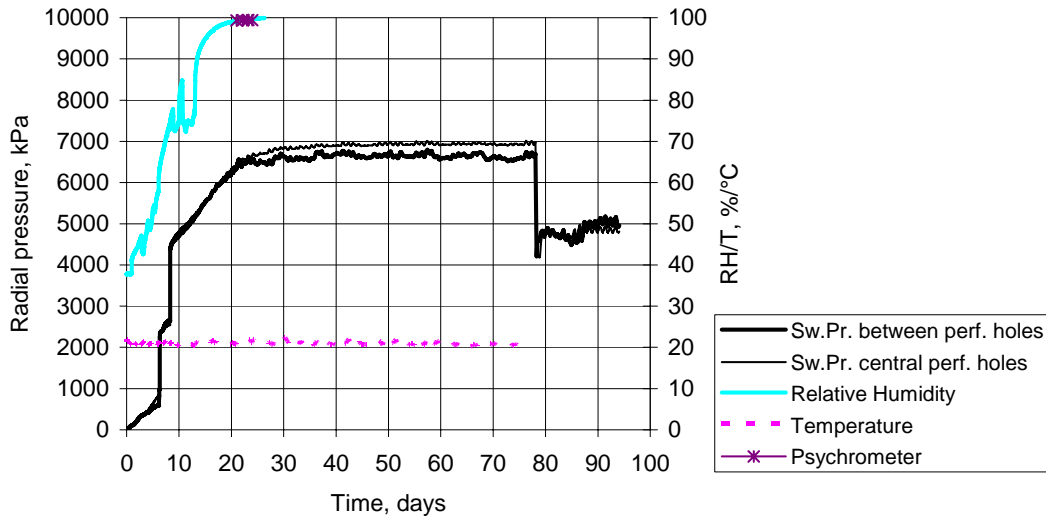


Figure 4-14. Diagram showing the radial pressure build up during saturation for the test with distilled water. The diagram also shows the Relative Humidity in the centre of the bentonite. The pore water pressure was raised to 4 MPa in two steps. The dip in pressure after 78 days is caused by a decrease in water pressure during the hydraulic conductivity measurement.

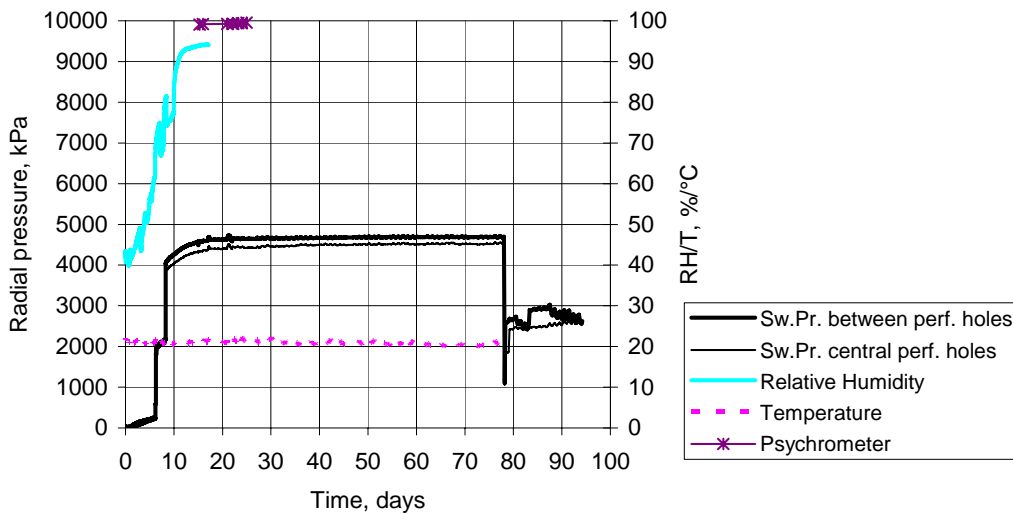


Figure 4-15. Diagram showing the radial pressure build up during saturation for the test with 3.5% CaCl_2 water. The diagram also shows the Relative Humidity in the centre of the bentonite. The pore water pressure was raised to 4 MPa in two. The dip in pressure after 78 days is caused by a decrease in water pressure during the hydraulic conductivity measurement.

Flow testing for measurement of the hydraulic conductivity

In order to determine the sealing effects, an attempt has been made to measure the hydraulic conductivity of the bentonite that has swelled out between the perforated tube and the “rock” after finalized wetting. The measuring principle was to set the water pressure in the lower filter (see Figure 4-8) to 2300 kPa and the water pressure in the upper filter to 1800 kPa. After reaching steady state conditions the water inflow and outflow were measured. The hydraulic conductivity K (m/s) was calculated by assuming that all water was flowing through the bentonite in the slot outside the copper tube.

The results from the measurements are shown in Figure 4-16 and 4-17. The evaluation of the hydraulic conductivity was problematic since the amounts of water was very small and the influence of temperature variations very strong. Both the pressurizing devices and the clay samples contain water and the thermal expansion of this water volume is quite strong also for small temperature changes that take place in the laboratory between days and nights (about 1 °C).

The results from the flow test in the sample with distilled water yielded a net inflow in both mats after some time. This shows that water is either still taken up by the sample or that there is leakage somewhere. The hydraulic conductivity can thus be calculated either as only the inflow (conservative) or as the inflow minus the outflow. The former evaluation yields $9 \cdot 10^{-13}$ m/s and the latter yields $5 \cdot 10^{-13}$ m/s.

The results from the flow tests in the sample with salty water are more logic. The hydraulic conductivity for the sample percolated with 3.5% CaCl_2 water was found to be about $2 \cdot 10^{-12}$.

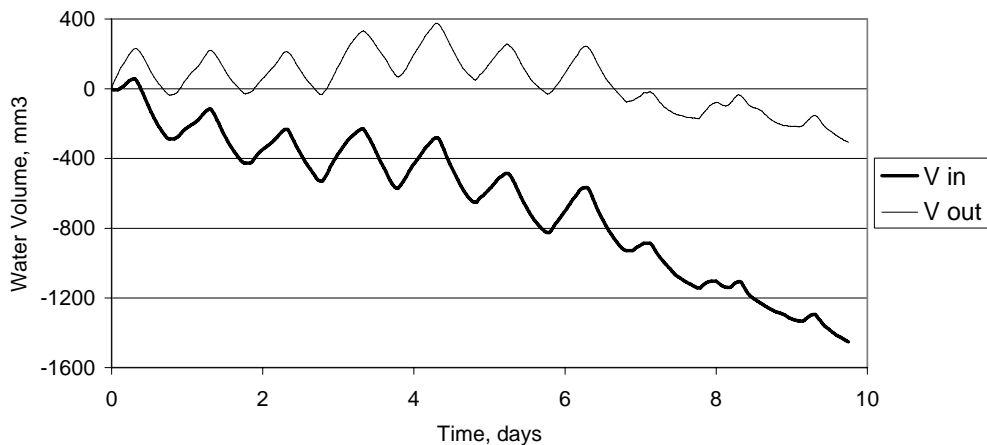


Figure 4-16. Diagram showing the water flow in the two filter mats in the sample with distilled water. The bold line shows the volume change in the lower filter which was pressurized with 2300 kPa and the thin line shows the water flow in the upper filter, which was pressurized with 1800 kPa. Minus stands for water inflow which means that water is still taken up by the bentonite.

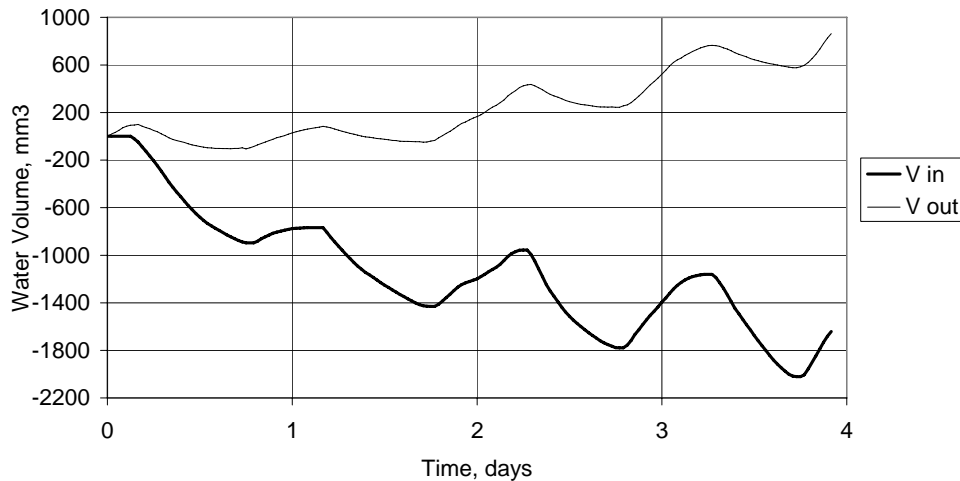


Figure 4-17. Diagram showing the water flow in the two filter mats in the sample with 3.5% CaCl₂ water. The bold line shows the volume change in the lower filter, which was pressurized with 2300 kPa and the thin line shows the water flow in the upper filter which was pressurized with 1800 kPa. Minus stands for water inflow.

Sampling after finalized test

The two long time tests were interrupted about 95 days after test start. The dismantling and sampling were done as follows:

1. The water pressure was lowered to atmospheric pressure.
2. All tubes and the load cells were disconnected.
3. The clay samples including copper tubes were pressed out from the steel cylinder by use of a hydraulic press.
4. Samples for determination of water ratio and density distribution of the bentonite was taken according to the following schedule:
 - **The slot between the copper tube and the “rock” (steel confinement).**
Water ratio was determined in four directions (A, B, C and D) on 10 levels (every 2.5 cm).
 - **The holes in the copper tube.**
Water ratio was determined in four directions on 5 levels (every 5 cm).
 - **Inside the copper tube.**
Water ratio and density was determined in two directions (A and C) on three levels (4, 12.5 and 21 cm).

When samples had been taken on the outer slot, the copper tube was cut in two pieces with an angle grinder in order to facilitate the sampling of the inner parts.

The borehole plugs could be pressed out in one piece as shown in Figure 4-18. By use of a ruler and a knife, samples could be taken with good precision. When cutting the inner parts a band saw was used.

The water ratio was determined by use of a laboratory balance and an oven where the samples were dried for 24 h at a temperature of 105°. The bulk density of the samples taken inside the perforated tube was determined by weighing the samples in air and immediately thereafter submerging them in paraffin oil. No density determination was done on the samples taken outside the tube and in the holes due to that the amount of material is too small. For calculations of the density of the samples taken in the outer slot and in the holes in the copper tube it has been assumed they are water saturated.

Figures 4-19 and 4-20 show pictures taken during dismantling.



Figure 4-18 Picture showing the sample saturated with distilled water immediately after dismantling. It was possible to see the pattern from the perforated tubes in the clay surface. Both samples looked very similar.

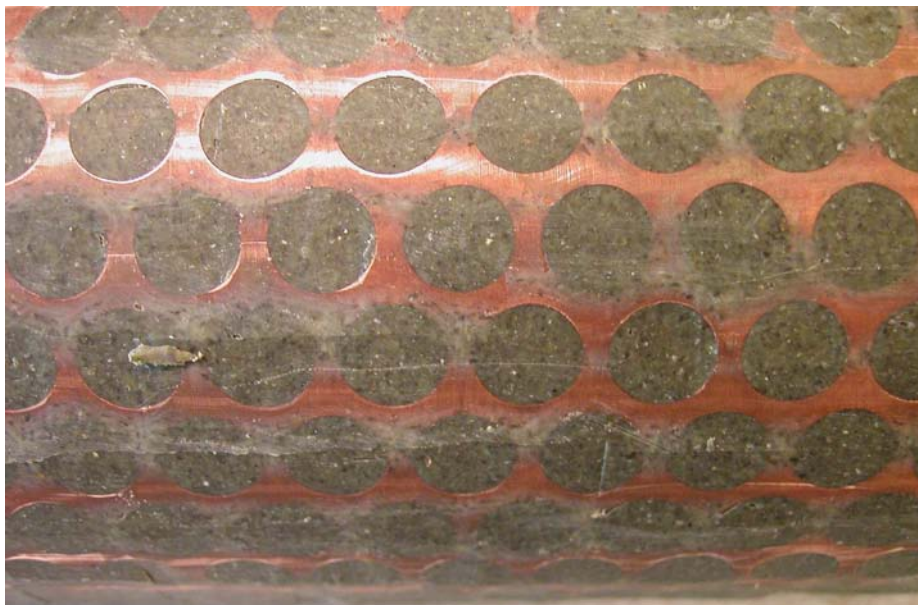


Figure 4-19 Picture showing the copper tube after removal and sampling of the bentonite outside the tube.



Figure 4-20 Picture showing the clay sample after dismantling of the copper tube. The clay from the holes is still solid and this facilitated the sampling.

The results of the sampling are summarized in Figures 4-21 to 4-25 for the plug supplied with distilled water and in Figures 4-26 to 4-30 for the plug supplied with salt water. The results show that the bentonite is as expected not homogeneous in radial direction. The friction during swelling through the holes have created a water ratio and density gradient in the plug. However, the plug is very homogeneous in tangential and axial directions, which was also expected since there is an axial symmetry and no difference in geometry in axial direction. For the bentonite in the slot it has not been possible to distinguish between the properties at the holes and between the holes, but an average value has been determined.

The difference between the plug supplied with distilled water and salty water is surprisingly small, considering the large difference in swelling pressure. The average water ratio, void ratio and density in the slot and in the holes are compared in Table 4-4. The water ratio is slightly higher and the density slightly lower in the plug with salty water than in the plug with distilled water.

Table 4-4. Comparison of the properties measured in the plug supplied with salty water and the plug with distilled water.

	Plug in distilled water		Plug in salty water	
	Slot	Holes	Slot	Holes
Water ratio (%)	42	34	43	36
Void ratio	1.16	0.95	1.20	0.98
Density (kg/m³)	1 830	1 920	1 810	1 890

The expected swelling pressure measured from constant volume tests of MX-80 saturated with distilled water is at the void ratio 1.16 is only 800 kPa compared to the measured swelling pressure 2800 kPa in the periphery of the plug. To yield 2800 kPa the void ratio needs to be about 0.9, which corresponds to a water ratio of 32%. This huge difference needs to be explained. One reason could be that the sample has taken up water during dismantling but an increase in water ratio of 10% is not very probable. A more plausible explanation is the complicated stress path in the plug test. The swelling pressure relations stem from constant volume tests but the bentonite in the periphery of the plug first swells to a very loose gel, which then consolidates by the pressure from the expansive bentonite inside the perforated tube. At consolidation from a very soft gel an average stress of about 2500 kPa has been both measured and modelled during oedometer tests (Figures 3-3 and 5-8 in /2/).

The expected swelling pressure from the test with salty water at the void ratio 1.2 is according to the relations taken from constant volume tests about 250 kPa compared to the measured swelling pressure 600 kPa. There is thus the same kind of difference although it is not as large. The reason that the difference is smaller is probably that the gel will not be as soft in salty water as in distilled water.

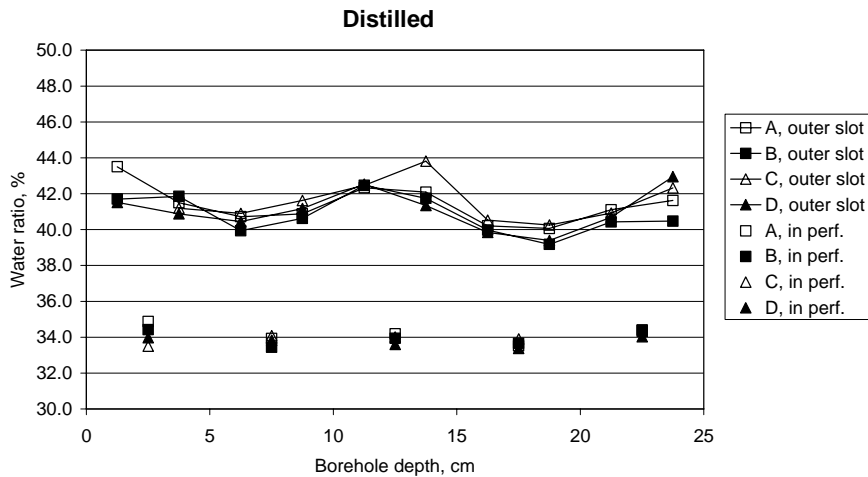


Figure 4-21. Diagram showing the water ratio distribution in the slot between the copper tube and the “rock” and in the perforated holes.

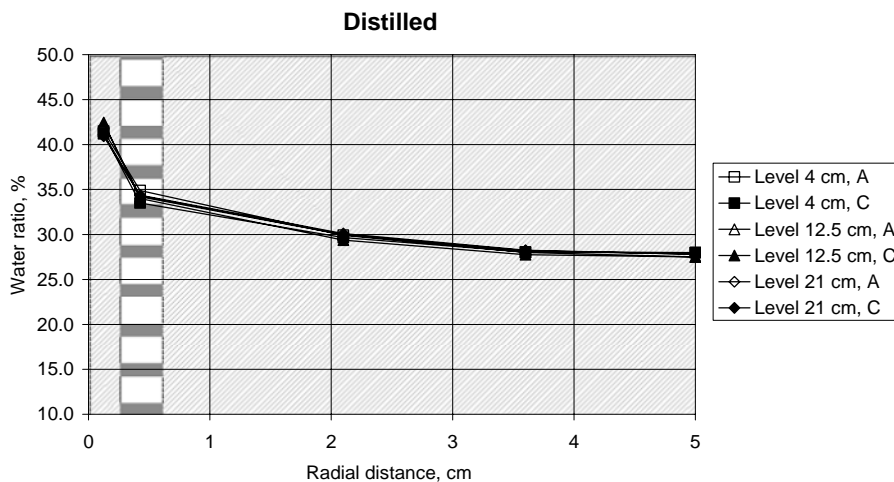


Figure 4-22. Diagram showing the radial water ratio distribution on three levels and in two directions.

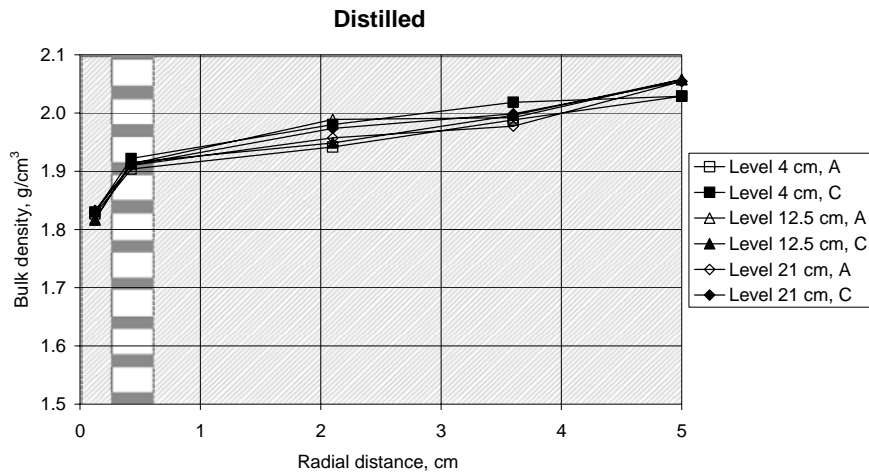


Figure 4-23. Diagram showing the radial bulk density distribution on three levels and in two directions. For calculating the density in the outer slot and in the holes in the perforation it has been assumed that the samples are water saturated.

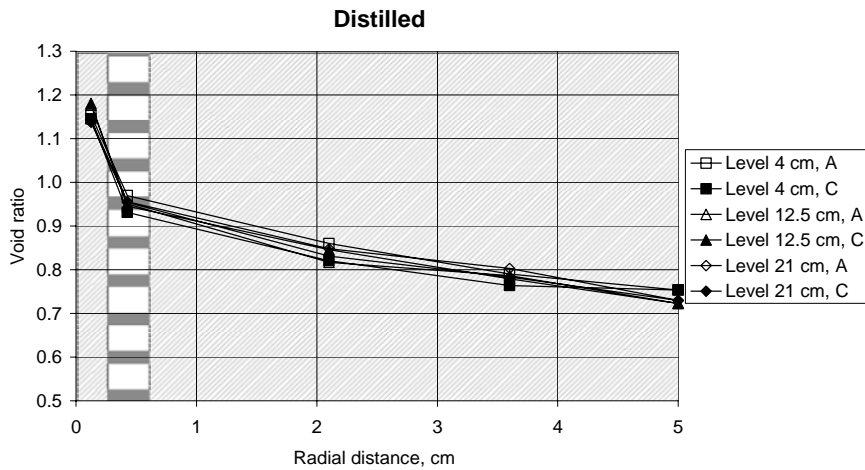


Figure 4-24. Diagram showing the radial void ratio distribution on three levels and in two directions. For calculating the void ratio in the outer slot and in the holes in the perforation it has been assumed that the samples are water saturated.

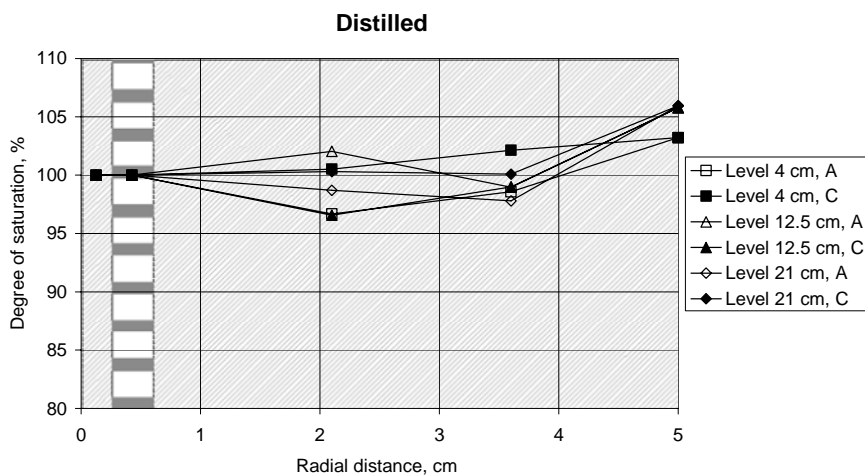


Figure 4-25. Diagram showing the radial degree of saturation distribution on three levels and in two directions.

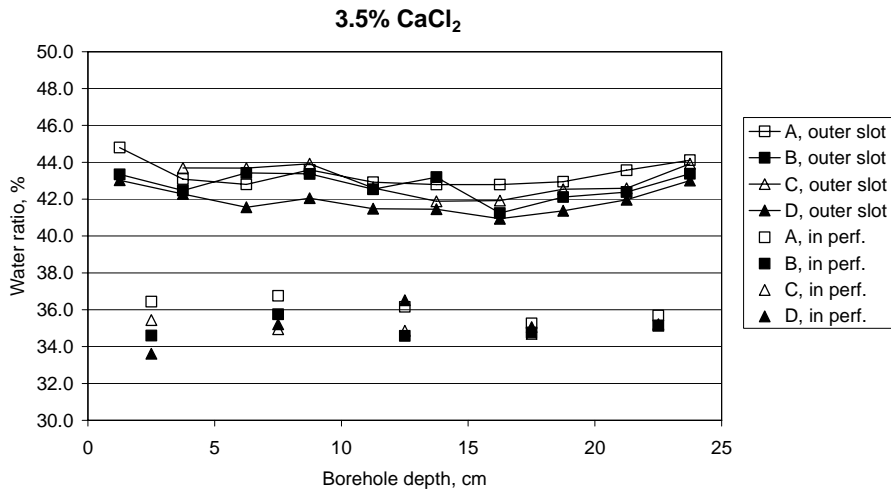


Figure 4-26 Diagram showing the water ratio distribution in the slot between the copper tube and the “rock” and in the perforated holes.

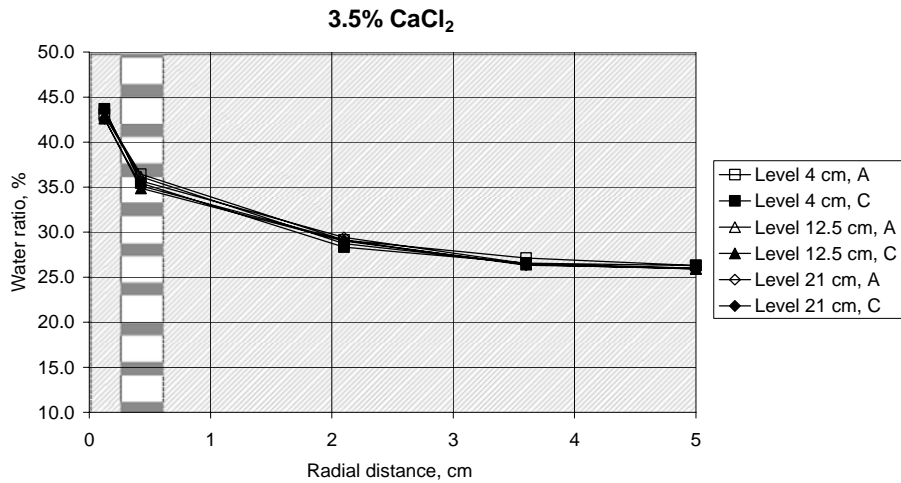


Figure 4-27 Diagram showing the radial water ratio distribution on three levels and in two directions.

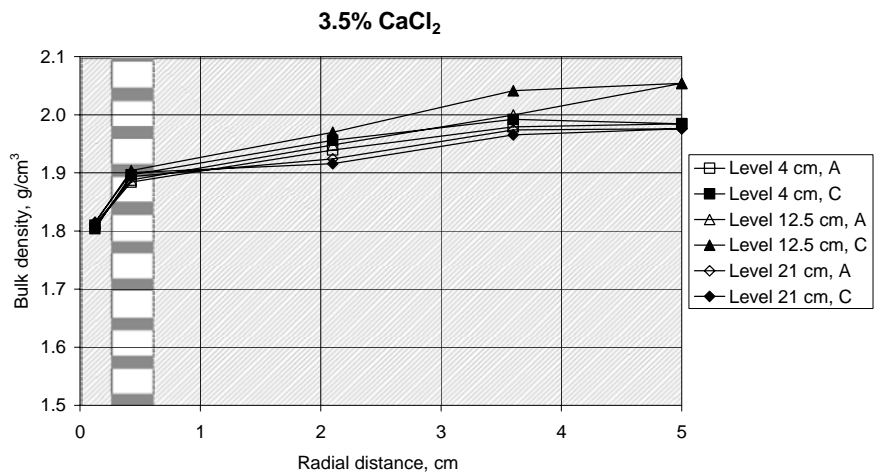


Figure 4-28 Diagram showing the radial bulk density distribution on three levels and in two directions. For calculating the density in the outer slot and in the holes in the perforation it has been assumed that the samples are water saturated.

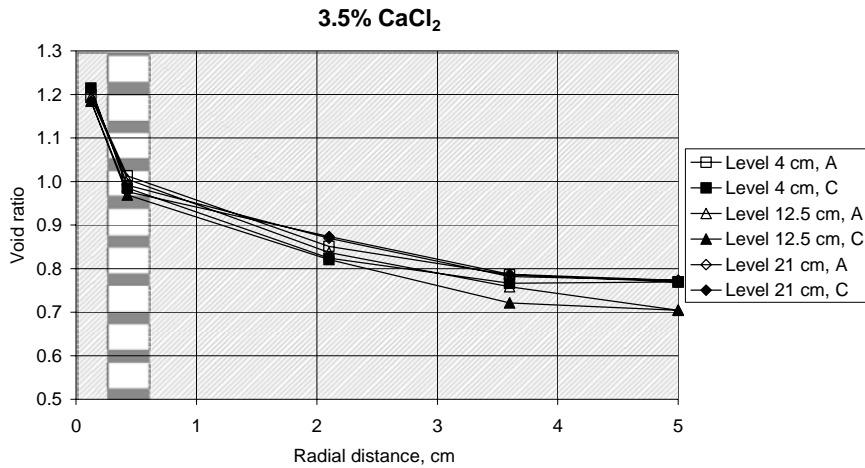


Figure 4-29 Diagram showing the radial void ratio distribution on three levels and in two directions. For calculating the void ratio in the outer slot and in the holes in the perforation it has been assumed that the samples are water saturated.

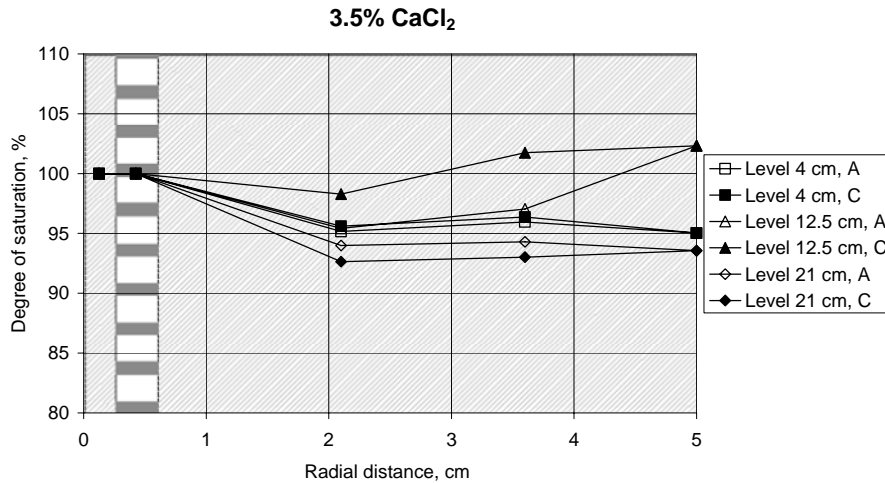


Figure 4-30 Diagram showing the radial degree of saturation distribution on three levels and in two directions.

4.3.5 Comparison between the measured results and the models

In chapter 3 the average swelling pressure was predicted for the two cases tested in the laboratory. A comparison yields that the predicted average swelling pressure for the plug in distilled water 2840 kPa agrees extremely well with the measured value 2800 kPa. However, for the plug in 3.5% CaCl₂ the agreement is rather bad since the predicted value was 1890 kPa and the measured only 600 kPa. A reason for the latter disagreement could be that the predictions were based on NaCl water instead of CaCl₂ water.

5 Summary of results and conclusions

This study has yielded the following results and conclusions:

The swelling of bentonite is considerably faster in water with 3.5% CaCl₂ content than in distilled water. Salt water can have maximum a one-hour stop during installation while fresh water can have a 5-10 hours stop before the parcel gets stuck.

The installation of a plug parcel at 500 m depth in fresh water results in almost a 10% loss of bentonite. The technique thus needs to be modified.

A theoretical model of the swelling of bentonite has been made and this shows that the optimum hole diameter is 10 mm for the predicted geometry, and that the minimum swelling pressure against the rock between the holes is 1 960 kPa for fresh water and 950 kPa for salt water.

The long term tests show that complete swelling and homogenisation is obtained after 10-20 days. The measured mean swelling pressure against the rock was 2 800 kPa for the fresh water case and 600 kPa for salt water. This mean pressure is in good agreement with the predicted mean pressure for fresh water (2 860 kPa) but not for salt water (1 950 kPa). The reason for the latter deviation might be that data for the bentonite has been obtained from tests with NaCl in the water instead of CaCl₂. The mean void ratio between tube and rock was fairly high in both cases (1.15-1.2).

Measurement of the hydraulic conductivity between tube and rock shows that it was 5-9 10⁻¹³ m/s for fresh water and 2 10⁻¹² for salt water.

References

Pusch R., 2004. Pilot study of borehole plug maturation. Draft report.

Börgesson L., Johannesson L.-E., Sandén T. and Hernelind J.; 1995. Modelling of the physical behaviour of water saturated clay barriers. Laboratory tests, material models and finite element application. SKB TR-95-20.

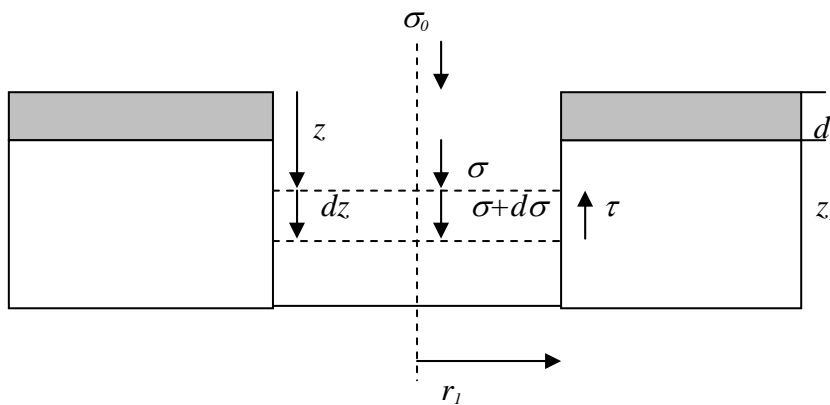
Simplified calculation of the swelling of bentonite through the holes of the perforated container

Lennart Börgesson

Clay Technology AB

Round holes are considered. Only the stage after completed swelling and homogenisation is considered. The calculation is made in two steps. The first step regards the stresses after swelling through the holes and considers a state of equilibrium in only the direction perpendicular to the rock surface (axial direction in relation to the holes in the container). The second step regards the stresses after swelling into the slot between the tube and the rock and considers a state of equilibrium in only the direction parallel to the rock surface (radial direction in relation to the holes in the container).

Step 1. Equilibrium after swelling through the holes:



d = container thickness

z_1 = distance between container and the rock

r_1 = hole radius

σ_0 = swelling pressure at $z = 0$

Force equilibrium in axial direction:

$$d\sigma \cdot \pi r_1^2 = \sigma \tan \phi \cdot 2\pi r_1 \cdot dz$$

$$\frac{d\sigma}{\sigma} = \frac{2 \tan \phi}{r_1} \cdot dz$$

$$dz = \frac{r_1}{2 \tan \phi} \cdot \frac{d\sigma}{\sigma}$$

Integrating:

$$\int_0^z dz = \frac{r_1}{2 \tan \phi} \int_{\sigma_0}^{\sigma} \frac{d\sigma}{\sigma}$$

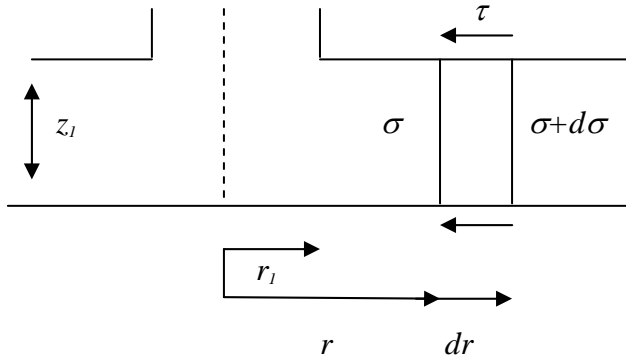
$$z = \frac{r_1}{2 \tan \phi} (\ln \sigma - \ln \sigma_0)$$

σ_1 = average swelling pressure in the slot (at $z = d+z_1/2$)

$$e^{(\ln \sigma_1 - \ln \sigma_0)} = e^{-\frac{2z \tan \phi}{r_1}}$$

$$\sigma_1 = \sigma_0 \cdot e^{\frac{-2(d+z_1/2) \tan \phi}{r_1}} \quad (1)$$

Step 2a. Equilibrium after swelling into the slot without considering in-plane stresses



Force equilibrium in radial direction:

$$\sigma \cdot 2\pi r z_1 - (\sigma + d\sigma) 2\pi (r + dr) z_1 = [\pi (r + dr)^2 - \pi r^2] \left(\sigma + \frac{d\sigma}{2} \right) \cdot \tan \phi \cdot 2$$

$$-\sigma dr - rd\sigma = \sigma dr \cdot \frac{2 \tan \phi}{z_1}$$

$$-\frac{dr}{r} - \frac{d\sigma}{\sigma} = dr \frac{2 \tan \phi}{z_1}$$

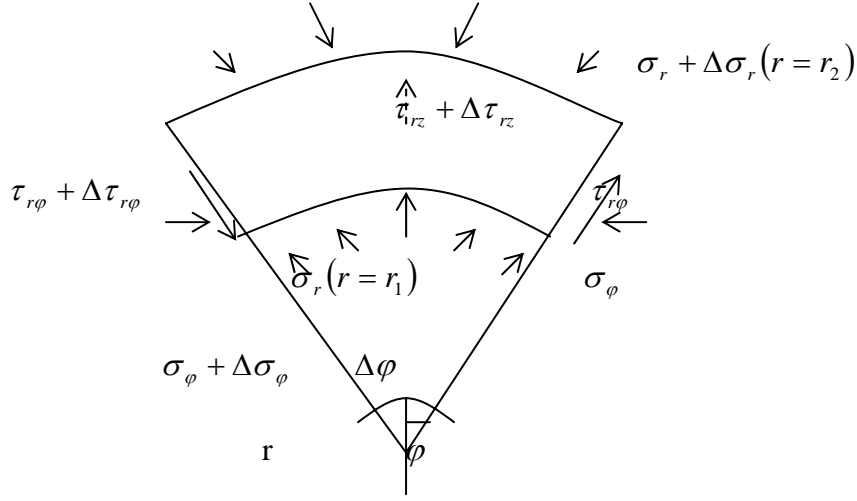
Integrating from r_1 to a specified maximum distance between the holes r_2 :

$$-\int_{\sigma_1}^{\sigma_2} \frac{d\sigma}{\sigma} = \int_{r_1}^{r_2} \frac{dr}{r} + \frac{2 \tan \phi}{z_1} \int_{r_1}^{r_2} dr$$

$$\ln \sigma_1 - \ln \sigma_2 = \ln \frac{r_2}{r_1} + (r_2 - r_1) \frac{2 \tan \phi}{z_1}$$

$$\ln \sigma_2 = \ln \sigma_1 - \ln \frac{r_2}{r_1} - \frac{r_2 - r_1}{z_1} \cdot 2 \tan \phi \quad (2)$$

Step 2b. Equilibrium after swelling into the slot (general case):



$$P_1 - (\sigma_r + \Delta\sigma_r)(r + \Delta r)\Delta\phi \cdot \Delta z + \sigma_r \cdot r\Delta\phi\Delta z + \tau_{r\phi} \cdot \Delta r \cdot \Delta z - (\tau_{r\phi} + \Delta\tau_{r\phi}) \cdot \Delta r\Delta z + \cdot$$

$$(\sigma_\phi + \sigma_\phi + \Delta\sigma_\phi) \cdot \Delta r \cdot \Delta z + \frac{\Delta\phi}{z} + [(\tau_{rz} + \Delta\tau_{rz}) - \tau_{rz}] \cdot \Delta\phi \cdot \left[\frac{(r+\Delta r)^2}{2} - \frac{r^2}{2} \right] = 0$$

$$- \sigma_r r \Delta\phi \Delta z - \sigma_r \Delta r \Delta\phi \Delta z - \Delta\sigma_r r \Delta\phi \Delta z - \Delta\sigma_r \Delta r \Delta\phi \Delta z + \sigma_r r \Delta\phi \Delta z - \Delta\tau_{r\phi} \Delta r \Delta z + \sigma_\phi \Delta r \Delta z \Delta\phi + \Delta\sigma_\phi \Delta r \frac{\Delta\phi}{2} \cdot \Delta z + \Delta\tau_{rz} \cdot \Delta\phi \left(r \cdot \Delta r + \frac{\Delta r^2}{2} \right) = 0$$

$$\left(\sigma_\phi - \sigma_r \right) - \Delta\sigma_r \left(\frac{r}{\Delta r} + 1 \right) + \Delta\sigma_\phi / 2 - \frac{\Delta\tau_{r\phi}}{\Delta\phi} + \frac{\Delta\tau_{rz}}{\Delta z} \left(r + \frac{\Delta r}{2} \right) = 0$$

$$\Delta\sigma_\phi = 0$$

$$\frac{\Delta\tau_{r\phi}}{\Delta\phi} = 0$$

$$\Delta\tau_{rz} = -2\sigma_r \cdot \tan\phi$$

\Rightarrow

$$\left(\sigma_\phi - \sigma_r \right) - \Delta\sigma_r \frac{r}{\Delta r} - \frac{2\sigma_r \tan\phi}{\Delta z} \cdot r = 0 \quad (3)$$

Assuming isotropic swelling pressure:

$$\begin{aligned}
 \sigma_r &= \sigma_\phi \\
 \Rightarrow \\
 -\Delta\sigma_r \frac{r}{\Delta r} - \frac{2\sigma_r \tan \phi}{\Delta z} \cdot r &= 0 \\
 -\frac{d\sigma_r}{\sigma_r} \Delta z &= 2 \tan \phi \cdot \Delta r \\
 -\left(\ln \frac{\sigma_2}{\sigma_1} \right) \cdot z_1 &= 2 \tan \phi (r_2 - r_1) \\
 \sigma_2 &= \sigma_1 \cdot e^{\frac{2 \tan \phi (r_2 - r_1)}{z_1}} \quad (4)
 \end{aligned}$$

Assuming unisotropic swelling pressure:

$$\begin{aligned}
 \sigma_\phi / \sigma_r &= \nu / (1 - \nu) \Rightarrow \\
 \sigma_\phi - \sigma_r &= \sigma_r \left(\frac{\nu}{1 - \nu} - 1 \right) \\
 K &= \left(\frac{\nu}{1 - \nu} - 1 \right) \Rightarrow \\
 \sigma_\phi - \sigma_r &= \sigma_r \cdot K \quad (5)
 \end{aligned}$$

Eqn 5 applied to Eqn 3 yields

$$\begin{aligned}
 -\Delta\sigma_r \frac{r}{\Delta r} + \sigma_r \left(+K - \frac{2 \tan \phi}{\Delta z} \cdot r \right) &= 0 \\
 \frac{d\sigma_r}{\sigma_r} \Delta z &= \left(K \frac{dr}{r} \Delta z - 2 \tan \phi dr \right) \\
 \left(\ln \frac{\sigma_2}{\sigma_1} \right) z_1 &= K \cdot z_1 \cdot \ln \frac{r_2}{r_1} - 2 \tan \phi (r_2 - r_1) \\
 \frac{\sigma_2}{\sigma_1} &= \cdot e^{\frac{K \ln(\frac{r_2}{r_1}) - 2 \tan \phi (\frac{r_2 - r_1}{z_1})}{z_1}} \\
 \ln \sigma_2 &= \ln \sigma_1 + K \ln \frac{r_2}{r_1} - \frac{r_2 - r_1}{z_1} \cdot 2 \tan \phi \quad (6)
 \end{aligned}$$

ν	K
0	-1
0.3	-0.57
0.5	0

Thus $\nu=0$ in Eqn 6 yields Eqn 2 and $\nu=0.5$ yields Eqn 4.

Appendix II

1 Homogenization of borehole plugs of Basic Type – 1 month tests

1.1 Test layout

Tests of this type have been made earlier within this project but not with the final decided geometry and with the right type of bentonite cylinders.

Two sets of test equipment have been manufactured in order to simulate a short part of a borehole, Figure 1-2 and 1-3. The test equipment contains a perforated copper tube and pre compacted bentonite cylinders. The radial swelling pressure is measured in two positions and the relative humidity in two positions.

In this test series totally four tests will be performed:

1 1 month tests.

- One test will be performed simulating a loss of material due to erosion of 7.5%. The material will be mechanically eroded.
- One test will be performed simulating a loss of material due to erosion of 7.5%. The material will be eroded in a water flow.

2 1 year tests.

- One test will be performed simulating a loss of material due to erosion of 7.5%. The material will be mechanically eroded.
- One test will be performed simulating a loss of material due to erosion of 7.5%. The material will be eroded in a water flow.

In this report are the results from the one month tests reported.

Table 1-1. Table showing the input data to the tests and the calculated saturated values of the bentonite.

Calculated test data	
Start values, bentonite samples	
Bulk density, kg/m ³	2145
Dry density, kg/m ³	2035
Water ratio, %	6.0
Degree of sat. %	45
Void ratio	0.364
Saturated values in borehole	
Saturated density, kg/m ³	1981
Dry density, kg/m ³	1521
Void ratio	0.824

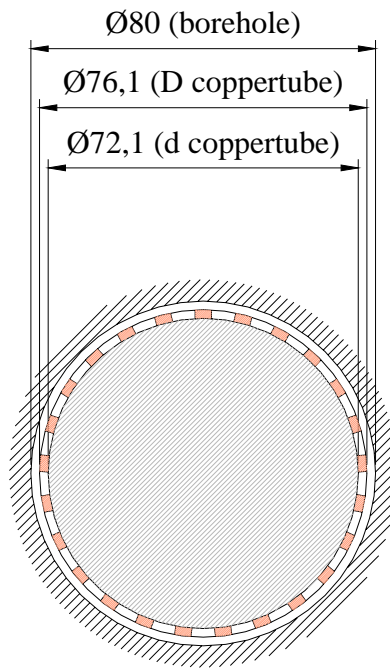


Figure 1-1. Picture showing the dimensions of the borehole and the copper tube.

Bentonite cylinders.

The bentonite used in these tests is Mx-80 Wyoming bentonite. In order to achieve a high dry density of the compacted material, the powder is dried to a water ratio of about 6%. The bentonite cylinders are compacted with a pressure of 200 MPa. The cylinders have a height of about 50 mm and a diameter of 71.3/70.9 mm (somewhat conical). The input data of the bentonite is shown in Table 1-1.

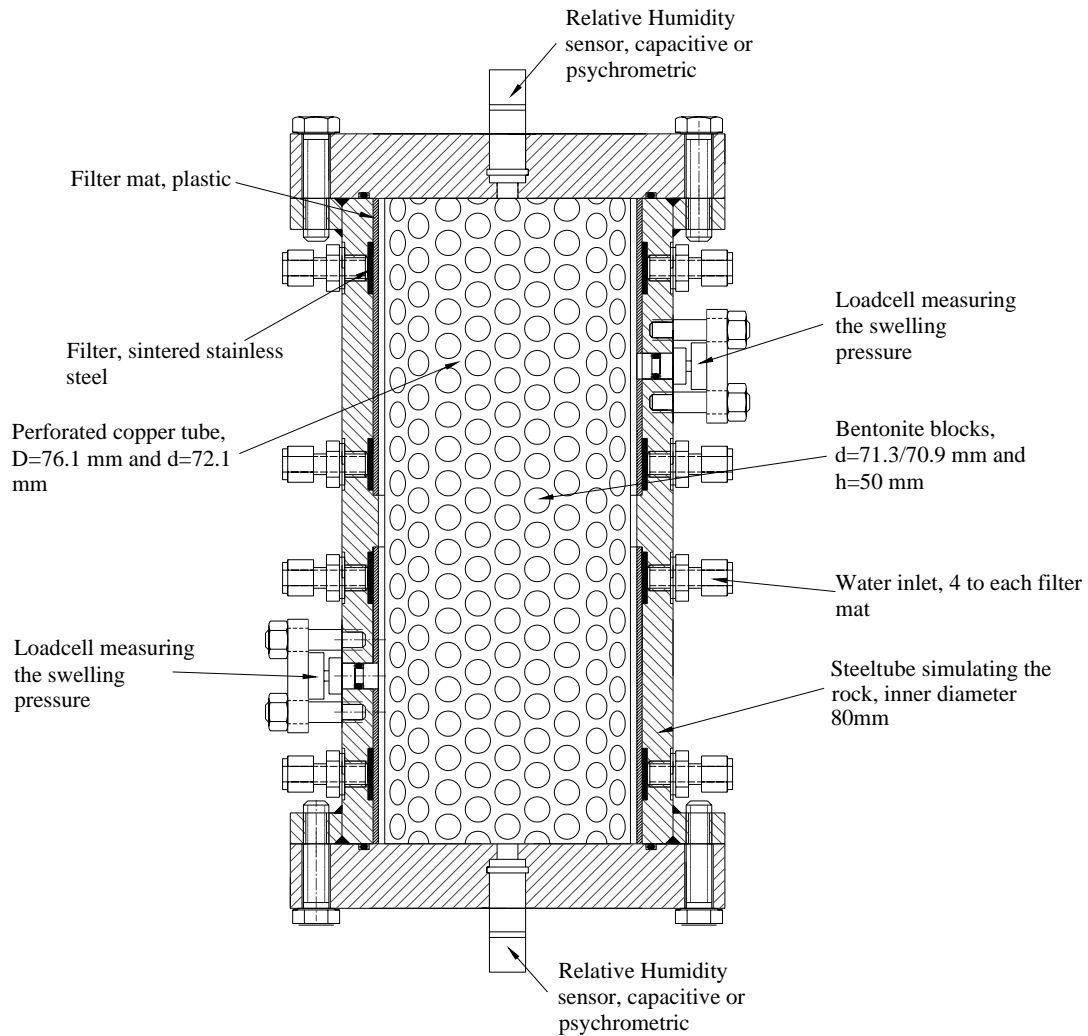


Figure 1-2. Schematic view showing the equipment used in these tests. The samples have had free access to water during the test period. A water pressure of 2 MPa was applied after 5-6 day.

Test start

After preparation of the two tests, water was filled up slowly from the bottom in order to de-air the volume. The samples had access to water from burettes for about 5-6 days (in order to not flow water directly on the RH sensors) before a water pressure was applied. The water pressure was raised in two steps up to 2 MPa.

1.2 Test result from the 1 month tests

Measurement of swelling pressure and the wetting process

The radial swelling pressure was measured in the periphery outside the perforated tube in two points as shown in Figure 1-2. The pressure was measured by use of a small piston with the diameter $d=10$ mm in contact with a load cell.

Relative humidity (RH) was measured in two points in the centre of the samples as shown in Figure 4-8. A capacitive sensor was placed in the top and a psychrometer in the bottom. The reason for using two different devices is that although the measuring range for the capacitive sensors is 0-100% the accuracy between 90 and 100% is not good (+/- 2%). The measuring range for the psychrometer is only 95-100% but the accuracy in that limited range is very high.

The tests in this series were left for about 30 days for wetting and homogenization. The measured results are shown in Figures 1-4 and 1-5.

$\sigma_s = 1700-2200$ kPa for the sample which have had a mechanical erosion

$\sigma_s = 1300-1400$ kPa for the sample which have had a erosion in water.

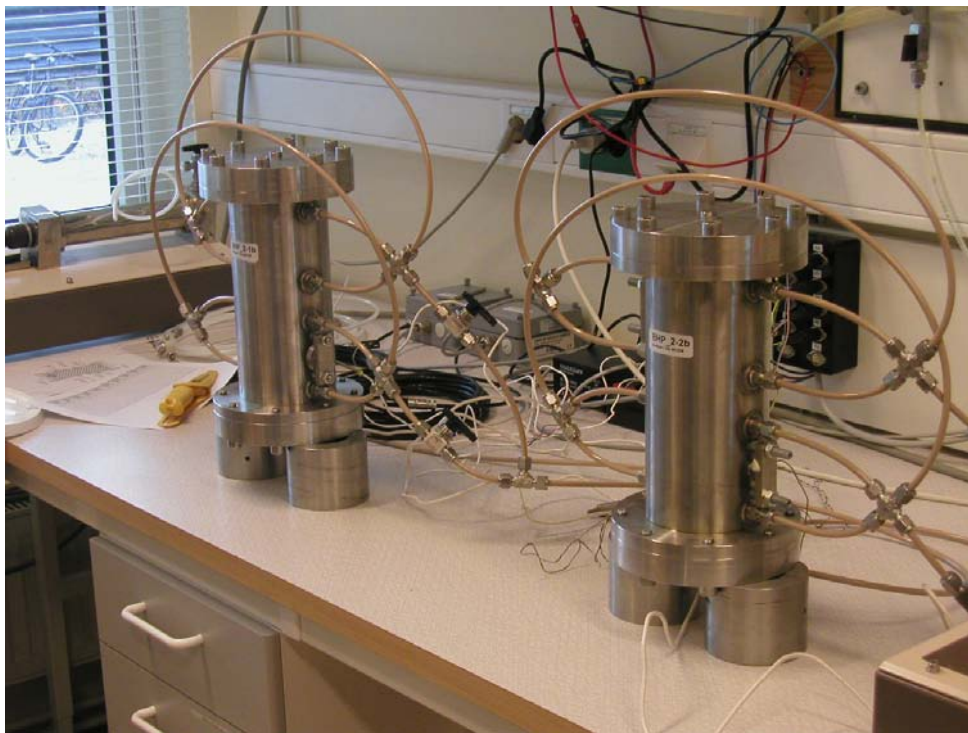


Figure 1-3. Picture showing the test equipment for the long time tests.

1 month test, 7.5% eroded mechanically

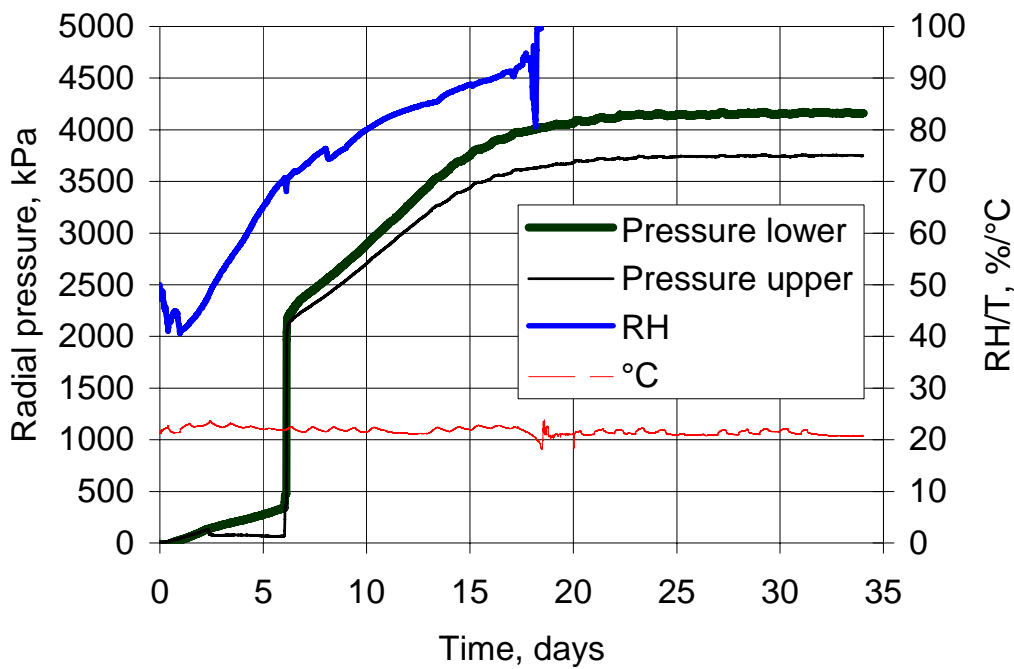


Figure 1-4. Diagram showing the radial pressure build up during saturation for the test. The diagram also shows the Relative Humidity in the bentonite. After 5-6 days the pore water pressure was raised to 2 MPa.

1 month test, 7.5% eroded in water

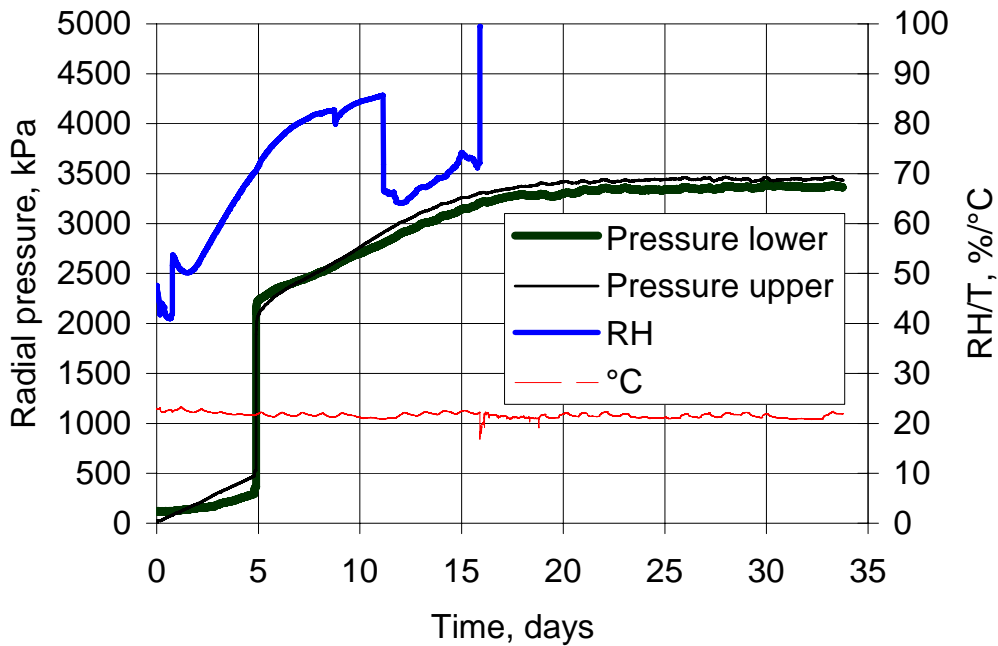


Figure 1-5. Diagram showing the radial pressure build up during saturation for the test. The diagram also shows the Relative Humidity in the bentonite. After 5-6 days the pore water pressure was raised to 2 MPa.

Interruption of tests

The two tests were interrupted about 30-35 days after test start. The work was done as follows:

1. The water pressure was lowered to atmospheric pressure.
2. All tubes and the load cells were disconnected.
3. The clay samples including copper tubes were pressed out from the steel cylinder by use of a hydraulic press.
4. Samples for determination of water ratio and density was taken according to the following:
 - **Slot between copper tube and rock (steel).** Water ratio was determined in four directions (A, B, C and D) on 10 levels (every 2.5 cm).
 - **Clay in holes in copper tube.** Water ratio was determined in four directions on 5 levels (every 5 cm).
 - **Inside copper tube.** Water ratio and density was determined in two directions (A and C) on three levels (4, 12.5 and 21 cm).
5. When samples had been taken on the outer slot, the copper tube was cut in two pieces with an angle grinder in order to facilitate the sampling of the inner parts.

Both samples could be pressed out in one piece, Figure 1-6. By use of a ruler and a knife, samples could be taken with good precision. When cutting up the inner parts a band saw was used to facilitate the work.

The water ratio was determined by use of a laboratory balance and an oven where the samples were dried for 24 h at a temperature of 105°. The bulk density was determined by weighing the samples in air and immediately after submerged in paraffin oil. In the calculations it has been assumed that the samples taken in the outer slot and in the holes in the copper tube were water saturated.



Figure 1-6. Picture showing one of the samples immediately after dismantling. It was possible to see the pattern from the perforated tubes in the clay surface. Both samples looked very similar.



Figure 1-7. Picture showing the clay sample after dismantling of the copper tube. The clay from the holes is still solid and this facilitated the sampling.

Analyses of the clay from test performed with 7.5% mechanical erosion.

A compilation of the analyses from the clay in this sample is done in Figure 1-8 to 1-11.

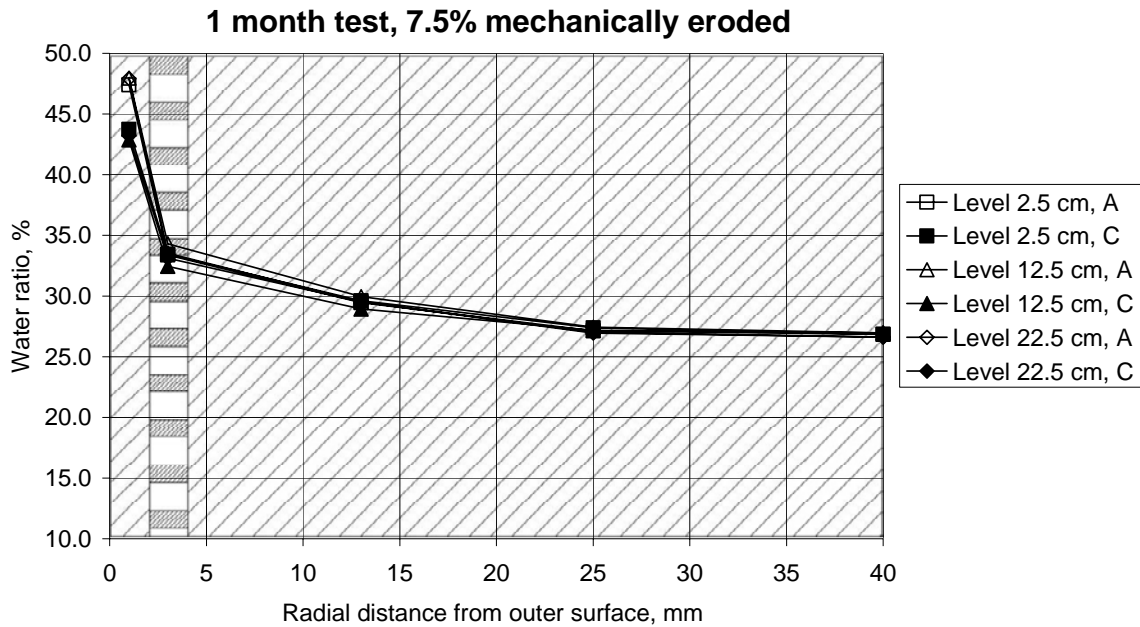


Figure 1-8. Diagram showing the radial water ratio distribution on three levels and in two directions.

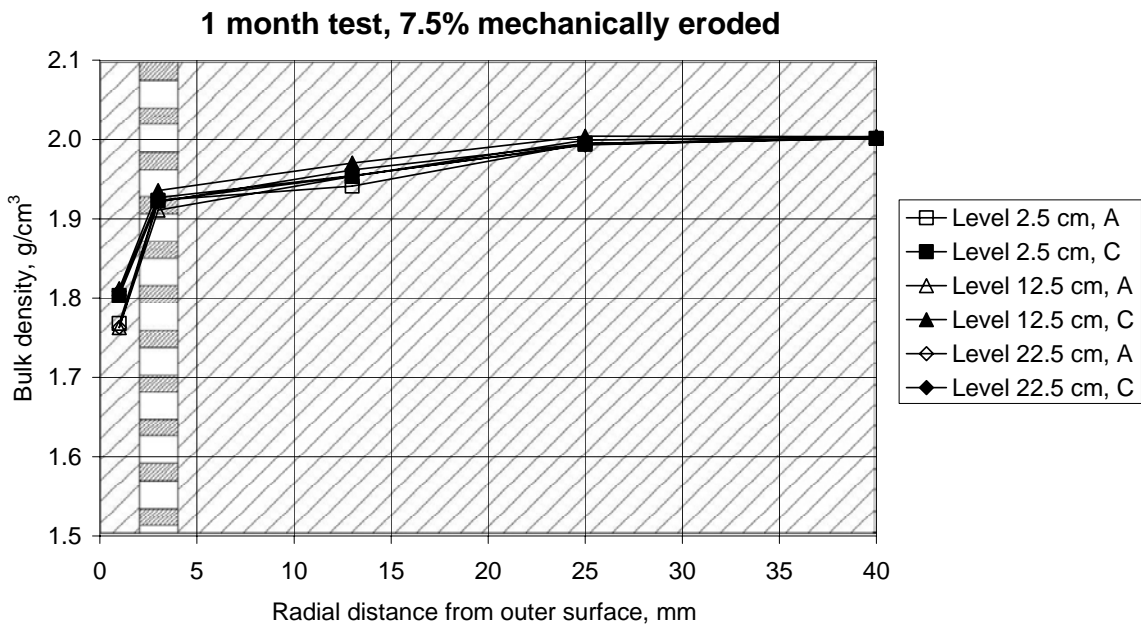


Figure 1-9. Diagram showing the radial bulk density distribution on three levels and in two directions. In the calculations it was assumed that the samples from the outer slot and from the holes in the perforation were water saturated.

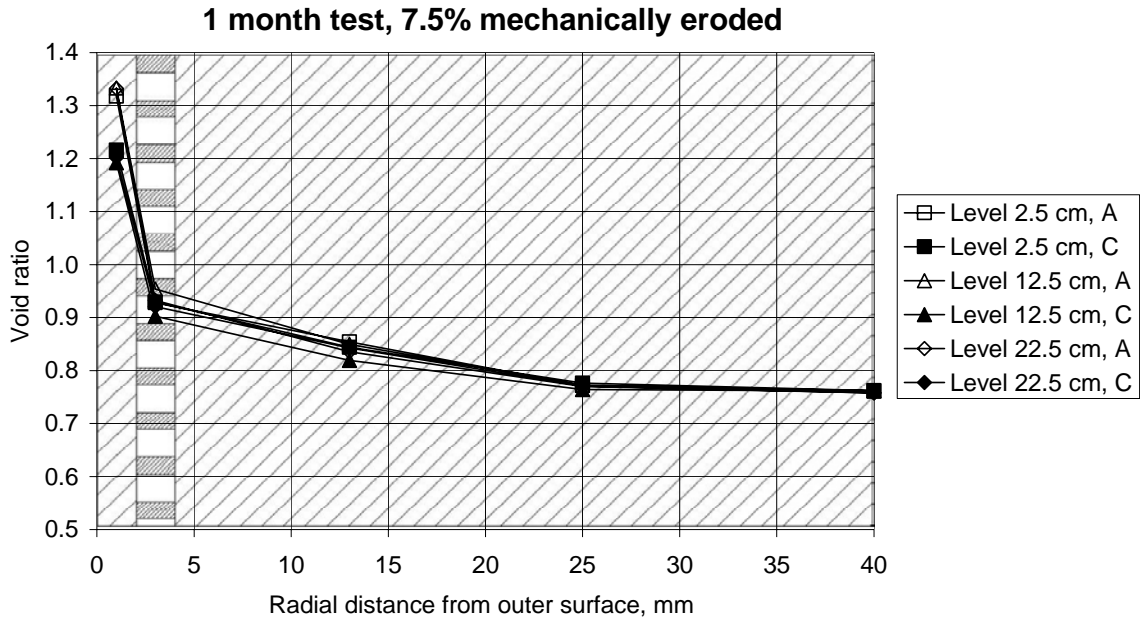


Figure 1-10. Diagram showing the radial void ratio distribution on three levels and in two directions. In the calculations it was assumed that the samples from the outer slot and from the holes in the perforation were water saturated.

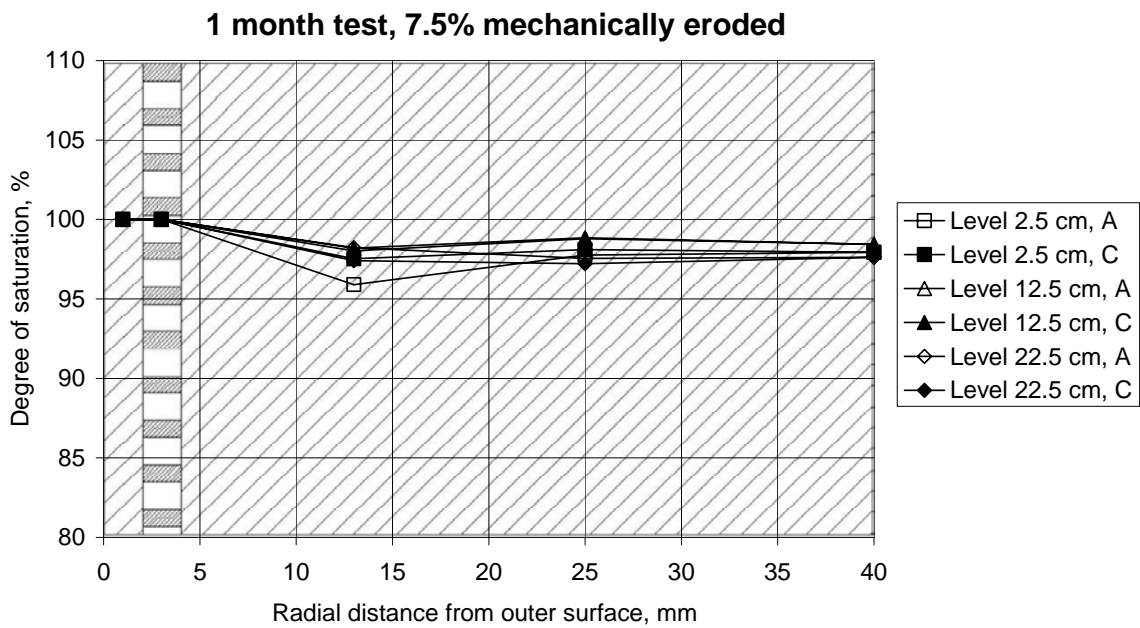


Figure 1-11. Diagram showing the radial degree of saturation distribution on three levels and in two directions. In the calculations it was assumed that the samples from the outer slot and from the holes in the perforation were water saturated.

Analyses of the clay from test performed with 7.5% erosion in water.

A compilation of the analyses from the clay in this sample is done in Figure 1-12 to 1-15.

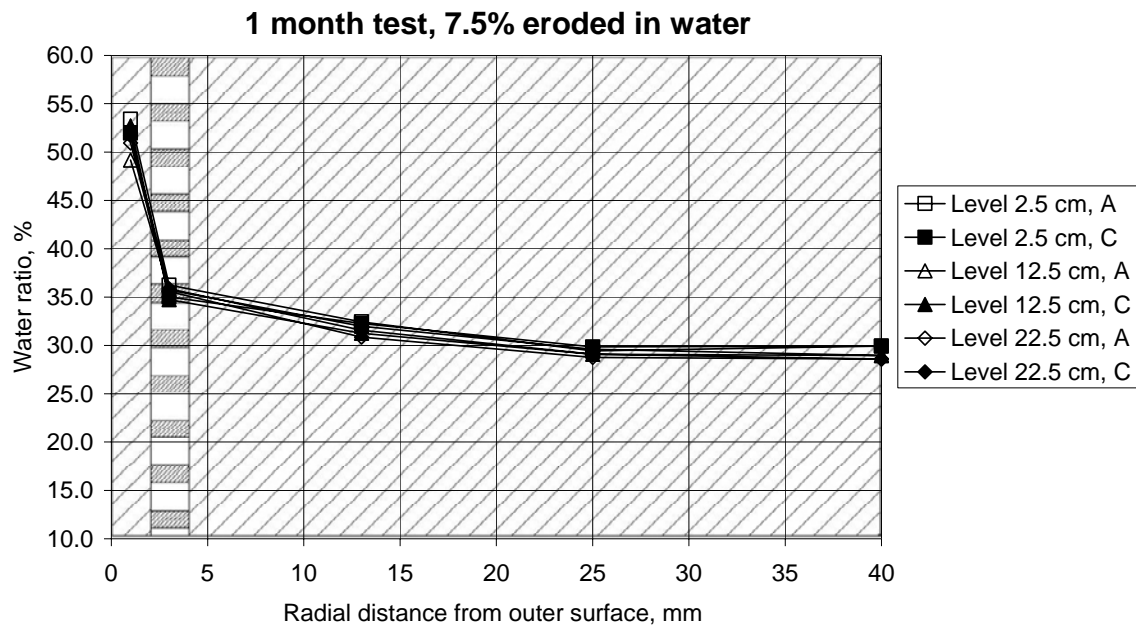


Figure 4-27. Diagram showing the radial water ratio distribution on three levels and in two directions.

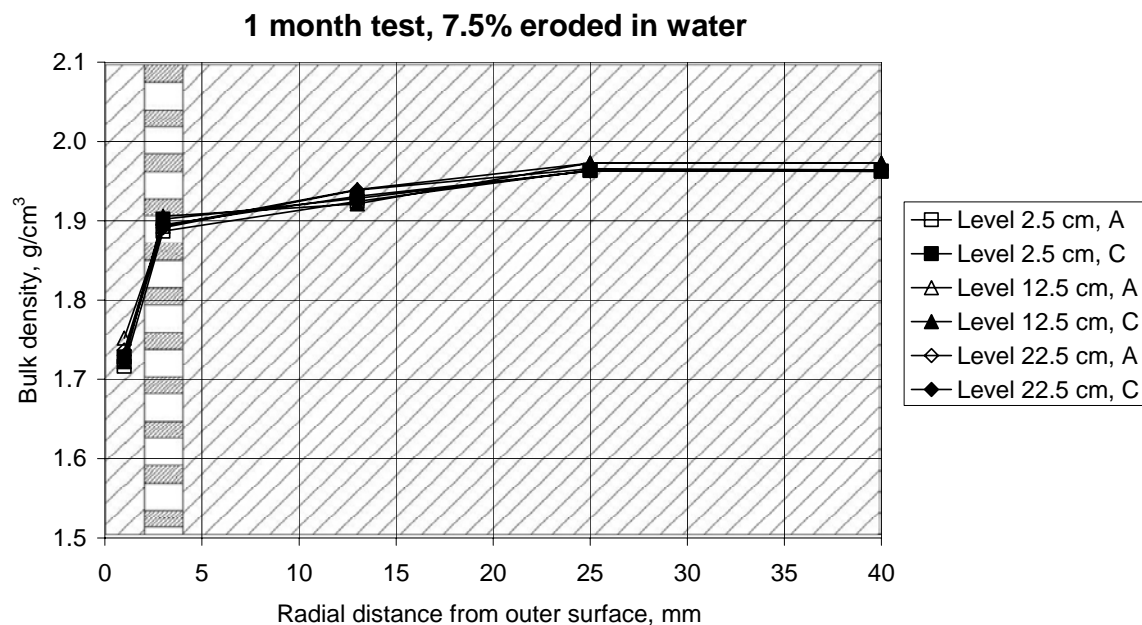


Figure 4-28. Diagram showing the radial bulk density distribution on three levels and in two directions. In the calculations it was assumed that the samples from the outer slot and from the holes in the perforation were water saturated.

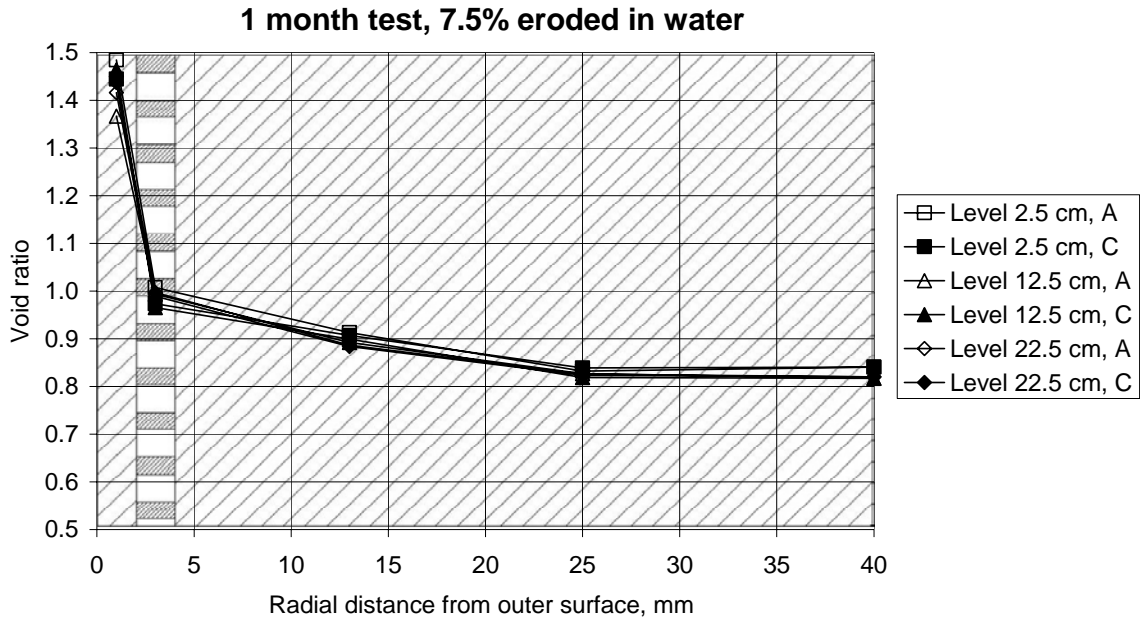


Figure 4-29. Diagram showing the radial void ratio distribution on three levels and in two directions. In the calculations it was assumed that the samples from the outer slot and from the holes in the perforation were water saturated.

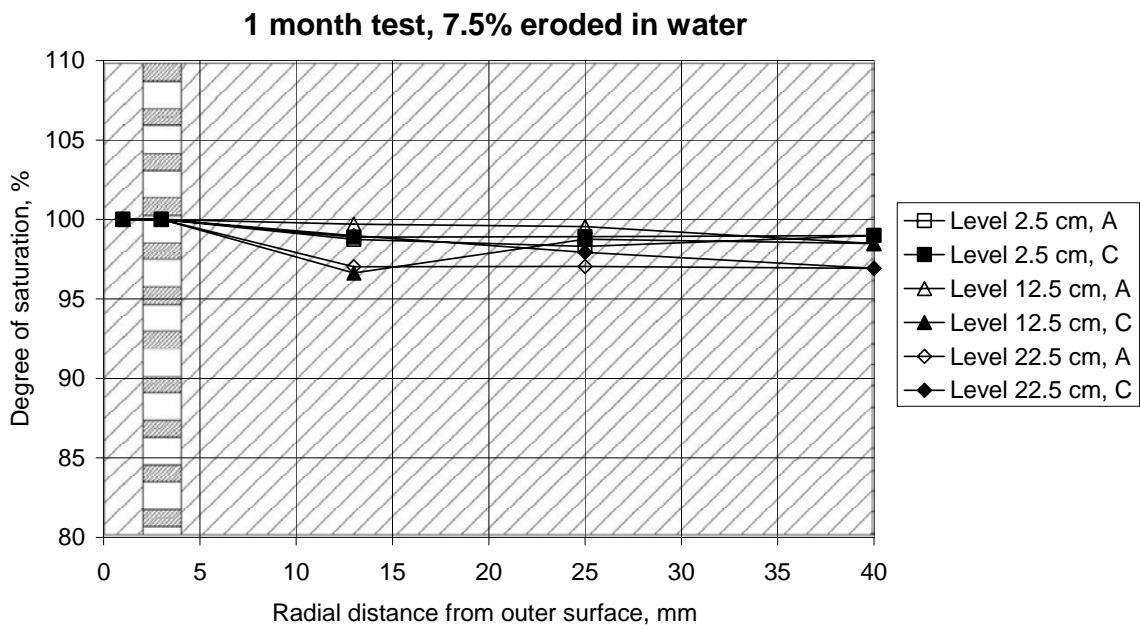


Figure 4-30. Diagram showing the radial degree of saturation distribution on three levels and in two directions. In the calculations it was assumed that the samples from the outer slot and from the holes in the perforation were water saturated.

Comments to the tests

- The input values to the sample which have had a mechanical erosion of 7.5% is well known. The erosion of the other sample (exposed to flowing water for 1 hour) was estimated based on earlier experiments. The analyses of the clay samples after interruption shows that the erosion has been higher, probably around 10%. This is very evident when comparing the radial water ratio distribution for the two samples.
- The degree of saturation is for both samples, 96-100%. In the calculations it was assumed that the samples taken in the outer slot and in the perforation were completely saturated (it was not possible to measure the density in these positions, only the water ratio).
- The saturated average density in the borehole (after 7.5% erosion) is calculated to be 1980 kg/m^3 . The density gradient is after 1 month very strong, 2.00 at the inner parts and down to about 1.72 at the outermost parts.

Appendix III

Borehole plugging test – Piping Experiments

"Basic" type

Case: 2.5 m perforated copper tube filled with compacted MX-80 blocks. Tap water filled from lower end. Figures 1 and 2 show the water pressure history and the amount of water taken up by the clay. Figure 3 illustrates the preparation of the plug and Figures 4 and 5 the test arrangement.

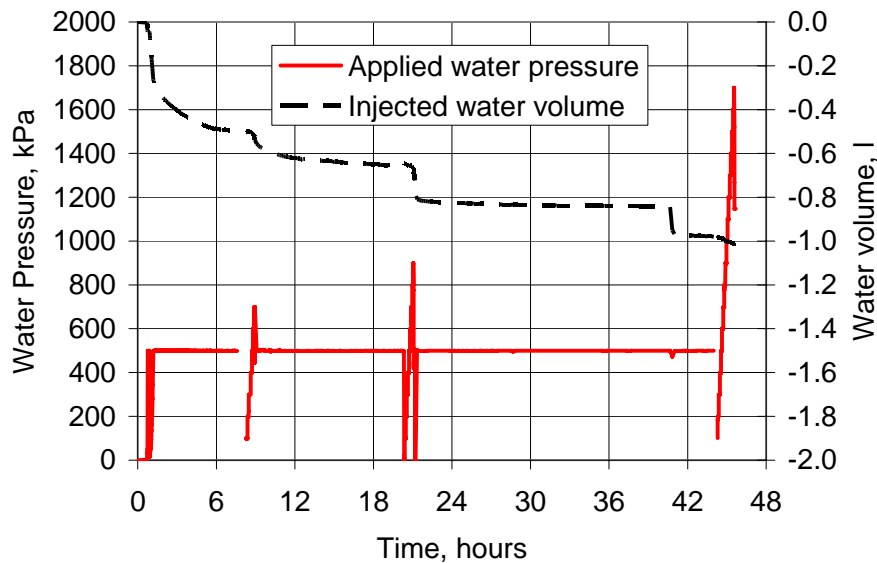


Figure 1. Diagram showing the water pressure evolution after filling the tube with water, and the amount of water taken up. The peaks represent the pressure tests.

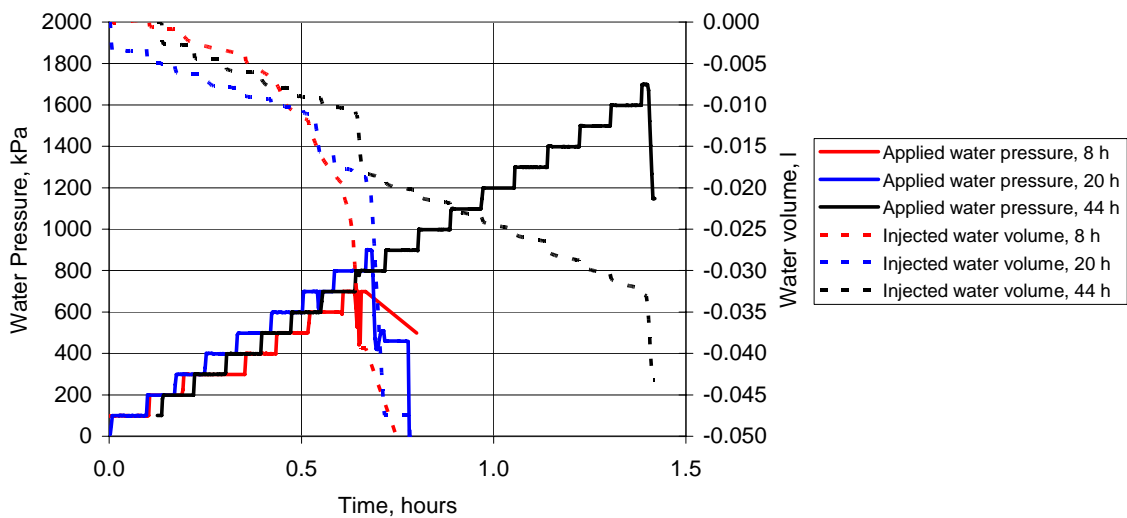


Figure 2. Diagram showing the detailed evolution of injected water.



Figure 3. Preparation of the "Basic" plug for the experiments.

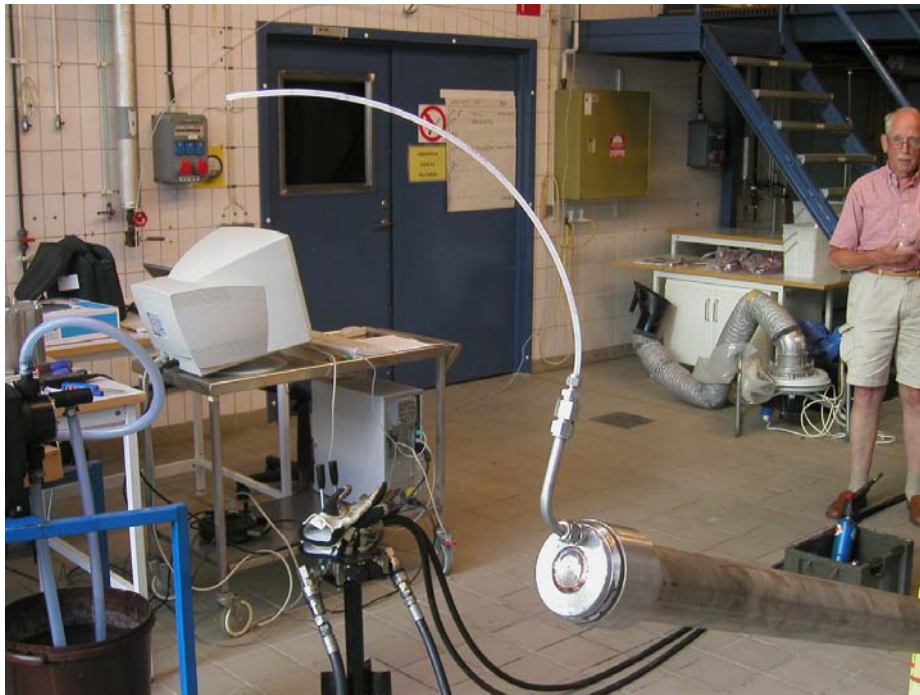


Figure 4. Details of the test arrangement. The upper end of the confining tube with a plastic tubing for direct observation when through-flow occurred.



Figure 5. Equipments. Upper: The tube representing a borehole with the plug inserted. Lower: The GDS unit.

The water contents determined of clay scraped off from the tube (“skin”) was determined for three sections:

0.5m	1.25m	2m
105%	94%	93%

”Container” type

Case: The tube filled with compacted MX-80 blocks. Tap water filled from lower end. Figures 6 and 7 show the water pressure history and the amount of water taken up by the clay.

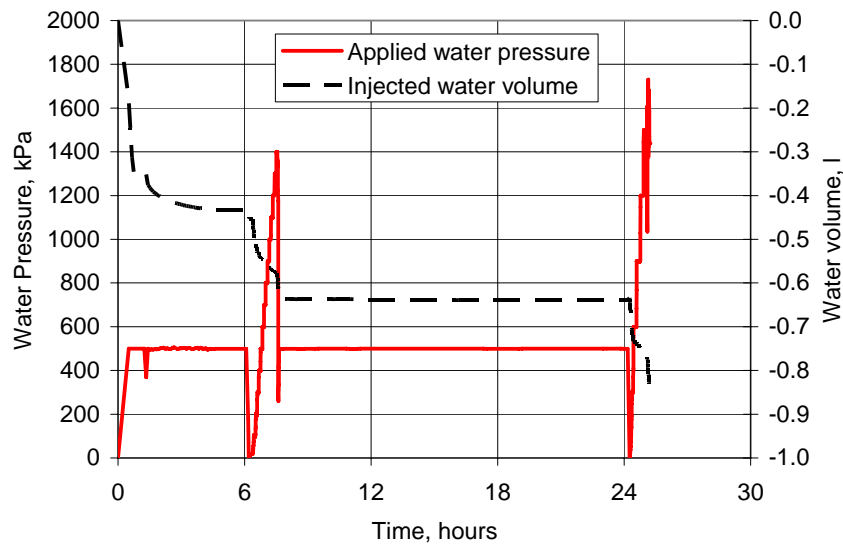


Figure 6. Diagram showing the water pressure evolution after filling the tube with water, and the amount of water taken up. The peaks represent the pressure tests.

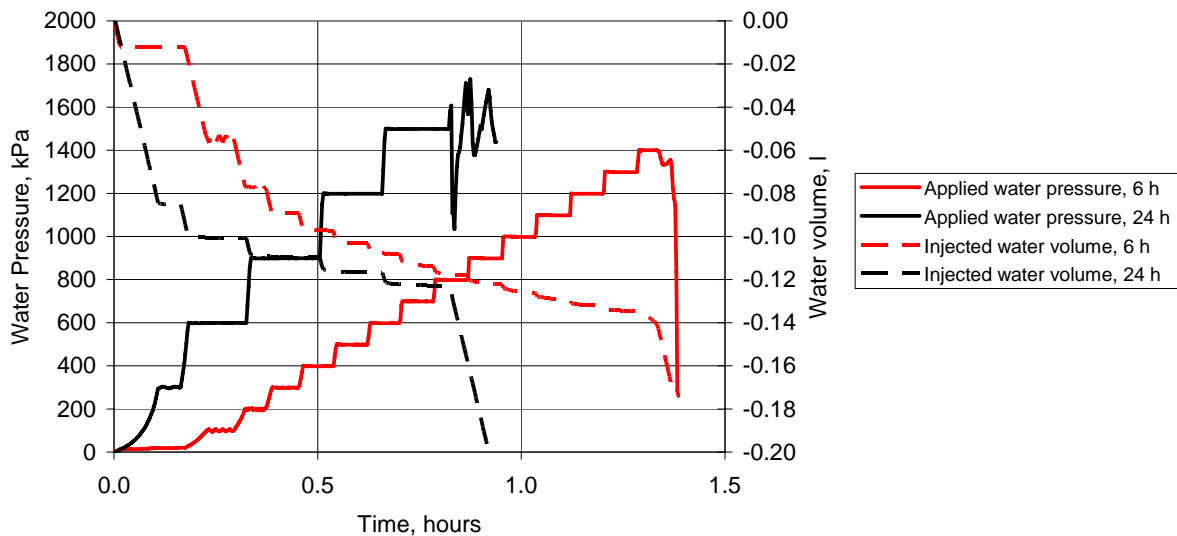


Figure 7. Diagram showing the detailed evolution of injected water.

"Pellet" type

Case: The tube filled with compacted MX-80 pellets. Tap water filled from lower end. Figures 8 and 9 show the water pressure history and the amount of water taken up by the clay.

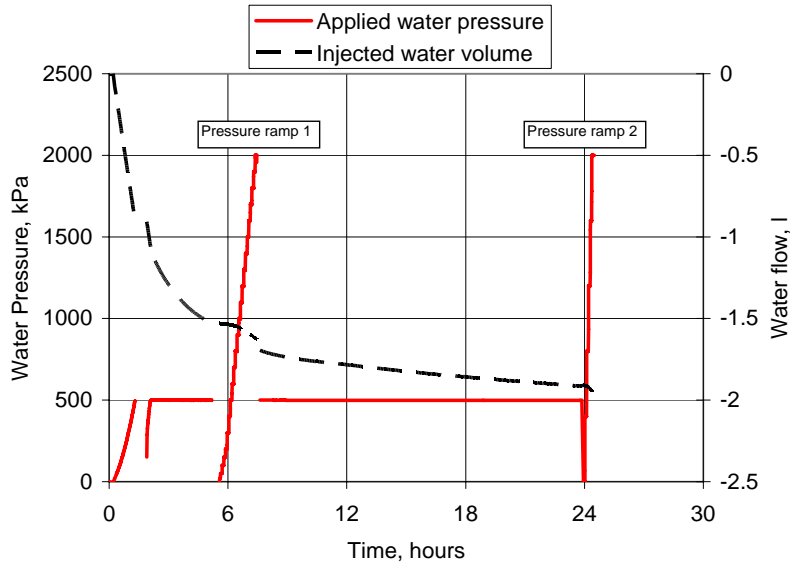


Figure 8. Diagram showing the water pressure evolution after filling the tube with water, and the amount of water taken up. The peaks represent the pressure tests.

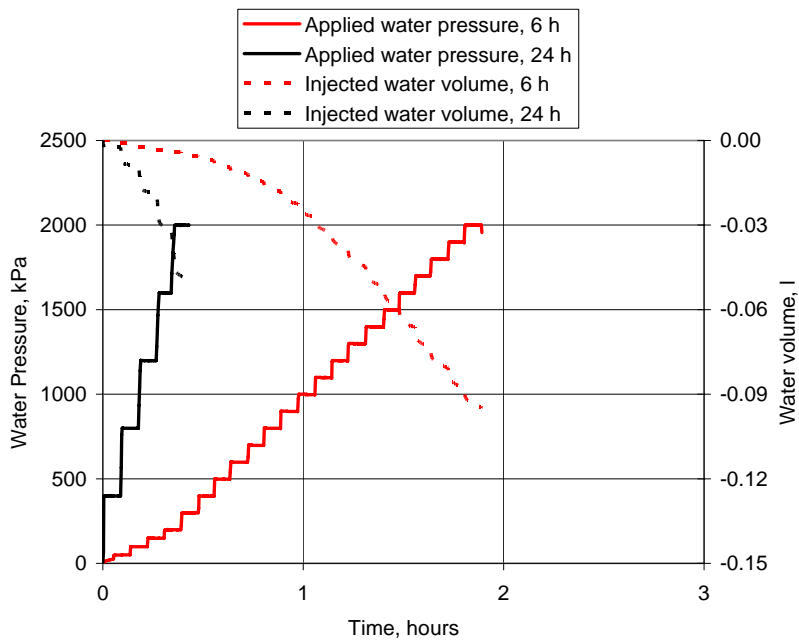


Figure 9. Diagram showing the detailed evolution of injected water.

The water contents were determined in three sections, shallow and central:

0.2 m from low end		1.5 m from low end		2.5 m from low end	
Core	Shallow	Core	Shallow	Core	Shallow
53 %	76 %	54 %	66 %	48 %	86 %

Appendix IV

Manufacturing of bentonite plugs with very high density

Torbjörn Sandén
Lennart Börgesson
Clay Technology AB

Contents

1	Manufacturing of bentonite cylinders	141
1.1	Compaction	141
1.2	Tensile strength	144
1.3	Swelling capacity	149

1 Manufacturing of bentonite cylinders

1.1 Compaction

In order to determine the influence of the compaction pressure and of the water ratio of the bentonite affect the final dry density and water uptake properties of the compacted bentonite plugs, a number of tests have been performed. Samples have been compacted with 100, 150, 200, 250 and 300 MPa. For each pressure, samples with a water ratio of 2.5%, 5%, 7.5%, 10% and 12.7% were compacted.

Figure 1-1 shows a diagram where the final saturated density in the borehole is plotted against the dry density of the bentonite plugs. The lower line shows the case when the tube is removed after installation. The figures are valid with the given dimensions of borehole, copper tube and bentonite plugs.

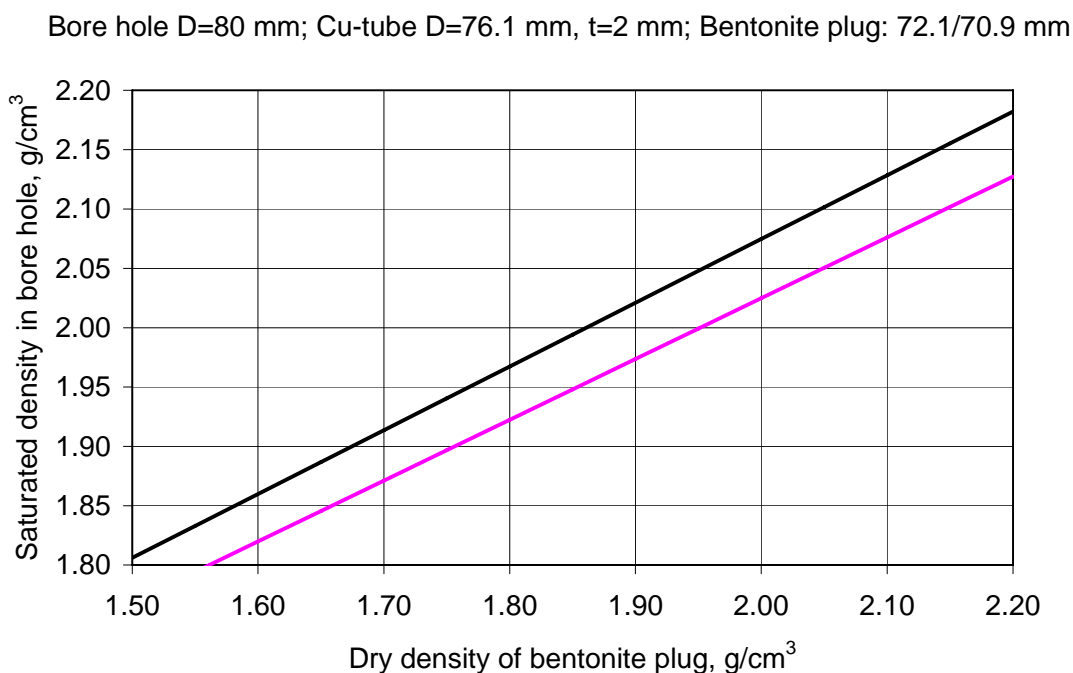


Figure 1-1. Diagram showing the saturated density of the bentonite installed in a borehole as a function of the dry density of the compacted bentonite cylinders. The figures are valid for the given dimensions of the borehole, the copper tube and the bentonite cylinders. The lower line shows the case when the tube is retrieved after installation.

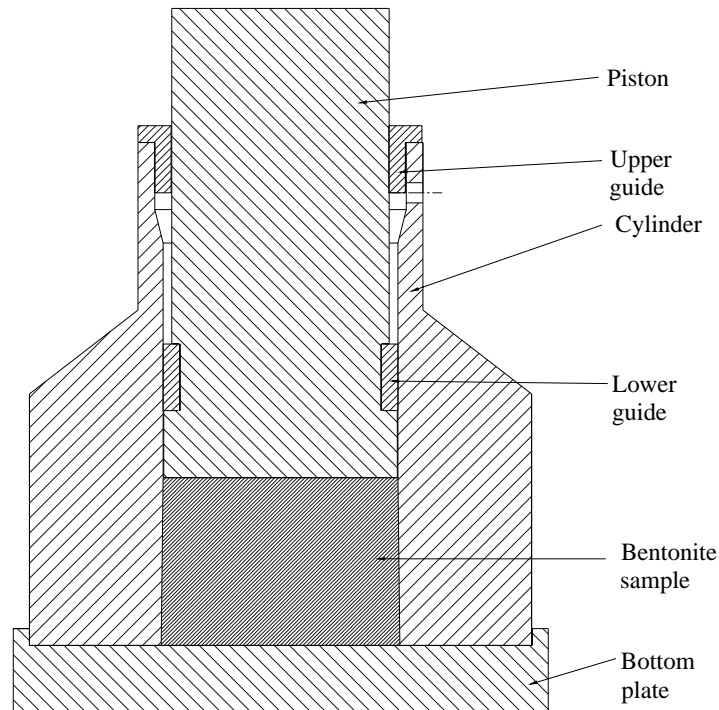


Figure 1-2. Schematic drawing of the equipment used when producing the bentonite plugs.

A special mold was manufactured in order to handle the high pressures, Figure 1-2. The mold is somewhat conical in order to facilitate the removal of the form and to get the plugs out in one piece. Due to the rather high elastic expansion of the bentonite plugs it is very difficult to make them cylindrical. Before removing the form the bentonite plugs have a height of about 50 mm and a diameter of 71.4 mm in the bottom and 70.2 in the top. The elastic expansion of the plug after unloading and removing the mold is a function of the water ratio and of the compaction pressure.

The different water ratios of the material were achieved by mixing dried bentonite (dried in 105°C) and bentonite with a water ratio of 12.7%. After mixing, the material was left in sealed containers for about 2 weeks in order to ensure a homogenous material.

In order to facilitate the compaction and the removal of the compacted plugs, the mold was lubricated with a thin layer of MoS₂ before each compaction. The results of the compaction tests are shown in Figure 1-4 and 1-5.

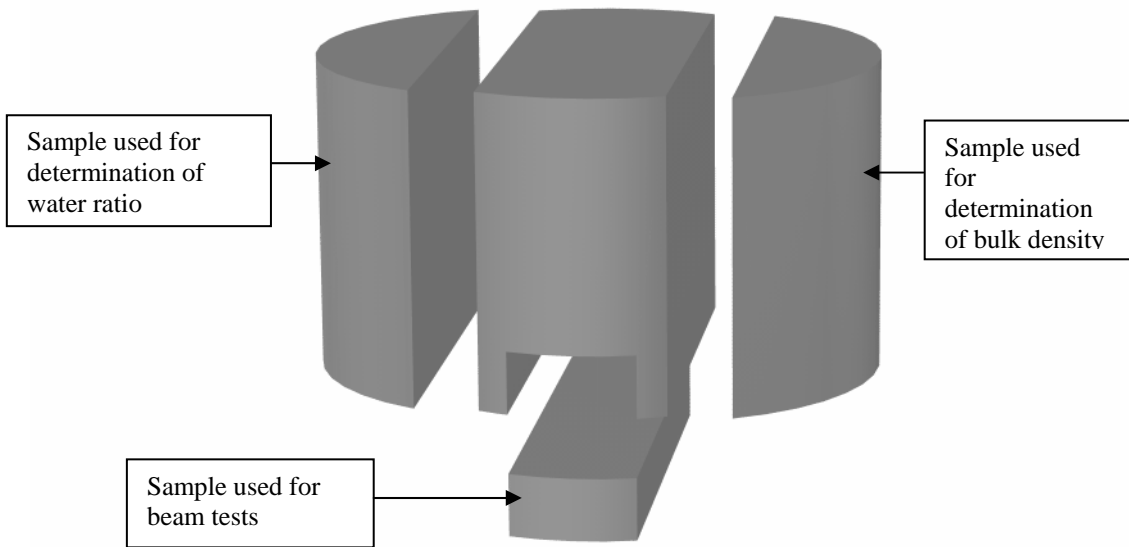


Figure 1-3. Schematic drawing showing the partition of the bentonite plugs.

Each compacted plug was split according to Figure 1-3. The density and the water ratio were determined. A beam was sawed out from the bottom part in order to test the tensile strength, see next chapter.

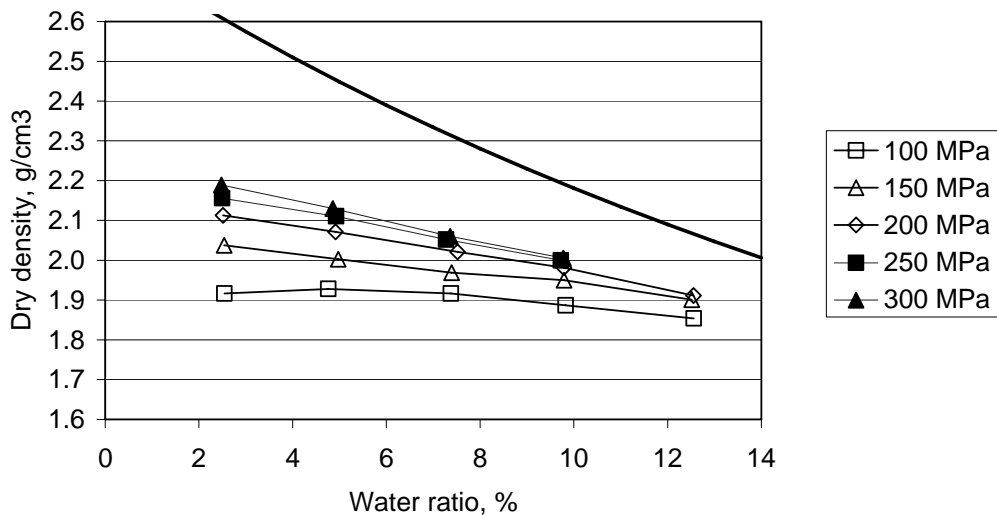


Figure 1-4. Diagram showing the dry density of the compacted bentonite cylinders as a function of the water ratio for different compaction pressures. The maximum dry density for a certain water ratio corresponding to complete water saturation is also plotted.

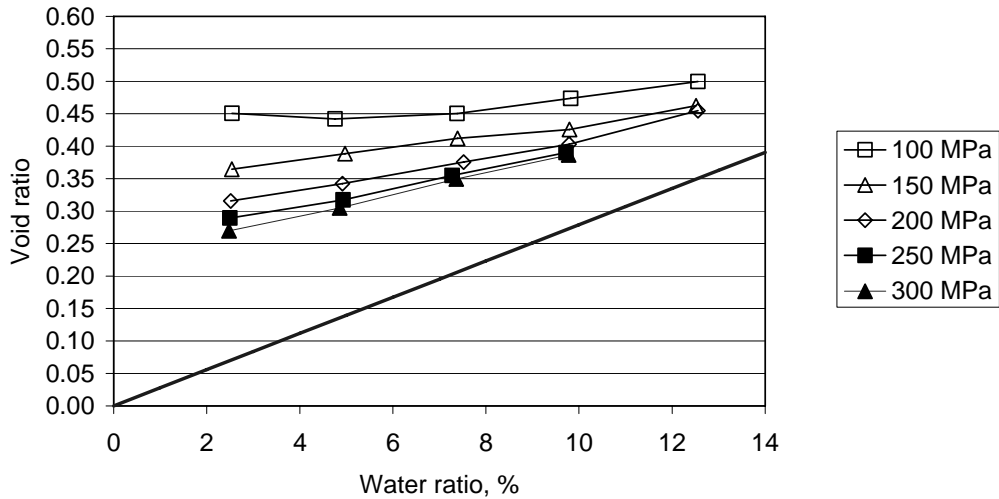


Figure 1-5. Diagram showing the void ratio of the compacted bentonite cylinders as a function of the water ratio for different compaction pressures.

1.2 Tensile strength

The tensile strength and the strain at failure are two important parameters in order to evaluate the handle of the compacted bentonite plugs without damaging them. Bending tests were performed in order to determine these properties. Beams with the dimensions 70 x 20 x 10 were sawed out from each compacted bentonite plug, Figure 1-3. The beams were supported in the ends and a gradually increasing force was applied in the center of each sample, Figure 1-6.

The deformation and the force were continuously measured during the tests. By using the recorded data, the maximum stress and strain at failure could be calculated, Figure 1-7 to 1-13 and Table 1.



Figure 1-6. Picture showing the test arrangement for determination of the tensile strength.

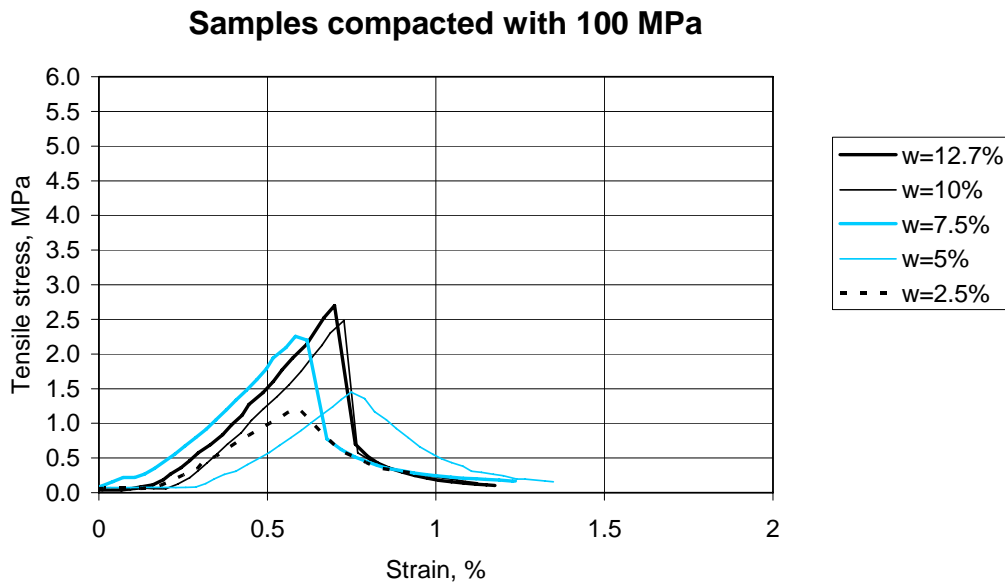


Figure 1-7. Diagram showing the tensile stress as a function of the strain for the samples compacted with 100 MPa..

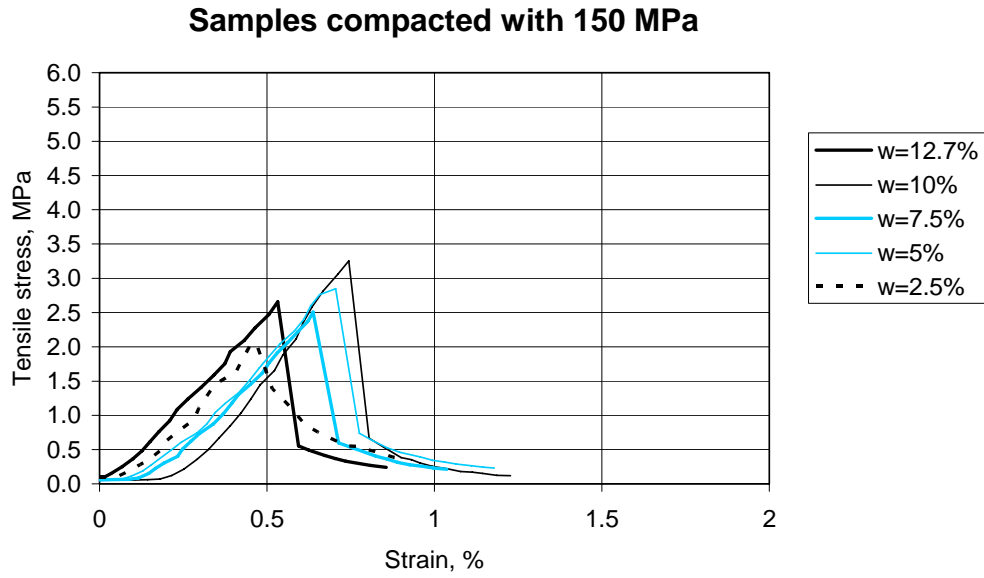


Figure 1-8. Diagram showing the tensile stress as a function of the strain for the samples compacted with 150 MPa..

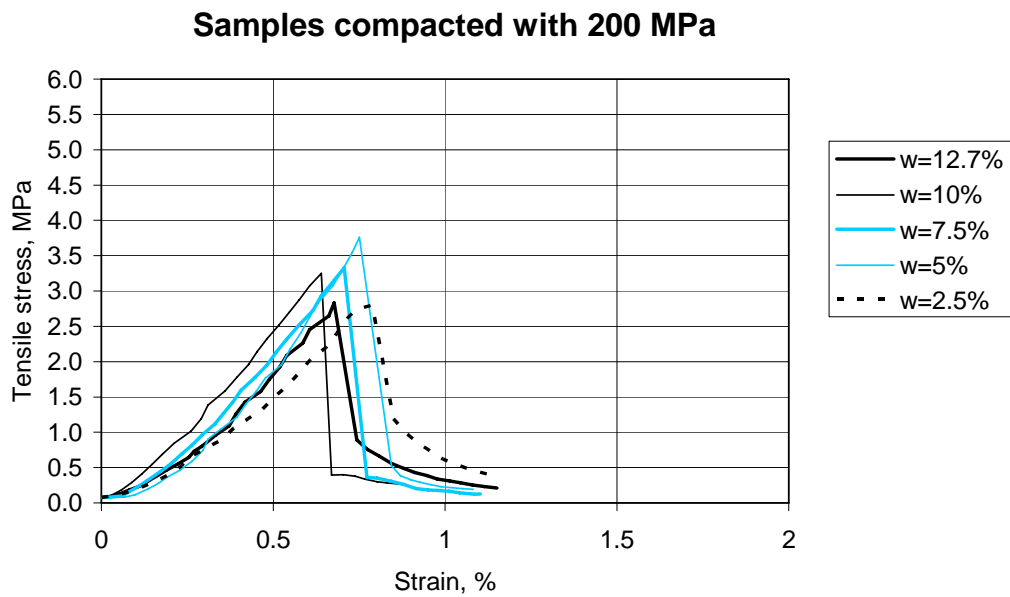


Figure 1-9. Diagram showing the tensile stress as a function of the strain for the samples compacted with 200 MPa..

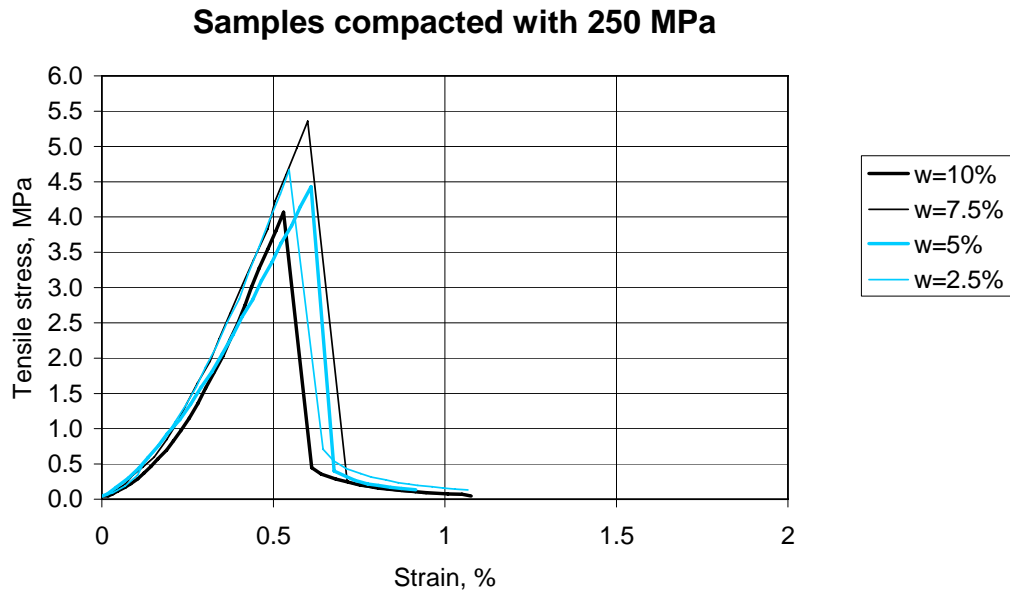


Figure 1-10. Diagram showing the tensile stress as a function of the strain for the samples compacted with 250 MPa..

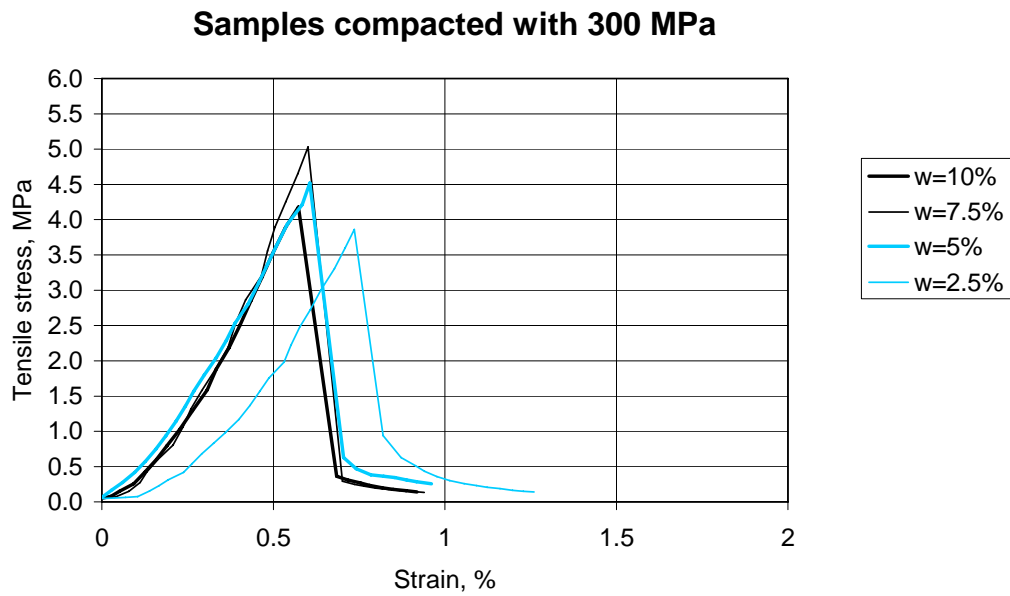


Figure 1-11. Diagram showing the tensile stress as a function of the strain for the samples compacted with 300 MPa..

Table 1. Table showing the maximum tensile strength and the strain for the tested bentonite samples.

Bentonite type	Comp. Pressure MPa	w %	e	Sr %	Tensile strength MPa	Max tensile strain
Mx-80	100	12.7	0.499	69.9	2.7	0.7
Mx-80	100	10.0	0.474	57.7	2.5	0.7
Mx-80	100	7.5	0.450	45.5	2.2	0.6
Mx-80	100	5.0	0.442	29.9	1.4	0.7
Mx-80	100	2.5	0.451	15.7	1.2	0.6
Mx-80	150	12.7	0.462	75.3	2.7	0.5
Mx-80	150	10.0	0.426	63.9	3.3	0.7
Mx-80	150	7.5	0.412	49.9	2.5	0.6
Mx-80	150	5.0	0.388	35.6	2.8	0.7
Mx-80	150	2.5	0.364	19.4	2.1	0.5
Mx-80	200	12.7	0.455	76.8	2.8	0.7
Mx-80	200	10.0	0.403	67.5	3.2	0.6
Mx-80	200	7.5	0.376	55.7	3.3	0.7
Mx-80	200	5.0	0.342	39.9	3.8	0.7
Mx-80	200	2.5	0.316	22.2	2.8	0.8
Mx-80	250	10.0	0.390	69.3	4.1	0.5
Mx-80	250	7.5	0.355	57.0	5.4	0.6
Mx-80	250	5.0	0.317	43.2	4.4	0.6
Mx-80	250	2.5	0.289	24.0	4.7	0.5
Mx-80	300	10.0	0.386	70.3	4.2	0.6
Mx-80	300	7.5	0.350	58.6	5	0.6
Mx-80	300	5.0	0.305	44.3	4.5	0.6
Mx-80	300	2.5	0.270	25.6	3.9	0.7

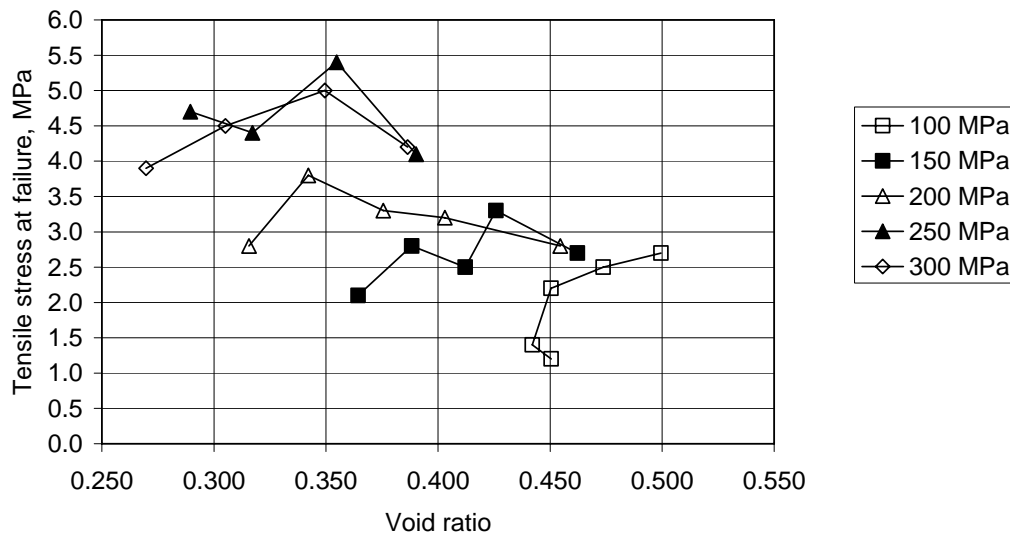


Figure 1-12. Diagram showing the tensile stress as a function of the void ratio.

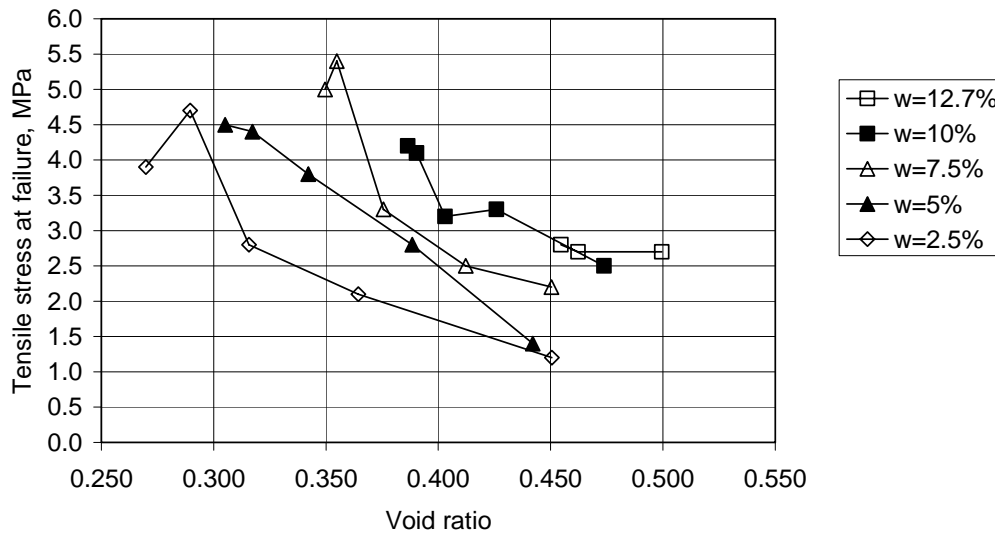


Figure 1-13. Diagram showing the tensile stress as a function of the void ratio.

1.3 Swelling capacity

A standard control of bentonite includes a test of the swelling capacity. This test is done with powder, which is carefully poured into water in a measuring glass. In order to do a quick test of the swelling ability and swelling rate of the compacted bentonite, a modified swelling test has been performed. A cubical sample was sawed out from each plug. Each sample had a solid mass of 3.65 g. The samples were put in measuring glasses filled with water. The swelling was registered by photo at different elapsed time. Four samples were tested:

1. w=10%, Compaction pressure=100 MPa
2. w=10%, Compaction pressure=300 MPa
3. w=2.5%, Compaction pressure=100 MPa
4. w=2.5%, Compaction pressure=300 MPa

The results of the test are shown in Figure 1-14. No obvious difference in swelling capacity and swelling rate could be detected with this simple test. These tests indicate that the compaction pressure and the water ratio of the plugs do not affect the erosion properties.



Figure 1-14. Pictures showing the swelling capacity of four materials. From left: $w=10\%$ 100 MPa, $w=10\%$ 300 MPa, $w=2.5\%$ 100 MPa, $w=2.5\%$ 300 MPa. The upper picture shows the result after 5 min, next picture after 1 hour, next 24 hours and the lower after 48 hours.

Appendix V

Silica concrete for plugging of deep bore holes

Design, performance and long time durability

Björn Lagerblad & Carsten Vogt

Swedish Cement and Concrete Research Institute

Mars 2007

This report concerns a study, which was conducted for SKB. The conclusions and viewpoints presented in the report are those of the authors and do not necessarily coincide with those of the client.

Summary

There is a need to permanently plug bore holes made during investigation for suitable areas for deposition of radioactive waste. Concrete can be a suitable material for the plug.

The demands are that the concrete shall not contaminate the ground water, i.e. it shall not give a pH higher than 11. Moreover, the concrete shall be formulated so that it remains stable even if the binder is decomposed by leaching, i.e. the amount of aggregate shall be as large as possible. For technical purposes it must be pumpable and self compacting.

For this purpose a special concrete has been developed. It is formulated with normal aggregate. The amount of binder is minimized by the help of ultrafine filler. The concrete contains 60 kg of Portland cement and 60 kg of silica fume per m^3 concrete (density of concrete is 2300 kg/m^3). This is around 1/3 of the normal amount of binder in a concrete.

As a consequence of the large amount of silica fume it will not behave as a normal concrete, thus not to confuse it with normal concrete it is called silica concrete.

The silica concrete has due to the small amount of Portland cement relatively slow strength gain but it will with time get strength of more than 60 MPa, which is more than enough for the purpose. The permeability and shrinkage is low.

When leached the concrete gives the water a maximum pH of around 10. It will leach congruently and in contrast to normal concrete leach as much silica as calcium ions. The silica will, however, redeposit at pH 8. The silica concrete will, when decomposed, loose only around 42 kg of CaO per m^3 and thus it will remain physically stable after decomposition.

As the binder is so rich in silica the binder will polymerize with time and one can presume that with time in repository conditions will crystallise.

Contents

1	Introduction	1
1.1	Silica concrete for the bore hole plug.....	1
1.1.1	Demands on the silica concrete	2
2	Concept for the bore hole concrete	3
2.1	Chemical composition and leaching.	3
2.2	Concrete mix.	4
2.3	Concrete recipe.....	4
3	Results	6
3.1	Rheology	6
3.2	Strength	6
3.3	Shrinkage.....	7
3.3.1	Autogeneous shrinkage	7
3.3.2	Shrinkage in water.....	8
3.4	Concrete texture and porosity	9
3.5	Chemical composition of the cement paste.....	12
3.6	Leaching experiments	13
3.6.1	Discussion of leaching results.....	14
4	Effect on ground water and long time durability	16
4.1	Stability of amorphous calcium-silicate hydrate (C-S-H).....	16
4.2	Structural order and crystalline C-S-H phases	19
4.2.1	Structural order of C-S-H.....	20
4.2.2	Possible crystalline compounds	21
5	Discussion	23
6	Conclusions	25
7	References	26
Appendix 1	pH bestämning av silika betong.....	28

1 Introduction

In Sweden radioactive waste will be stored in underground repositories in granitoid rock formations. To find a proper place the geology of the rock formation must be investigated, which demands a large number of drill cores. In the rock formation the drill holes will act as conductive transport channels and must thus be sealed off. The choice of material and application technique will be important both for the function, durability and interaction with the repository.

The drill holes normally have a diameter of around 75-100 mm and the length can be up to 1500 meters. The inclination normally varies between 45 and 90 degrees but in some sections the drill holes can even be horizontal.

The life length of the plugs must be as long as that of the repository, i.e., they must hinder water transport for more than 100 000 years. During this period the hydraulic conductivity shall be lower than that of the surrounding rock and the properties of the plug shall be such that no water flows in the contact zone between the plug and the surrounding rock.

The suggested basic concept is to use bentonite clay for the sealing. Compacted bentonite in perforated copper tubes will be placed in the drill holes and the swelling of the bentonite will seal the drill holes. In some places and as a complementary material concrete will be used. For safety reasons, however, normal concrete can not be used as it will give to high pH to the surrounding water. Thus a low pH concrete must be used. The low pH is achieved by adding silica in different forms to a normal concrete (with pure ordinary Portland cement). The large amounts of silica will change the properties of the concrete both as regard pH and the structure of the binder. Thus it is named silica concrete so that it shall not be directly compared to normal cementitious concrete.

Silica concrete will also be used to stabilise the drill holes so that the tubes with compacted bentonite can be put in place. The procedure is described in Vogt et al. (2004).

This report treats the silica concrete and its applications. The silica concrete must, however, have such properties that the function of the bentonite is not jeopardized.

1.1 Silica concrete for the bore hole plug

In the borehole-plugging process concrete will be used in two different ways. Firstly the borehole must be stabilized to allow the application of the bentonite tubes. How to stabilize the boreholes is investigated in another project "low alkali mortar for selective stabilization of deep drill holes" in the PLU programme. Low alkali means low pH, which in turn means that it is silica concrete. One of the concepts here is to enlarge the damaged section of the borehole and fill it with ultrahigh strength silica concrete containing glass fibres. When this concrete has hardened a new hole will be drilled with the same diameter as the original hole. This will result in a "tube" in the rock that will stabilize the drill hole. Other concepts are also being investigated.

The borehole plug will be casted at the desired position where it shall fill the section and hinder water movement. The technique to get the concrete in place is being developed in another part of the project. Basically a special canister with fresh concrete will be lowered to the desired depth where it will be emptied. The geometry of the canister will put a limit to D-max of the aggregates. As the geometry is not fully developed the silica concrete recipe must be designed in such a way that it will be possible to adjust.

The casting technique, spacing, and chemistry put special demands on the silica concrete, both in the fresh and the hardened state.

Both the silica concrete used for stabilisation and bore hole silica concrete has been tested in borehole KR 24 at Olkiluoto.

1.1.1 Demands on the silica concrete

- 1 The geometry of the application canister and the diameter of the borehole restrict the largest size of aggregates. The D-max is around 1/3 of the diameter of the opening in the canister. A D-max of 4 mm is set for the basic recipe.
- 2 The silica concrete shall be self-compacting, i.e. there shall be no need for vibration to get the fresh silica concrete compacted.
- 3 The shrinkage shall be at a minimum.
- 4 The fresh silica concrete may be placed in an area with pecculating water. Thus the silica concrete must have a good cohesion.
- 5 The silica concrete shall have good resistance to leaching
- 6 The silica concrete shall have a good stability after leaching.
- 7 The silica concrete will be in direct contact with bentonite. A high pH will reduce the swelling capacity of the bentonite. Thus the concrete shall not contaminate either the bentonite or the surrounding ground water. Preferably the concrete shall not increase the pH of the surrounding groundwater to more than 11.

2 Concept for the bore hole concrete

The special and demanding requirements are to get a low pH when the concrete is leached, make it self-compacting and to minimize the amount of cement paste.

2.1 Chemical composition and leaching.

The cement paste of hardened concrete is water-soluble. How fast the leaching goes and the effect on ground water depends on the composition of the cement paste. The mechanism of leaching is complicated and will only be briefly described here. A more detailed description can be found in Lagerblad (2001).

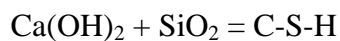
Basically cement paste is porous and the pore water is in contact with ground water. If a chemical component is removed from the pore water the solid phases of the cement paste will reequilibrate and solid phases will dissolve or change composition. Submerged in water the ionic transfer from the pore solution to the ground water will be by diffusion that is controlled by concentration gradient, transport distance through leached concrete and porosity. Thus to control the effect on ground water the focus must be on the pore water composition. If the pore water has a pH of less than 11 the concrete will presumably not give a pH of above 11 to the ground water.

The pore water composition is controlled by the composition of the cement paste phases and residual ions from the cement hydration. The bulk effect comes from hydration phases. Thus to control the effect on the ground water the composition of the cement paste must be regulated.

Pure Portland cement mixed with water gives crystalline portlandite (CH, calciumhydroxide), semi crystalline calcium silicate hydrate (C-S-H), crystalline ettringite (AFt, calcium aluminate sulphate), crystalline monosulphate (AFm, calcium aluminate sulphate), remaining cement clinker and residual alkali hydroxide in the pore solution. The amount of the different phases depends on the composition of the cement and the degree of hydration. Each of the crystalline phases gives a specific pH when in contact with water. The C-S-H dissolves incongruent by releasing CH, i.e. lowering its CaO/SiO₂ ratio.

The pore solution of ordinary concrete is above 13. This is due to residual easily soluble alkali hydroxide. The amount of alkali ions is limited, but to get a low pH concrete low alkali cement must be chosen. Of the different types of cement available on the Swedish market Aalborg A/S white cement contains least alkalis, around 0.2 wt. % alkalis when recalculated to pure Na₂O.

Of the solid phases CH gives the highest pH, around 12.4 in pure water. Thus this phase must be eliminated. This can be achieved by mixing the cement with reactive silica (puzzolana) that will give more C-S-H.



The most reactive silica is silica fume that is extremely fine-grained amorphous silica. To eliminate all CH around 15 wt. % silica fume is needed in the binder (cement + silica fume).

This C-S-H will, however, give a C-S-H with a CaO/SiO₂ ratio of around 1, 6 and it will give a pH of above 12 when leached. To lower the pH further more silica fume is needed. To get a pH of less than 11 the CaO/SiO₂ ratio must be less than 1, 1 (Stronach and Glasser 1997, Fig 1). The effect on pH diminishes with the ratio. One must, however, also to consider the composition of the ground water, as this will effect the composition of the pore water, equilibrium with the hydrate phases and thus the pH.

SiO₂ + C-S-H (1) = C-S-H (2) where C-S-H (2) has a lower CaO/SiO₂ ratio than C-S-H (1)

To get a C-S-H with a CaO/SiO₂ ratio of 1.1 around 30 wt. % silica fume is needed in the binder (Lagerblad et al. 2004). One must, however, consider that fine-grained quartz also reacts with the Ca and thus will lower the CaO/SiO₂ ratio further.

In a concrete with this large amount of silica fume AFm (monosulphate) will not form, as it requires a pH of 11.6 to form. The Aft (ettringite) is stable at a pH above 10.6. Thus with enough silica fume there will be no solid phase that can dissolve and give the ground water a pH of above 11.

For the basic recipe a mix with 50/50 white cement and silica fume was chosen to be certain to get a pH of below 11. This will give a Ca/Si ratio of less than 1 and the pH will be distinctly less than 11 and when the paste (C-S-H) is leached it will dissolve congruently and release more silica than calcium ions (see chapter 4.1, figure 9, 11, 12)

2.2 Concrete mix.

The silica concrete shall be cohesive, contain a minimum of cement/binder and it shall be self-compacting. The two first demands can be met with large amount of filler. To reduce the amount of binder part of the filler shall be ultrafine. This concept has been developed and is described in Lagerblad & Vogt 2004. Fillers are particles with a size of less than 63 µm and ultra filler are particles with a size of less than 10 µm.

The ultra filler shall be of quartz as this mineral will react with the cement paste and thus lower the CaO/SiO₂ ratio of the C-S-H. The fine ground types of quartz chosen for the mixes were fine ground α-quartz (M300) and fine ground cristobalite quartz (M6000). They are both commercial products from Sibelco. M300 has a size similar to cement and thus allows the amount of cement to be lowered without disturbing the particle packing. The M6000 is much finer than cement and will thus act as ultra filler and can thus replace cement without reducing the strength or increase the porosity (Lagerblad & Vogt 2004).

The concrete shall be self-compacting. This can be achieved by having a large amount of filler in the mix. A superplasticizer is necessary to make the silica concrete workable.

2.3 Concrete recipe

Based on the concept of silica fume and ultra fine filler a sequence of mixes was tested. The goals were to minimise the amount of Portland cement and maximize the amount of aggregate and filler. Earlier experience has shown that to large amounts of silica fume can give a

concrete that is difficult to mix and with a large shrinkage due to polymerisation (Lagerblad et al. 2004) Mixing and flowability is regulated by superplasticizer. The shrinkage is related to the amount paste. Thus small amounts of binder (cement-silica fume-water) will diminish shrinkage. During leaching it is part of the paste that is removed thus one will get a more stable product after leaching with a small amount of binder. The recipe is a balance depending on the desired properties.

Based on a sequence of mixes and preliminary tests the recipe below was chosen for further testing.

Table 1. Concrete recipe shown as kilogram of component per m³ of silica concrete. Brand name of product and producers in bracket.

Components	Kilograms per m ³ of concrete
White cement (Aalborg Portland)	60
Water (tap water)	150
Silica Fume (Elkem)	60
Fine ground α -quartz (M 300, Sibelco)	200
Fine ground cristobalite quartz (M6000, Sibelco)	150
Superplasticizer (Glenium 51 BASF)	4.38 (dry weight)
Aggregate 0-4 mm (Underås, Jehanders Grus)	1679

The silica concrete was mixed in a forced mixer. At Olkiluoto a simple paddle mixer was used.

3 Results

3.1 Rheology

The silica concrete composed according to the recipe was self-compacting, i.e. it flows and fills a given space by gravity. To measure the ability to self-compact a flow set measurement is normally used. It is based on a normal set cone but instead of measuring the set the spread is measured. The flow set (Figure 1) was 650 mm, which is enough to define it as self-compacting. Compared to ordinary concrete it was fairly viscous, i.e. it flows slowly (like syrup). The silica concrete had a good adhesion. This can be noticed at the edge of the spread (Figure 1) where no water separation can be noticed. The rheological properties indicate that it can be applied and casted at position in the borehole.



Figure 1; Picture of flow for the borehole plug concrete. This concrete is self-compacting in a borehole.

3.2 Strength

There are demands both on stiffening, strength development, and final strength. Thus compressive strength was tested at different ages. The basic aim was to get cube strength of above 10 MPa. The strength and strength development is dependent on temperature. Thus the mix was tested both at 5 and 20 °C curing temperature. The temperature in the borehole depends on depth and is assumed to be between these two temperatures.

Table 2. Strengths development. Cube strength.

Curing time in days	5°C Cube strength in MPa	20°C Cube strength in MPa
2	1.9	4.5
3	4	6.6
7	7.5	10.6
28	14	40
72	32.9	55.2
91	35.4	57.4
365	Not tested	68.0

The demands on strength are low for this application. The strength is, however, linked to porosity which in turn is linked to leaching and is thus of importance. The strength development is relatively slow presumably due to the low amount of cement. It is, as expected, slower at lower temperatures. If necessary, strength development can be increased by adding CaCl_2 to the mix. Normal concrete for building purposes normally has strength of somewhat above 30 MPa after 28 days. No long time test has been done, due to lack of material, on the concrete stored at 5°C, but one can presume that it will get the same strength as the one stored at 20°C but it will take longer time. This means that the borehole concrete by time will become very strong and that it will have a low porosity. It was rather surprising that a concrete with this low amount of cement could get this high strength.

3.3 Shrinkage

In the borehole the silica concrete will never dry out. Thus drying shrinkage can be neglected. Only autogenous shrinkage and shrinkage with surplus water has to be considered.

3.3.1 Autogenous shrinkage

This is shrinkage under sealed conditions, i.e. water is not added or removed. In the test the concrete was put in a flexible plastic tube and the length change was measured over time (Figure 2).



Figure 2; Flexible tube for autogenous shrinkage.

The results are shown in Fig 3. The measurements started when the concrete was hard enough to handle the tubes. The shrinkage before this is of no importance as the concrete in the borehole will compact itself before stiffening.

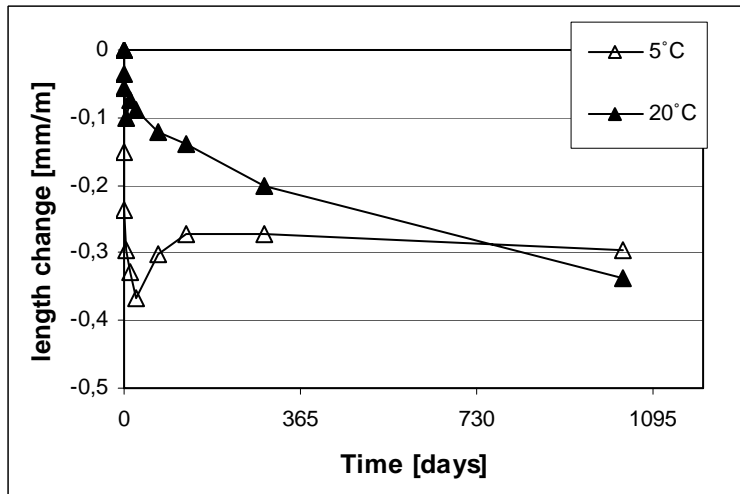


Figure 3; Autogeneous shrinkage of bore hole silica concrete.

The results show that, as expected, there is shrinkage at both temperatures. The reason for the difference is not known, but the shrinkage is fairly low even after three years and will only produce a negligible gap between the concrete and the rock.

3.3.2 Shrinkage in water

The casting and initial curing was done according to SS-13 72 15. After casting from the 100 x 100x400 mm³ prisms were water cured for one week before the measurements started. Then in contrast to SS-13 72 15 that stipulates storing at 50% RH the prisms were kept in tap water. In water there was a small initial shrinkage followed by a swelling which in turn was followed by shrinkage (Figure 4). The length change is small and it is close to the precision of the measuring device. The shrinkage is somewhat less than that of the autogeneous shrinkage. The results show that addition of water reduces the basic autogeneous shrinkage. This indicates that there will be a negligible gap between the concrete and rock.

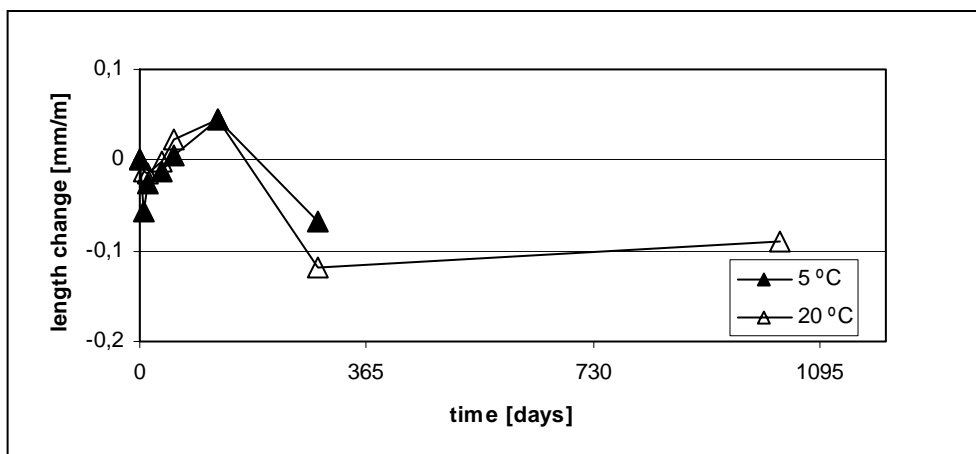


Figure 4: Shrinkage of bore hole concrete submerged in water.

3.4 Concrete texture and porosity

The porosity has been analysed in thin sections and by mercury intrusion porosity. A thin section is a specimen that has been polished so thin that light can penetrate it. This means that the concrete can be analysed in a polarising microscope. The thin sections have been impregnated with epoxy containing fluorescent dye. When analysed with UV light one can estimate the porosity. A porous material will absorb more epoxy/dye. Normal concretes with different water/cement ratios are used as reference. Mercury intrusion porosity is a method where a small piece of the dry material (larger aggregate fragments are removed) is put in liquid mercury. By increasing the pressure successively smaller pores are filled. By measuring the pressure and the amount mercury absorbed a porosity curve can be calculated. One error in the method is that it can only measure dry material and in concrete the pores are at least partly filled with water. Drying gives irreversible changes of the cement paste and the pore size will thus be larger than in reality.

The results from the thin sections (Figure 5) show that the silica concrete has porosity similar to common concrete with a water/cement ratio of 0.5 to 0.6. This is in accordance with the strength. Normal concrete contains around 300 kg cement and 150 kg of water. The borehole silica concrete contains 150 kg of water. As the amount of water decides the porosity this porosity is reasonable. The mercury intrusion (Figure 6) shows that the size of the pores of the silica concrete is lower than that of normal concrete. The amount of porosity is, however, similar. This will give the silica concrete other properties than normal concrete.

The effect is presumably due to the ultra filler that gives a dense structure. This can be better observed in scanning electron microscope (SEM) that gives a greater enlargement. Pictures from SEM are shown in Figure 6. In these photos one can observe a texture dominated by fine quartz grains, grains finer than cement. In samples water cured for 2 weeks we can still observe some remaining cement grains but these cement grains disappear with time. This remaining cement will react with time and give a more dense texture. The bottom two pictures in Figure 6 shows a normal Portland cement concrete with 300 kg of cement and similar strength. The water/cement is 0.5. The texture of this concrete is different with much more remaining cement grains and portlandite.

The main reason for the strength of the bore hole plug silica concrete seem to be that the fine grained quartz flour becomes an integrated part of the cement paste the binder. The cement is fully used up.

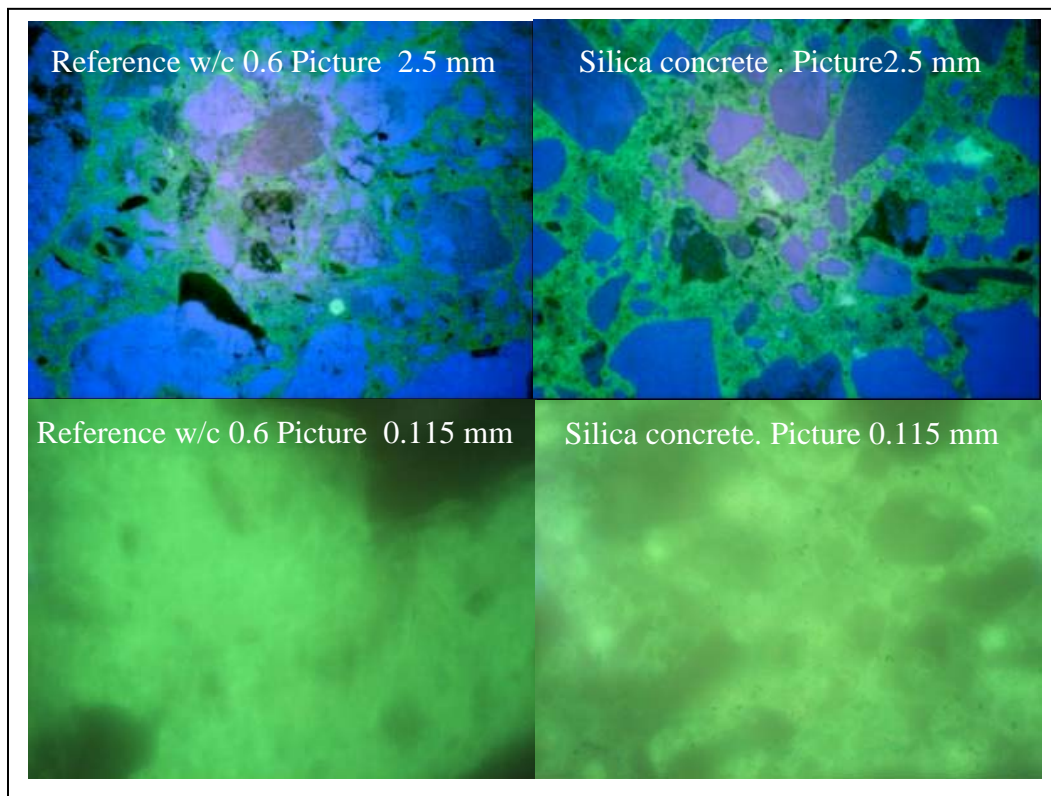


Figure 5: Thin section of bore hole silica concrete cured for 14 days in water compared to ordinary concrete with a water/cement of 0.6. Fluorescence pictures in petrographic microscope. The blue or dark grains are non porous aggregates while the yellow colour comes from fluoresces dye absorbed by the porous cement paste.

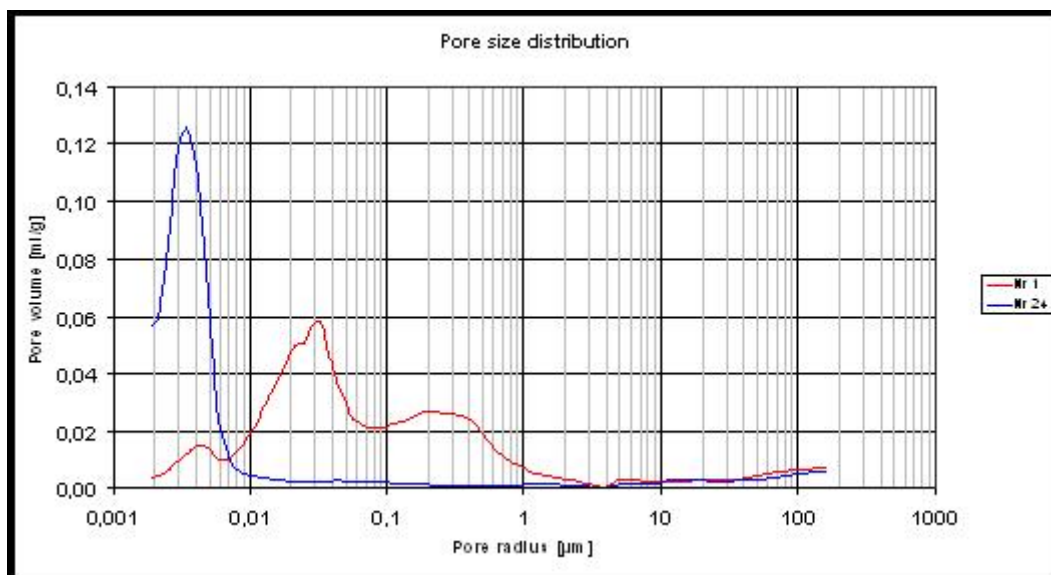


Figure 6; Mercure intrusion porosimetry. Blue line shows the silica concrete and red line normal good quality Portland cement concrete.

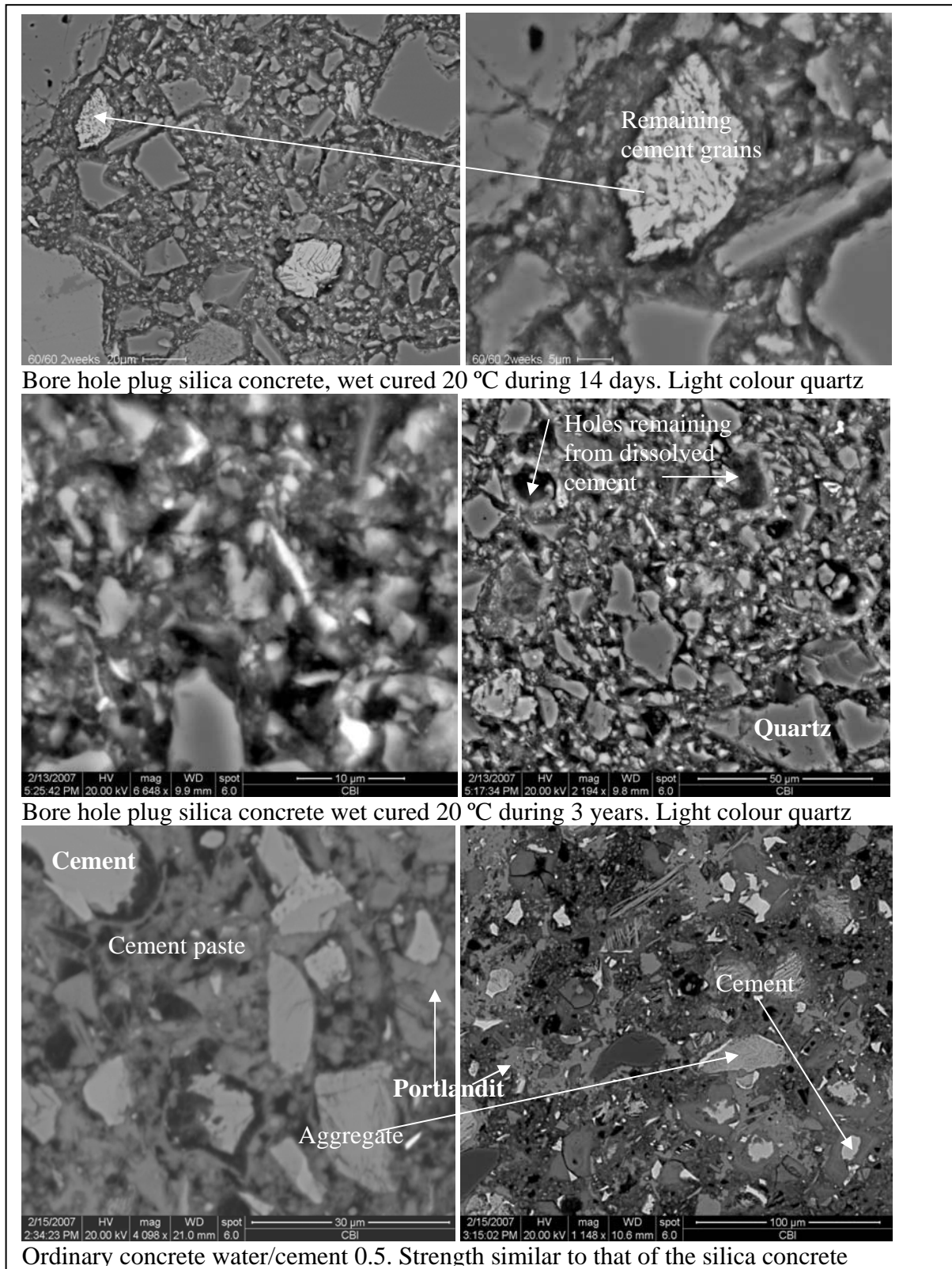


Figure 7. Scanning electron microscope image of flat polished surfaces in backscatter mode of bore hole silica concrete and a normal concrete with similar strength for comparison.

3.5 Chemical composition of the cement paste

The binder dominantly consists of calcium-silicate-hydrate (C-S-H). The cement, however, also contains some aluminate and sulphate (Table 2). In normal paste these two components form ettringite and monosulphate. X-ray diffraction, that identifies crystalline phases, shows that none of these formed; instead the peaks indicate calcium-aluminate-silica zeolites. This is presumably due to that the pH is below the stability limit of ettringite (pH 10.6). No sulphate minerals could be identified.

In SEM the chemical composition in a small area (spot) can be analysed by energy dispersive analysis. This technique was used to analyse the cement paste. It was, however, difficult to find a good spot away from the quartz filler due to the small amount of paste. Thus a large number of spots was analysed and those with the highest amount of Ca was chosen as representative of the paste. The paste contains water and thus the analyses were normalised to 100 % oxides. Representative analyses are presented in table 2. Analyses on three years old silica concrete gave similar values with a CaO/SiO₂ ratio between 0,25 and 0,50.

Table 2 Chemical composition of cement paste in bore hole concrete. In the table are also included compositions of white cement and silica fume (company declared compositions). In the cement the content of alkalis are put together as Na-equivalent.

Oxide	6°C age 14 d	6°C age 14 d	20°C age 14 d	20°C age 125 d	20°C age 125 d	White cement	Silica Fume
	Close to cement	In matrix	In matrix	In matrix	Close to cement	Bulk composition	
CaO	36,1	17,18	15,80	18,72	24,36	69,28	0,5
SiO ₂	52,29	72,09	75,99	70,84	66,71	24,9	93,8
Al ₂ O ₃	5,90	6,60	3,62	4,06	3,50	1,91	1,2
TiO ₂	0,28	0,25	--	--	--	--	--
Fe ₂ O ₃	2,40	1,33	1,58	3,07	2,87	0,33	0,5
Na ₂ O	0,49	--	0,37	0,33	0,21	0,15	0,27
K ₂ O	0,55	0,35	0,78	0,94	0,83		1,04
MgO	1,05	1,31	0,68	1,15	0,86	0,58	0,6
SO ₃	1,29	0,89	1,17	0,68	0,45	2,11	0,4
LOI						0,7	2,1
CaO/SiO ₂	0,69	0,24	0,20	0,26	0,37		

The paste contains 50 wt. % cement and 50 wt. % silica fume. The paste is totally dominated by C-S-H. It seems like most of the aluminates, sulphates and alkalis are incorporated in the C-S-H, i.e. no ettringite but some zeolites are formed. Thus we can assume that most of the calcium and silicates are in the C-S-H. Thus the chemistry of the cement and the silica fume suggest a CaO/SiO₂ of somewhat less than 0.6. The measured ratio in the analyses is less. The highest ratio was found close to a remaining cement grains and was only 0.69 but the mean value is between 0.2 and 0.4. There are some errors in the analyses due to the low atomic density and the abundant small quartz fragments but the data still suggest that some quartz is dissolved, which would lower the CaO/SiO₂. This low ratio will give a pH of distinctly less than 11.

3.6 Leaching experiments

Some simple leaching experiments were done to confirm the effect of silica on the composition of the paste. Later more precise measurements were done in glove boxes at Chalmers (appendix 1). The problem with leaching is that it is a slow process and that carbon dioxide from the atmosphere can interact with the leaching water. Carbon dioxide will dissolve to carboniferous acid that will react with the calcium hydroxide and lower the pH of the fluid. Thus interaction with carbon dioxide must be hindered.

The device that was set up for the test consists of 800 ml Teflon beakers with Teflon lids. In the lid of the beaker a 10 mm sawn slab is hung in platinum treads. The slabs are 70x 80 mm, i.e. the slab has a volume of around 56 cm^3 and an area of 142 cm^2 . The surface liquid area is around $1.8 \text{ cm}^2/\text{ml}$. In the bottom a Teflon coated magnetic stirrer keep the liquid in motion. To avoid carbon dioxide contamination the beakers are modified in such a way that the empty space is filled with argon gas and the argon gas is used to squeeze out the sample water (Figure8).

The samples were water cured for 48 days. After this period they were sawn and the slabs were water cured (tap water) for 2 days. Following this they were put in the beakers. The first pH measurement was taken after one day in the beakers. The leaching process is fairly slow and is linked to water turnover. Thus four experimental series was set up. In one of them the water was continuously replaced while in other the concrete slabs were kept in the water. A glass electrode calibrated with a buffer solution at pH 10 measured the pH.

When leached there is first a surface reaction, which gives the highest pH. As the test slabs were sawn there may be some cement grains at the surface. This will not be the case with casted concrete, as it will get a surface skin. Thus the slabs were first put in water to hydrate these cement grains. The last 40 days was during summer holiday. During this period no Argon gas was added which increases the risk for carbon dioxide contamination.

After this test of the pH, the bore hole silica concrete was tested on pH in a glove box (appendix 1). The test was done in the same type of Teflon beaker in nitrogen atmosphere to avoid carbon dioxide contamination. The water was of granitic type "Allard Water". The water was changed after 1, 2, 4, 6 and 10 weeks and at each change the pH was measured inside the glove box. The pH was 9.62, 9.50, 9.75, 9.72 and 9.72 respectively. The total alkalinity was 1.05 mmole after 4 weeks and 1.33 mmole after 10 weeks. The pH is slightly lower in the glove box but this is expected as Allard water contains some salt that will lower the pH. This water is, however, what one will find in shallow bore holes. The leach ability of the superplasticizer was also tested and the results are presented in SKB PIR-06-10.

Table 4. Influence on deionised water of borehole concrete. The pH is measured by glass electrode calibrated at pH 10 (buffer solution). pH measurement followed by *exchange of water.

Days	1	4	7	10	12	14	17	19	21
Serie 1	*10.3	*10.43	*10.28	*10.24	*10.14	*10.15	*10.23	*10.29	*10.08
Serie 2	10.21		*10.18			*10.30			*10.13
Serie 3	10.23					10.23			
Serie 4	10.22			10.25			10.14		

24	27	31	33	35	38	40	42	82
*9.94	*9.90	*9.97	*10.01	*10.06	*9.99	*10.16	*10.17	8.98
	*10.32			*10.37			10.36	9.49
	10.38	*10.37					10.38	10.30
	10.02						9.88	9.51

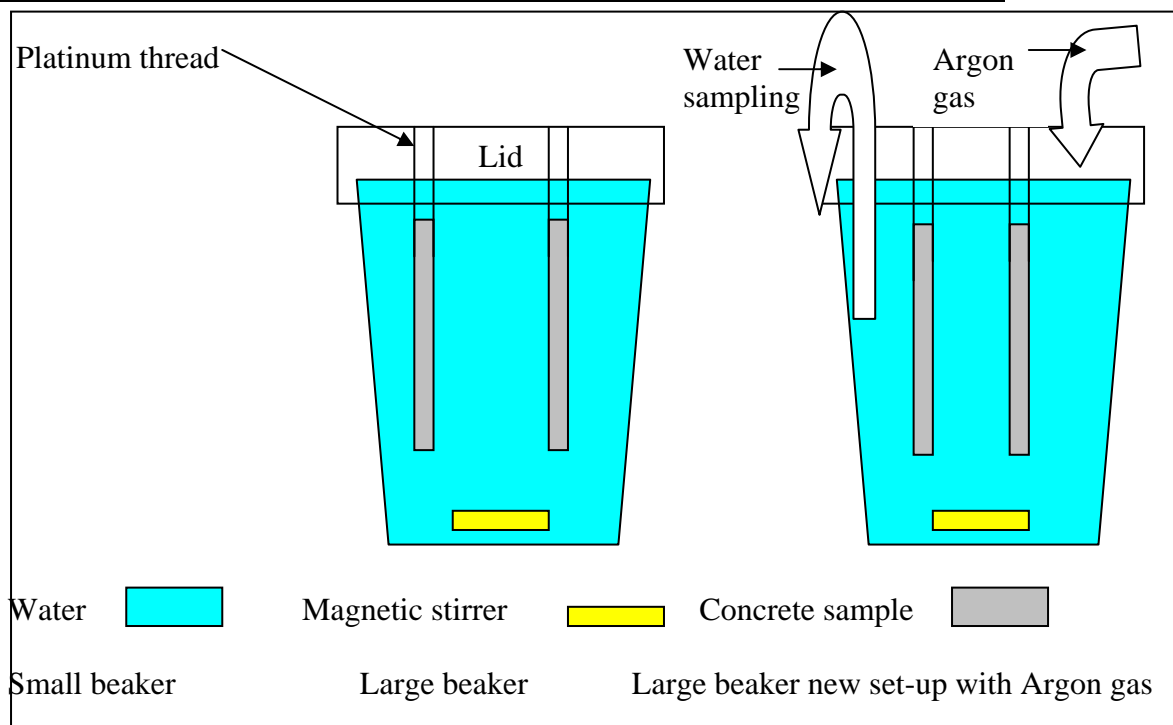


Figure 8. Set-up of leaching devices.

3.6.1 Discussion of leaching results

Leaching is a complicated process. To start with it is a chemical reaction between the surface and the water. Later leaching is a diffusion-controlled process between the pore water of the concrete and the surrounding water. Moreover the cement paste changes as the concrete becomes older. It will take some time before the cement clinker is totally consumed and has reacted with the silica fume and especially with the less reactive fine-grained quartz and the C-S-H will polymerise or crystallize with time. In the leaching experiments the concrete is fairly young and the sawn surface is fresh. In all of the four experimental series the pH was less than 10.5. The data from experimental series 1 show that the pH declines somewhat with every water change. This indicates that it takes a certain time for the leaching process to increase the pH. In series 4 the pH remains fairly constant. There is a small decline in pH over

time. This is not logical and indicates some minor leakage of carbon dioxide. With time and more mature concrete the pH will presumably decline somewhat. The more reliable glove box test gives a pH of less than 10. This is in accordance with the low CaO/SiO₂ of the C-S-H (see chapter 4.1).

4 Effect on ground water and long time durability

Effect on ground water, effect of leaching and material changes over time of the silica concrete must be considered in coherence.

All three aspect are linked to the stability of the in the silica concrete dominant amorphous C-S-H. The C-S-H in the silica concrete is very different from that of normal concrete. In normal mature concrete the CaO/SiO_2 of the C-S-H is around 1.7, while it in the silica concrete formulated for the plug is less than 0.6. This material will polymerize and probably form crystalline components with time (see chapter 4.2)

4.1 Stability of amorphous calcium-silicate hydrate (C-S-H)

The bulk of information comes from amorphous C-S-H as it is an essential part of normal cement paste. Normal C-S-H will dissolve incongruently by releasing Ca(OH)_2 until the CaO/SiO_2 drops to around 0.8-0.9 (Harris et al 2002) from where congruent dissolution of both SiO_2 and Ca(OH)_2 starts. Thus with a CaO/SiO_2 of less than 0.6 the leaching will be congruent from the start releasing both silica and calcium ions (Figure 9).

In the case of silica concrete the solubility of silica must be considered. In a closed system with small amounts of water equilibrium between the C-S-H and the water will be established. Experiments (Chen et al 2004) show that with a C-S-H with a C-S-H gel with a CaO/SiO_2 of 0.56 will be in equilibrium with a water containing 0.95 mMol Ca and 2.9 mMol Si ions per dm^3 water at a pH of around 10. Harris et al (2002) comes to similar values when leaching synthetic C-S-H gels. A thermodynamic model of dissolution (Atkinson et al. 1991 and Sugiyama & Fujita 2006) precipitation of C-S-H also gives similar values. However, none of these have considered the effect of salty water on the leaching behaviour.

If the concrete is in contact with slowly percolating water another system will appear. Silica will be released when the pH is around 10 but when the pH will drop amorphous silica will precipitate (Figure 10). This means that we will get a gap between pH of around 8 to around 11 where silica is soluble. This corresponds to what one can find in leaching (Table 4). In the material investigated by Lagerblad (2001) one can observe a porous layer (zone 3) followed by a denser layer where the silica has precipitated.

In the repository one can presume that when the silica concrete comes in contact with ground water it will slowly dissolve congruently. Silica will be released but it will later precipitate when the pH of the ground water goes down (like in Table 5). The high salt content in the deep ground water may, however, change the conditions.

The silica concrete is dense with a fine porosity. Normal concrete contains both portlandite and ettringite (Table 4). Portlandite is relatively soluble. Thus in normal concrete the portlandite dissolves first and leaves holes that increase the porosity. The silica rich C-S-H will dissolve much slower and thus the leaching will presumably be less. Moreover, when totally leached the pH will be down to normal groundwater chemistry where silica gel is stable. Thus most of the material will remain intact. Considering the low amount of binder one can thus expect the remaining material to be stable. The leaching experiments show that the leaching is slow.

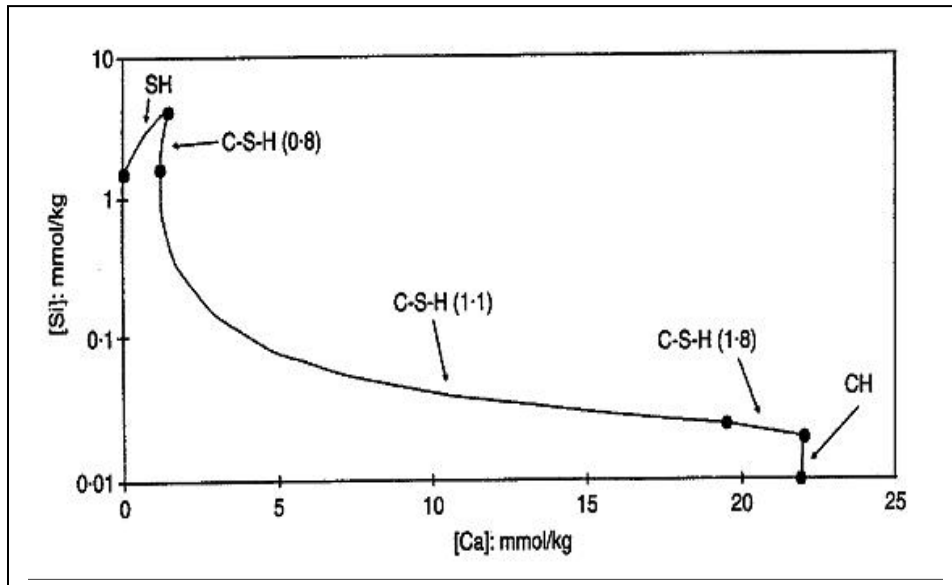


Figure 9. Relation between Ca and Si in solution and composition of C-S-H. The values in () marks the CaO/SiO₂ ratio. Figure and data from Stronach and Glasser 1997. The contents of Si and Ca in solution define the pH. SH is a silica gel. Similar diagram with a discussion and references can be found in Harris et al (2002) and in Chen et al (2004)

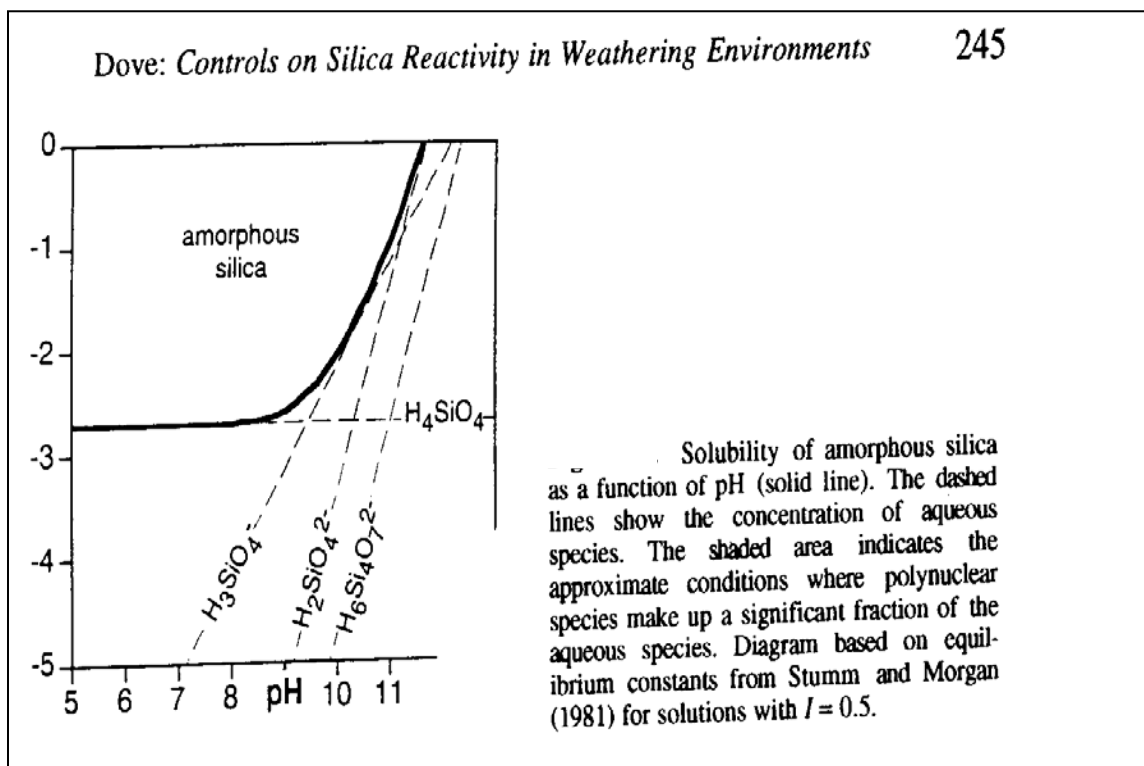


Figure 10. Solubility of amorphous silica. Dove 1995.

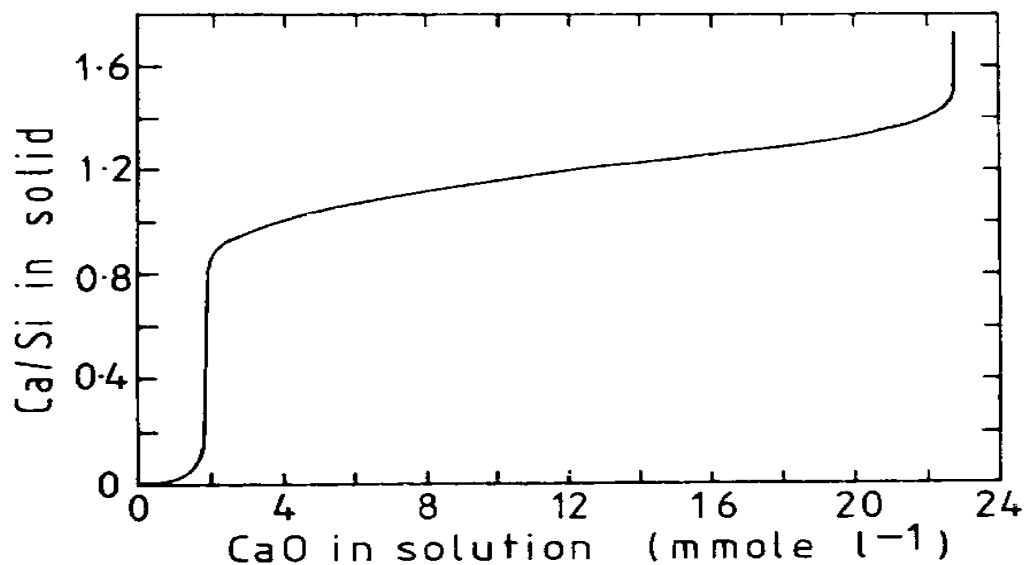


Figure 11. Measured and modelled relationship between Ca concentration and Calcium/silica ratio of C-S-H. From Rahman et al. 1999. Similar diagram with a discussion and more references can be found in Harris et al (2002), in Chen et al (2004) and Sugiyama & Fujita (2005)

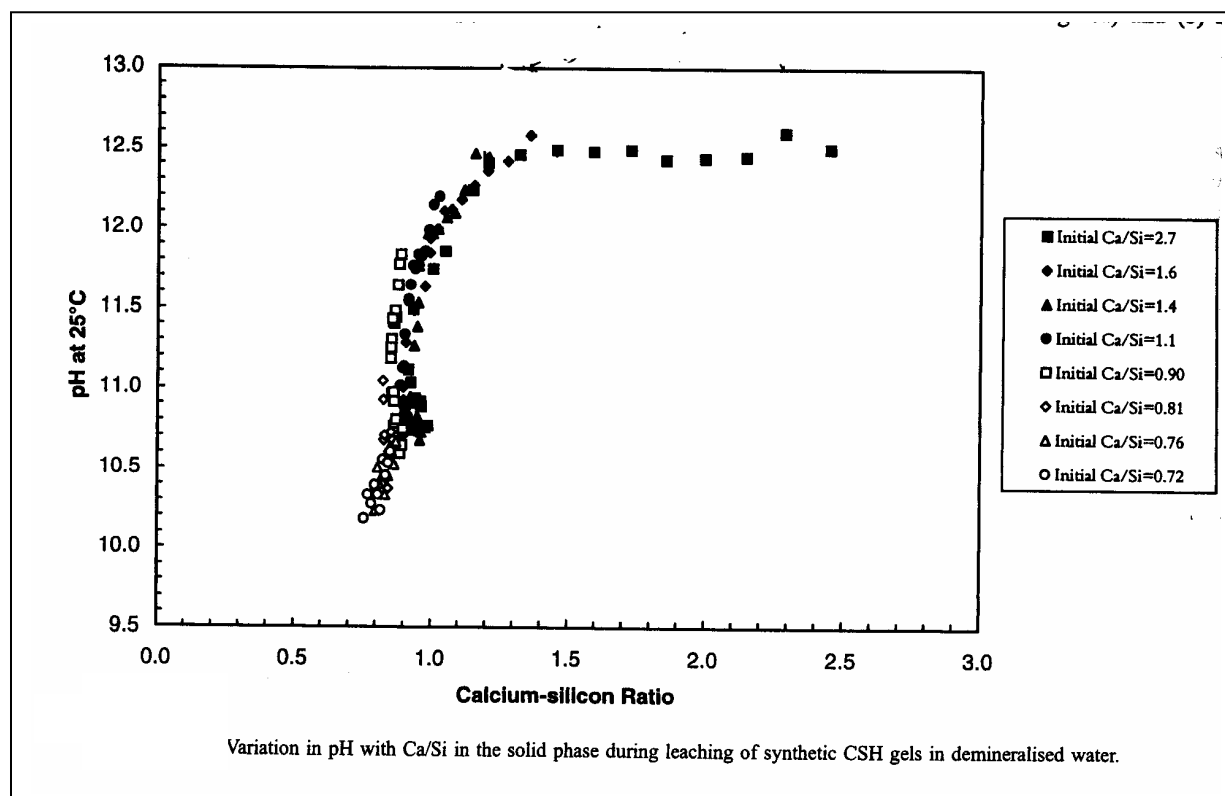


Figure 12. Diagram showing relationship between CaO/SiO_2 and pH. The ratio in investigated silica concrete is < 0.6 . From Harris et al (2002)

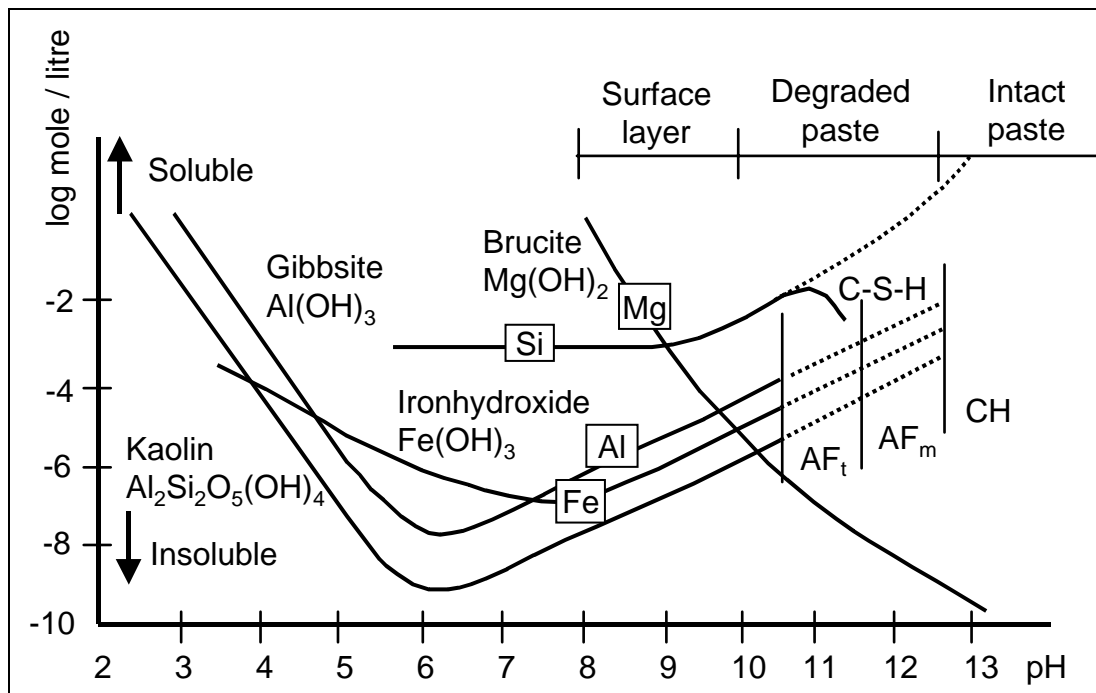


Figure 13. Solubility of pure hydroxides. From Lagerblad 2001

Table 5. Zonal pattern in leached concrete. From Lagerblad 2001

	Zone 1	Zone 2	Zone 3	Zone 4	Zone 5	Zone 6
Phases	Calcite Silica-gel Hydroxides	Silica-gel Calcite Hydroxides	Silica-gel / C-S-H Hydroxides	C-S-H Ettring.	C-S-H Ettringite (Cement)	C-S-H, CH Ettringite (Cement)
Al ₂ O ₃	High	Medium	low	low	low	low
*MgO	High	Medium	Low	None	None	None
*CaO/SiO ₂	< 0.1	< 0.5	0.5-1.0	Around 1	1.0-1.6	1.6-1.7
[Ca] mmol/kg	low	< 2	< 4	< 10	10-20	>20
[Si] mmol/kg	1.5	4.2	1.5	1.5	<1	<1
pH	7	Around 10	10.0-10.5	> 10.5	10.5-12.4	> 12.4
Porosity	Low	Medium	High	Medium	Low	Very Low

4.2 Structural order and crystalline C-S-H phases

In cement paste the C-S-H is amorphous but all amorphous products will try to form a crystalline compound. In the normal cement paste the C-S-H is cryptocrystalline with short silica chains. Even in old concretes no crystalline structure can be found. This is probably due to that the large Ca ion can not fit into the orthorhombic sites and thus hinders the formation of long Si chains. At lower Ca contents linked to lower pH, however, longer SiO₄ tetrahedra chains may form. This is treated in chapter 4.2.1.

C-S-H minerals can, however, be synthesized and be found in nature. This is especially the case with low CaO/SiO₂ C-S-H and thus the silica concrete C-S-H will probably try to crystallize with time. This is treated in chapter 4.2.2.

4.2.1 Structural order of C-S-H

The structure of the C-S-H can be identified with ²⁹Si MAS NMR. One can measure Q⁰, Q¹, Q², Q³ and Q⁴ where Q⁰ is a single silica tetrahedra, Q¹ two tetrahedra, Q² a chain of tetrahedra, Q³ a two dimensional and Q⁴ a three dimensional silicate structure. In a study (Lagerblad et al 2004) the chain length of new and old concrete with different amount of silica fume was investigated. This shows that the mean chain length increases both with amount of silica fume and age. Data is summarized in table 5. Normal concrete gets a mean chain length of around 5 silica oxide tetrahedra with time. With 40 wt. % silica fume the chain length will increase to around 10 and with 50 % silica fume the one dimensional chain length will be infinite. The chain length is linked to the CaO/SiO₂ of the C-S-H. This indicates that normal C-S-H will not crystallize but that a paste with 50 % silica fume, like silica concrete investigated, will get infinite chains that can be organised to a crystalline structure. Leached concrete (with low Ca/Si) will also get silica chains with infinite chain length Lagerblad (2001). Moreover, in leached concrete with low CaO/SiO₂ one can also get Q³ that indicate a two dimensional sheet like structure (Lagerblad 2001). The appearance of Q³ peaks at low pH has also been demonstrated by Matsuyama & Young (2000). With a silica chain or two dimensional structures a crystalline compound may form. Thus one can presume that the low pH plug concrete with time will crystallise and thus one must look on possible C-S-H crystalline compounds. The polymerisation will release water that will result either in shrinkage or increased porosity.

Table 6. Summary of ²⁹Si MAS NMR results. Degree of cement hydration comes from $(Q^1+Q^2) / (Q^0 + Q^1+Q^2)$. Since Q⁰ reflects the proportion of unhydrated cement, a low value indicates a low degree of hydration while a value of 1 indicates full hydration. The mean chain length is calculated from $2(Q^1+Q^2)/ Q^1$. The uncertainty is +/- 6 %. From Lagerblad et al 2004.

Laboratory specimen

Silica fume (%)	Age days	Degree of hyd.	Mean chain length	Age days	Degree of hydr.	Mean chain length	Age days	Degree of hyd.	Mean chain length
5	40	0.70	3.5	167	0.79	3.7	470	0.81	3.2
15	83	0.76	3.5	167	0.78	3.9	470	0.83	3.6
25	85	0.80	3.8	167	0.79	4.6	470	0.89	5.2
40	40	0.82	7.1	172	0.89	12.4	470	0.92	9.3

Old concrete from water dams and 20+ years old side beams with silica fume.

Cased year 100% OPC	Degree of hyd.	Mean chain length	Side-beams. Cast around 1980	Degree of hyd.	Mean chain length
1910	1.0	5.3	5E2, 50% SF	1.0	Only Q ²
1916	1.0	4.3	1B5, 20% SF	0.78	4.7
1927	1.0	5.4	2E19, 20% SF	0.82	4.6
1944	1.0	5.2	2C25, 17% SF	0.80	5.3
1960	1.0	4.7			

4.2.2 Possible crystalline compounds

Calcium silicate hydrate (C-S-H) minerals can be found in nature or are produced in laboratory. By comparing these and their structure we can evaluate the long term stability and the factors controlling the solubility and effect on pH.

Thus we must understand the conditions for the formation of C-S-H minerals. Two different types of possible low Ca/Si synthetic C-S-H minerals formed in the laboratory have been described.

Synthetic C-S-H minerals

1. Xenotlite $\text{Ca}_6\text{Si}_6(\text{OH})_2$, (CaO/SiO₂= 0.93)
This mineral is formed from normal cement paste when it is autoclaved to more than 180 °C.
2. Tobermorite (14-Å) $\text{Ca}_5\text{Si}_6(\text{O}, \text{OH})_{18} \times 5 \text{H}_2\text{O}$ (CaO/SiO₂ = 0.83)
This mineral is made by mixing lime (CaO) with silica in stoichiometric proportions and water 60 °C.

Natural C-S-H minerals

3. Okenite $\text{Ca}_5\text{Si}_9\text{O}_{24} \times 9\text{H}_2\text{O}$ (CaO/SiO₂= 0.5)
Triclinic, Dens. 2.28-2.33
Okenite is commonly found in amygdules in basalts together with zeolites, apophyllite, prehnite, calcite, quartz and chalcedony.
4. Gyrolite $\text{NaCa}_{16}(\text{Si}_{23}\text{Al})\text{O}_{60} \times 14 \text{H}_2\text{O}$ (CaO/SiO₂=0.65).

Triclinic, pseudo hexagonal, Dens 2.39

Gyrolite is found as replacement of wall rocks, in vugs, amygdules, as veinlets in basalt; in hydrothermally altered rhyolites and sediments; and in some ore deposits.

5. Tobermorite (14-Å) $\text{Ca}_5\text{Si}_6(\text{O}, \text{OH})_{18} \times 5 \text{H}_2\text{O}$ (CaO/SiO₂ = 0,83)
The natural Tobermorites also contain some Al and will thus give a lower value.

Orthorhombic or monoclinic, pseudo-orthorhombic, D= 2.42-2.458

Tobermorite is a hydrothermal alteration product of calcium carbonate rocks, due to contact metamorphism and metasomatism. It can be found filling vesicles and cavities in basaltic rocks. It can be found together with zeolites, ettringite, portlandite and calcite.

6. Clinotobermorite $\text{Ca}_5\text{Si}_6(\text{O}, \text{OH})_{18} \times 5\text{H}_2\text{O}$ CaO/SiO₂ = 0,83.

Monoclinic, D=2.58

Clinotobermorite can be found in gehlenite-spurrite-bearing skarns. (Gehlenite and spurrite occur in contact metamorphic environments)

7. Xonotlite, $\text{Ca}_6\text{Si}_6(\text{OH})_2$, ($\text{CaO}/\text{SiO}_2 = 0.93$)

Monoclinic, $D=2.71$

Xonotlite can be found contact metamorphic deposits, in limestone, serpentinite, and metavolcanic rocks.

Of these mineral one can presume that a C-S-H with a CaO/SiO_2 value of less than 0,8 will form tobermorite. Xenolite needs high temperatures and will thus probably not form in repository conditions. Tobermorite that has a structure based on one-dimensional silica chains will probably form. Sodium ions are available in the ground water thus one can also presume that some gyrolite and okenite may form. As magnesium ions also are available one can presume that talk-like structures may form (Lagerblad 2001).

5 Discussion

The tests show that it is possible to make low pH silica concrete with very low content of binder. The strength is sufficient to fulfil its purpose. In contact with ground water it will give this ground water a pH of maximum 10. The pH has been measured and is in accordance with what can be expected from the composition of the dominant C-S-H.

Earlier unpublished experiments (Qualification of low-alkali cementitious products in the deep repository-Feasibility study) give that the pH of leaching declines with the salt content of the ground water. The influence of more salt water than granitic water is not known.

The cement paste mainly consists of C-S-H. The CaO/SiO₂ in the of the C-S-H in the examined silica concrete is less than 0.6 compared to around 1.7 in normal mature cement paste. This is presumably not only due to the silica fume but also to that the fine-grained quartz filler has reacted and formed more C-S-H. A C-S-H with such low CaO/SiO₂ will not have the same properties as normal C-S-H. Thus it can not be directly compared to normal cement paste. The C-S-H is dominated by the silica system and thus the concrete is termed silica concrete not to confuse it with normal Portland cement concrete.

At a CaO/SiO₂ of 0.6 the C-S-H dissolves congruently in water and release both Ca and Si ions. In pure water the dissolution will give around 2 mmole Ca and 2 mmole Si ions per dm³ water at a pH of 10. The porosity is fairly low and thus one can expect a low solubility of the silica concrete. The solubility of silica increases with pH but at higher pH it is controlled by precipitation of C-S-H (Figure 12). The solubility of silica is much lower at pH 8 than pH 10 (Figure 10). Leaching involves equilibrium with surrounding pH neutral groundwater (pH 8). Thus the released silica will presumably precipitate again after a short transport. Only the Ca ions will presumably leave the system. When totally leached the cement paste will be dominated by silica gel, zeolites and metal hydroxides (Figure 13).

The concrete contains 60 kg of cement per m³ of concrete. The cement contains 69 % CaO, which shows that the concrete may lose 41.4 kg CaO. The CaO will be bound as Ca(OH)₂ with a weight of 54.7 kg in the C-S-H. If we assume that all CH will be leached out and that the C-S-H will shrink with the same volume, the concrete will lose 23.8 dm³ of paste. This gives a volume reduction or increased porosity of 2.4 %. This assumes that the remaining silica gel will shrink according to the amount of removed CH, which probably is not the case. In any case with a volume loss of around 2.4 % the concrete will still be fairly intact. It will consist of aggregates glued together with a silica gel.

As regard long term properties we must consider the stability of the C-S-H, how will the paste change over time and what the final aging product will be. The C-S-H is a cryptocrystalline phase formed rapidly during the hydration process. In normal C-S-H the structure is regulated by the Ca ions that do not allow polymerisation or crystallisation. This, however, changes when the content of Ca ions is low as in the silica concrete. When the CaO/SiO₂ drops below around 1 the C-S-H can polymerize (Lagerblad et al 2004). Thus in a long time perspective we can assume that the C-S-H in the borehole concrete will crystallise. One of the possible phases is Tobermorite (14-Å). It has the composition Ca₅Si₆(O,OH) x 5 H₂O. The CaO/SiO ratio in the borehole concrete C-S-H is however, even lower than in the tobermorite (0.83). With a CaO/SiO₂ ratio around 0.5 there is a whole range of natural minerals like okenite

($\text{Ca}_5\text{Si}_9\text{O}_{24} \times 9\text{H}_2\text{O}$) or gyrolite ($\text{NaCa}_{16}(\text{Si}_{23}\text{Al}) \text{O}_{60} \times 14 \text{H}_2\text{O}$). These mineral are normally found in hydrothermally altered volcanic rocks in nature. Crystallisation will result in release of water and shrinkage or increase in porosity. Presumably, however, it will take a long time.

6 Conclusions

The produced and examined silica concrete has properties which makes it a candidate for the borehole plugging.

The concrete is based on a concept with large amounts of quartz filler. It is possible to adjust the recipe so that it may contain larger stones (D-max). The concept demands the use of superplasticizer. By increasing the amount of binder and reduce the amount of filler the amount of superplasticizer can be lowered.

With time the silica concrete will reach strength of more than 60 MPa about the same strength as in normal high quality concrete. This will be more than enough for the purpose. The porosity is low and one can not expect water penetration over any long distances.

The shrinkage is low due to the small amount of cement paste. In wet conditions one can observe a small swelling. This means that there will be no gap between the concrete and the rock. Polymerization and eventually crystallization may give shrinkage and or increased porosity.

In contact with groundwater it will give this water a pH of around 10. The binder is dominated by C-S-H and this will leach congruently giving a Ca and Si concentration of around 2 mmole ions per dm³ of water.

The silica concrete will in contrast to normal concrete presumably crystallise with time.

7 References

- Atkinson, A., Hearne, JA., Knights CF., 1991, Thermodynamic modelling and aqueous chemistry in the CaO-Al₂O₃-H₂O system, Material Research. Society Symp. Proc. Vol. 212
- Chen, JJ., Thomas, JJ., Taylor, HFW., Jennings, HM., Solubility and structure of calcium silicate hydrate. Cement and Concrete Research. 34, pp 1499-1519, 2004.
- Dove, PM., Kinetic and Thermodynamic Controls on Silica reactivity in Weathering Environments. In Chemical Weathering Rates of Silicate Minerals, Eds White, A., F., Brantley, S. L., Reviews in mineralogy, Vol. 31, Mineralogical Society of America, 1995
- Harris, A.W., Manning, MC., Tearle, WM., Tweed, CJ., Testing of models of the dissolution of cements-leaching of synthetic CSH gels. Cement and Concrete Research. 32 pp 731-746, 2002.
- Jennings, HM., Aqueous solubility relationships for two calcium silicate hydrates, Journal of the American Ceramic Society. Vol 69, Nr 8, 614-618, 1986.
- Lagerblad, B., Jennings, HM., Chen, JJ., Modification of cement paste with silica fume-A NMR Study, 1st International Symposium on Nanotechnology in Construction, eds; Bartos, PjM, Trtic, P & Hughes, JJ., Zhu, W., In Royal Society of Chemistry, Special Publication No 292, 2004.
- Lagerblad, B., Conceptual model for deterioration of Portland cement concrete in water. SKB-TR 96-01, 1996
- Lagerblad, B., Leaching performance of concrete based on samples from old concrete constructions, SKB TR-01-27, 2001
- Lagerblad, B., Vogt, C., Ultrafine particles to save cement and improve concrete properties“, CBI report, 1:2004, 2004
- Matsuyama, H. & Young, JF., Effects of pH on precipitation of quasi-crystalline calcium silicate hydrate. Advances in Cement Research. 12 vol 1 pp 29-33, 200
- Rahman, M., Nagasaki, S., Tanaka, S., 1999, A model for dissolution of CaO-SiO₂-H₂O gel at Ca/Si > 1. Cement and Concrete Research, 29, 1091-1097, 1999.
- Richardson, I. G., The nature of the hydration products in hardened cement pastes., Cement. and Concrete Composites. 22, 97-113, 2000.
- Sugiyama, D., Fujita, T., A thermodynamic model of dissolution and precipitation of calcium silicate hydrate, Cement and Concrete. Research. 36, pp 227-237, 2006.
- Steinour, HH., The reactions and thermochemistry of cement hydration at ordinary temperatures, Proc. 3d Int. Symp. On the Chem of Cem, Cem & Conc. Ass., London 1952.

Stronach, SA., Glasser, FP., Modelling the impact of abundant geochemical components on the phase stability and solubility of the CaO-Si=2-H₂O system at 25 C. *Advances in Cement Research*. Vol. 9, No 36, 167-181, 1997

Taylor, HFW., *Cement Chemistry*, 2 ed, Thomas Telford, London, 1997.

Vogt. C., Lagerblad, B., Persson. T.H., "Optimization of UHPC for selective stabilization of deep boreholes". *International symposium on ultrahigh performance concrete*, Sept 13-15, 2004. *Schriftenreihe Baustoffe und Massivbau*, Universität Kassel, Heft 3 No 3, 2004.

Appendix 1 pH bestämning av silika betong.

pH-mätningar i Betonglakvatten - Arbetsrapport 060104

av Stellan Holgersson

Sammanfattning

På uppdrag av Cement och Betong Institutet (CBI) har pH mätts i lakvatten i fyra prov av lågalkalisk betong.

De fyra proverna med betong anlände Chalmers 050412 och dessa var då nedsänkta i destillerat vatten. Proverna togs omedelbart in i en handsbox med N₂ atmosfär. Vattnet byttes till Modifierad Allard 050511 och lakning startades genom att vattenbyten utfördes efter 1, 2, 4, 6 och 10 veckor.

Stamlösningen för Modifierad Allard som då användes visade sig emellertid vara instabil varför försöken startades på nytt 050905, men nu utgående från en ny stamlösning .

I slutet av varje laksteg, strax innan vattenbytet mättes pH i lakvattnen. Alla pH mätningarna gjordes inne i handsbox.

Resultatet av pH-mätningarna för de olika lakstegen redovisas i Tabell 1 nedan.

Tabell 1. pH i lakvatten från lågalkalisk betong.

Tid(veckor)	FB40SF Botten	FB40SF Topp	FB40SF Lab	60/60
1	11.04 ± 0.09	11.01 ± 0.09	10.87 ± 0.09	9.62 ± 0.09
2	11.02 ± 0.07	11.02 ± 0.07	10.86 ± 0.07	9.50 ± 0.06
4	11.09 ± 0.09	11.10 ± 0.09	10.87 ± 0.09	9.75 ± 0.08
6	11.04 ± 0.13	11.06 ± 0.13	10.81 ± 0.12	9.72 ± 0.12
10	11.00 ± 0.15	11.01 ± 0.15	10.75 ± 0.15	9.72 ± 0.14

Lakvattnen från vattenbytet vid vecka 4 och vecka 10 titrerades för total alkalinitet. Titringarna utfördes utanför box men med N₂ bubbling i titrerkarlet.

Resultatet av titringarna för de två lakstegen redovisas i Tabell 2 nedan.

Tabell 2. Total alkalinitet (mM) i lakvatten från lågalkalisk betong.

Tid(veckor)	FB40SF Botten	FB40SF Topp	FB40SF Lab	60/60
4	2.55 ± 0.01	2.72 ± 0.16	2.38 ± 0.01	1.05 ± 0.01
10	2.39 ± 0.01	2.57 ± 0.01	2.36 ± 0.12	1.33 ± 0.02

Utförande

Preparation av Modifierat Allardvatten

En stamlösning preparerades genom att lösa 0.819g NaCl, 0.1492g KCl, 0.7508g CaCl₂·2H₂O, 0.493g MgSO₄·7H₂O (samtliga Merck p.A.) samt 0.0576g MgCl₂·6H₂O (Fluka p.A.) i 1L MilliQ-vatten. Stamlösningen togs in i box.

En 35 vikts% NaSiO₃·9H₂O lösning preparerades genom att lösa 3.5g av saltet (Fisher) i 6.5g MilliQ-vatten. Denna lösning späddes sedan till 1.4% och togs in i box. (*

En 0.125g portion med NaHCO₃ (Fluka MicroSelect) togs in i box.

Vid spädning till Modifierad Allardvatten användes MilliQ-vatten som förvarats i box minst ett dygn.

50 mL av stamlösningen, 1 mL av den 1.4% silikatlösningen och 0.125g NaHCO₃ tillsattes till 1L mätkolv och detta späddes till märket.

Därefter justerades pH i lösningen till 8.4 med 0.1M HCl och, vid behov, med 0.1M NaOH.

En ny lösning gjordes för varje prov, alltså fyra lösningar vid varje vattenbyte, detta p.g.a. att större volymer än 1L inte kan hanteras inne i box.

Resultat av pH-justeringar visas i Tabell 3 nedan.

Tabell 3. Mätningar av pH i Modifierat Allardvatten, före och efter pH justering.

Tid (veckor)	Botten		Topp		Lab		60/60	
	före	efter	före	efter	före	Efter	före	efter
0	9.02	8.35	9.04	8.38	9.03	8.34	9.01	8.39
1	9.00	8.39	9.06	8.35	9.03	8.37	9.05	8.35
2	9.08	8.44	9.08	8.42	9.09	8.42	9.06	8.39
4	9.05	8.34	9.09	8.36	9.10	8.44	9.09	8.37
6	9.07	8.39	9.05	8.39	9.05	8.38	9.03	8.39
10	9.06	8.42	9.02	8.40	9.04	8.38	9.02	8.38

*) Problem uppstod när en stamlösning innehållande silikat gjordes. Denna innehöll 0.79g 35% NaSiO₃·9H₂O men lösningen visade sig efterhand bilda utfällningar.

Genomförande av vattenbyte

De fyra proverna med betong anlände Chalmers 050412 och dessa var då nedsänkta i 1 L destillerat vatten. Proverna, tillsammans med de medföljande magnetorrörarna, togs omedelbart in i en handskbox med N₂ atmosfär. Vattnet byttes till 1 L Modifierad Allard 050511 och omrörning och lakning startades.

Vattenbyten (laksteg) utfördes efter 1, 2, 4, 6 och 10 veckor.

Stamlösningen för Modifierad Allard som då användes visade sig emellertid vara instabil varför försöken startades på nytt 050905, men nu utgående från en ny stamlösning .

Vid varje vattenbyte torkades kärnen ur från betongpartiklar.

pH mätning

I slutet av varje laksteg, strax innan vattenbytet mättes pH i lakvattnen.

För mätning av pH användes en elektrod Radiometer pHC 3006L-9 och en voltmeter Radiometer MeterLab PHM240.

Vid laksteg 6 veckor byttes elektroden till ett annat exemplar av samma typ. All mätning gjordes inne i N₂-fylld handskbox.

Kalibrering av elektroden gjordes med tre buffertar: pH7, pH10 samt pH12.5 Radiometer IUPAC standard. Resultatet av elektrodkalibreringarna visas i Tabell 4, nedan.

Tabell 4. Resultat från kalibrering av pH elektrod.

Datum	Tid (veckor)	Temp. (°C)	Lutning (mV/pH)	% av teoretisk	Intercept (mV)
050905	0	23	-58.37 ±0.20	99.3	430 ±2
050912	1	24	-58.31 ±0.36	98.9	429 ±4
050919	2	23	-57.80 ±0.26	98.4	416 ±3
051004	4	23	-57.23 ±0.34	97.4	418 ±3
051024	6	23	-58.71 ±0.49	99.9	410 ±5
051116	10	23	-58.97 ±0.59	100	409 ±6

Uppmätt potential i lakvatten vid de olika tiderna för lakvattenbyte redovisas nedan i Tabell 5.

Tabell 5. Uppmätt potential (mV) i lakvatten från lågalkalisk betong.

Tid (veckor)	FB40SF Botten	FB40SF Topp	FB40SF Lab	60/60
1	-214.8	-212.9	-204.7	-132.0
2	-220.5	-221	-211.3	-132.8
4	-217.3	-217.6	-204.4	-140.2
6	-237.8	-239	-224.5	-160.5
10	-238.6	-238.9	-224.1	-163.1

Det beräknade pH i lakvatten, från uppmätt potential och kalibrering, har redan redovisats i Tabell 1 ovan.

Felet i pH, som angivits i Tabell 1, beräknades med felfortplantningsformeln enligt:

$$\sigma_{pH} = \sqrt{\sigma_{lutn}^2 \cdot \left(\frac{(IC - mV)}{lutn^2}\right)^2 + \sigma_{IC}^2 \cdot \left(\frac{1}{lutn}\right)^2}$$

Där σ_{lutn} och σ_{IC} är felen i respektive lutning och intercept från kalibrering (Tabell 4) och mV är uppmätt värde.

Titring för total alkalinitet

Vid varje vattenbyte sparades 250 mL av lakvattnet för titring. Titringar på vatten från laksteg 4 och 10 veckor utfördes efter den sista pH mätningen.

pH elektroden som användes var en Radiometer pHC 3006L-9, titratoren en Radiometer ABU91/TIM90 med 1 mL byrett.

Titringarna gjordes utanför box, men med N₂-bubbling av lösningen.

Vid varje titring vägdes omkring 50 g lakvatten in och detta titrerades med antingen 0.1M eller 1M HCl (Riedel de Haen, Titrisol). Vid beräkningen av total alkalinitet antogs lakvattnet ha densiteten 1000 g/L.

Varje prov titrerades fem gånger, vilket gav ett medelvärde med standardavvikelse. Dessa har redovisats i Tabell 2 ovan.

Resultatet från titring av laksteg 4 veckor och 10 veckor ges i Tabell 6 respektive Tabell 7.

Tabell 6. Resultat från titringar med HCl på lakvatten från laksteg 4 veckor.

Prov	Titration #	Volym HCl (mL)	Koncentration HCl (M)	Mängd lakvatten (g)	Total alkalinitet i lakvatten (mM)
Botten	1	1.233	0.1	48.6075	2.54
	2	1.379	0.1	54.0152	2.55
	3	0.157	1	61.488	2.55
	4	0.169	1	66.077	2.56
	5	0.098	1	38.2745	2.56
Topp	1	0.174	1	58.3618	2.98
	2	0.151	1	57.7562	2.61
	3	0.168	1	64.276	2.61
	4	0.119	1	43.1205	2.76
	5	0.129	1	49.4575	2.60
Lab	1	0.125	1	52.6631	2.37
	2	0.134	1	56.1092	2.39
	3	0.129	1	54.0516	2.39
	4	0.123	1	51.888	2.37
	5	0.134	1	56.3752	2.38
60/60	1	0.614	0.1	57.5763	1.07

	2	0.597	0.1	56.83	1.05
	3	0.564	0.1	53.804	1.05
	4	0.57	0.1	54.144	1.05
	5	0.456	0.1	43.5124	1.05

Tabell 7. Resultat från titreringar med HCl på lakvatten från laksteg 10 veckor.

Prov	Titr #	Volym HCl (mL)	Koncentration HCl (M)	Mängd lakvatten (g)	Total alkalinitet i lakvatten (mM)
Botten	1	0.128	1	53.6546	2.39
	2	0.131	1	54.9853	2.38
	3	0.128	1	53.8568	2.38
	4	0.13	1	54.1754	2.40
	5	0.143	1	59.8593	2.39
Topp	1	0.142	1	55.2923	2.57
	2	0.155	1	60.417	2.57
	3	0.139	1	53.9038	2.58
	4	0.132	1	51.3535	2.57
	5	0.129	1	50.0114	2.58
Lab	1	0.140	1	54.38	2.57
	2	0.126	1	54.85	2.30
	3	0.123	1	53.3171	2.31
	4	0.124	1	53.9122	2.30
	5	0.128	1	55.6707	2.30
60/60	1	0.61	0.1	45.1	1.35
	2	0.745	0.1	56.4	1.32
	3	0.578	0.1	44.1	1.31
	4	0.578	0.1	43.7	1.32
	5	0.483	0.1	43.9	1.33

Tryckhållfasthet hos kuber												
Konto	Maxlast	Hastighet	Sign									
	2500 kN	0,8 MPa/s	CV									
Prov	Tryckhållfasthet	Densitet	tillverkad	provad	ålder	tryckyta	vikt	brottlast	gjuthöjd	tryckbredd	tryckhöjd	volym
	MPa	kg/m ³	datum	datum	dygn	mm ²	g	kN	mm	mm	mm	mm ³
Sötvatten	29,1	2261		07-04-05		22875	7758	665,4	152,5	150	150	3431250
Formationsv	30,2	2286		07-04-05		22650	7768	683,4	151	150	150	3397500

